Plk4-induced Centriole Biogenesis in Human Cells

Dissertation

zur Erlangung des Doktorgrades der Naturwissenschaften

der Fakultät für Biologie der Ludwig-Maximilians Universität

München

Vorgelegt von

Julia Kleylein-Sohn

München, 2007

Dissertation eingereicht am:

27.11.2007

Tag der mündlichen Prüfung:

18.04.2008

Erstgutachter: Prof. E. A. Nigg

Zweitgutachter: PD Dr. Angelika Böttger

Hiermit erkläre ich, dass ich die vorliegende Dissertation selbständig und ohne unerlaubte Hilfe angefertigt habe. Sämtliche Experimente wurden von mir selbst durchgeführt, soweit nicht explizit auf Dritte verwiesen wird. Ich habe weder an anderer Stelle versucht, eine Dissertation oder Teile einer solchen einzureichen bzw. einer Prüfungskommission vorzulegen, noch eine Doktorprüfung zu absolvieren.

München, den 22.11.2007

TABLE OF CONTENTS

SUMMARY

It has previously been shown that overexpression of Plk4 in human cells causes the recruitment of electron-dense material onto the proximal walls of parental centrioles (Habedanck *et al.*, 2005), suggesting that Plk4 is able to trigger pro-centriole formation.

Here, we have used a cell line allowing the temporally controlled expression of Plk4 to study the formation of centrioles in human cells. We show that Plk4 triggers the simultaneous formation of multiple pro-centrioles around each pre-existing centriole. These multiple centrioles form during S phase and persist as flower-like structures throughout G2 and M phase, before they disperse in response to disengagement during mitotic exit, giving rise to a typical centriole amplification phenotype. Through siRNA-mediated depletion of individual centrosomal proteins we have identified several gene products important for Plk4-controlled centriole biogenesis and assigned individual proteins to distinct steps in the assembly pathway.

Furthermore, we have been able to correlate these functional data with morphological analyses using immuno-electron microscopy, revealing that Plk4, hSas-6, CPAP, Cep135, γ-tubulin and CP110 were required at different stages of pro-centriole formation and in association with different centriolar structures. Remarkably, hSas-6 associated only transiently with nascent pro-centrioles, whereas Cep135 and CPAP formed a core structure within the proximal lumen of both parental and nascent centrioles. Finally, CP110 was recruited early and then associated with the growing distal tips, indicating that centrioles elongate through insertion of α-/β-tubulin underneath a CP110 cap. Collectively, these data afford a comprehensive view of the assembly pathway underlying centriole biogenesis in human cells.

INTRODUCTION

In most animal cells, the centrosome orchestrates the formation of the cytoplasmic microtubule (MT) network during interphase and the mitotic spindle during M phase (Doxsey *et al.*, 2005; Luders and Stearns, 2007). The importance of the centrosome was already realized at the end of the 19th century upon its discovery by Theodor Boveri who posed many key questions about the regulation of centrosome number and its role during cancerogenesis. It has been now known for more than 30 years that centrosomes duplicate in S phase – simultaneously to DNA replication. Whereas the molecular mechanisms that restrict DNA replication to a single round per cell cycle are well understood (Blow and Dutta, 2005; Machida and Dutta, 2005), little is known about the mechanisms controlling centrosome duplication. However, any deviation from normal centrosome number may lead to the formation of either monopolar or multipolar spindles, characeristics that are often associated with aneuploidy, and that are a hallmark of many cancer cells (Brinkley, 2001; Carroll *et al.*, 1999; Lingle *et al.*, 1998; Pihan *et al.*, 1998). Therefore, both centrosome number and the coordination between chromosomal and centrosomal replication must be tightly controlled within the cell cycle. Here, the basic structure and function of the centrosome will be introduced. Then, recent studies and their implication for our understanding of centriole assembly itself, and the regulatory mechanisms controlling centrosome duplication, will be presented.

The structure of the centrosome

The centrosome is a non-membraneous organelle of ~ $1\mu m^3$ volume that is usually located in close proximity to the nucleus (Bornens, 2002; Doxsey, 2001). As the major microtubule organizing centre (MTOC) (Bornens, 2002; Doxsey, 2001) it participates in a range of functions, including cytoskeletal organisation, cell shape, motility, organelle transport and cell signalling during interphase. In mitotic cells, centrosomes organize the bipolar spindle and ensure accurate chromosome segregation and cytokinesis. Despite some morphological differences, specifically in *Drosophila* and *C. elegans,* basic centrosomal structure and functions are evolutionarily conserved from lower eukaryotes to mammals (Beisson and Wright,

2003). In some organisms that have lost their ability to form centrosomes, e.g. higher plants, a centrosome-independent mechanism ensures the formation of a bipolar spindle during mitosis (Gadde and Heald, 2004).
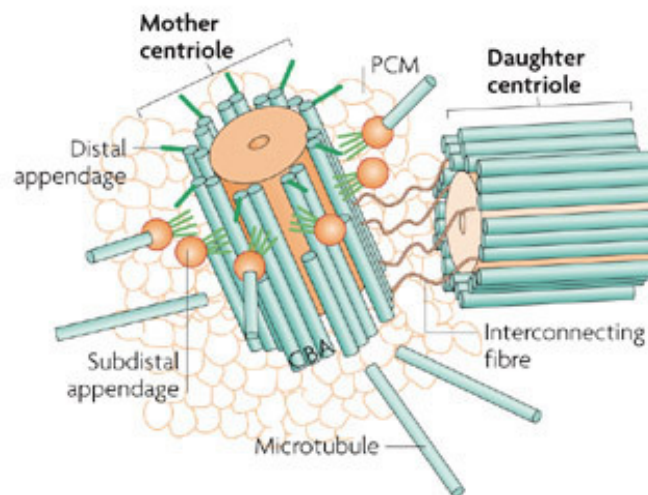
Figure 1. The structure of the centrosome.
Schematic view of the centrosome consisting of the centrioles and the surrounding PCM. At the proximal ends, the centrioles consist of microtubule triplets (A-, B-, C-tubule) while microtubule doublets are present at the distal ends (Bettencourt-Dias and Glover, 2007).

The single centrosome present in a G1 phase cell comprises two centrioles embedded in a protein matrix, the so-called pericentriolar material (Figure 1) (Bornens, 2002). This pericentriolar matrix is an electron-dense fibrous lattice (Dictenberg *et al.*, 1998) that is composed of more than 100 different proteins (Andersen *et al.*, 2003). It functions as a docking site for proteins involved in microtubule nucleation and anchoring, notably the evolutionarily conserved γ-tubulin ring complex (γ-TuRC) and large coiled-coil proteins like AKAP450 and PCM-1 (Balczon *et al.*, 1994; Keryer *et al.*, 2003).

The two centrioles at the core of the centrosome are symmetrical barrel-shaped arrays of nine microtubule triplets. They are structurally and functionally distinct in that only one is fully mature, as reflected by the presence of distal and subdistal appendages (Ishikawa *et al.*, 2005; Lange and Gull, 1996; Vorobjev and

Chentsov Yu, 1982). Centrioles are interconvertible with basal bodies which are essential for the formation of cilia and flagella (Dutcher, 2003).

During ciliogenesis, the mature centriole/basal body is positioned in close proximity to the plasma-membrane, and the ciliary axoneme extends from its distal end by the elongation of centriolar MTs (Figure 2). Depending on the structure of the axoneme, cilia and flagella can be motile or non-motile, determined by the presence (motile 9+2 structure) or absence (non-motile 9+0 structure) of two central MTs within the lumen of the axoneme. While motile cilia and flagella are important for locomotion and the transport of material over cellular surfaces, non-motile/primary cilia appear to function as transducers of sensory stimuli (Pazour and Witman, 2003; Satir and Christensen, 2007; Singla and Reiter, 2006).

Recent studies have established convincing genetic links between centriole-associated proteins implicated in ciliogenesis such as BBS proteins (Nachury *et al.*, 2007) and Odf2 (Ishikawa *et al.*, 2005) and several human diseases (Badano *et al.*, 2006; Bond *et al.*, 2005; Hildebrandt and Zhou, 2007; Singla and Reiter, 2006) For example, Odf2 localizes specifically to the distal appendages of the mature centriole and its knockout phenotype in mouse F9 embryonic carcinoma cells suggests a role of Odf2 in primary cilium formation (Ishikawa *et al.*, 2005). Interestingly, primary cilia are present on the surface of most quiescent somatic cells in vertebrates (Marshall and Nonaka, 2006; Singla and Reiter, 2006) and play important roles in physiology, development and disease. So far, studies on cilia formation have primarily focused on molecular components responsible for intraflagellar transport (IFT) or intracellular transport of membranes to growing cilia (Beales *et al.*, 2007; Nachury *et al.*, 2007) – both essential for ciliogenesis. However, the signalling network that controls ciliogenesis and particularly the interconversion between centrioles and basal bodies during cell cycle progression, remains to be elucidated.
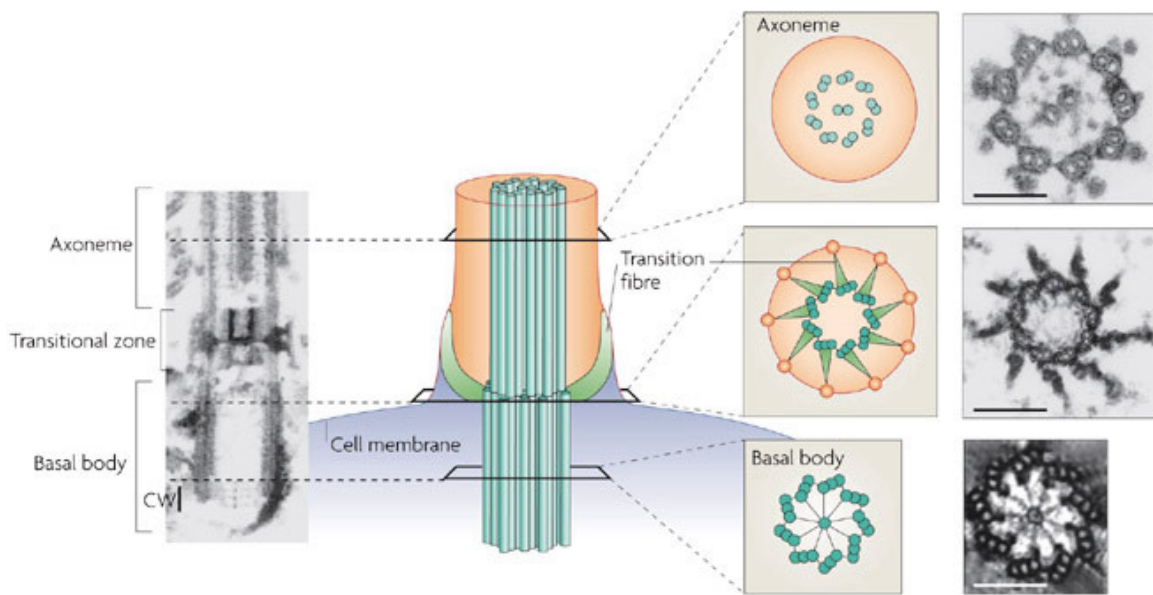
Figure 2. The Structure of cilia.

Electron micrographs and schematic views of the flagella of green algae. The axoneme is a cylindrical array of nine doublet MTs that surround either two singlet MTs (9+2 structure) or lack central MTs (9+0 structure). The transition fibers extend from the distal end of the basal body to the cell membrane. It has been suggested that they can be part of a pore complex that controls the entry of molecules into the cilium. Scale bar 0.25 µm. CW, cartwheel (Bettencourt-Dias and Glover, 2007).

The centrosome cycle

A somatic cell enters the centriole cycle at the G1/S-transition with a single centrosome comprising two loosely associated centrioles (Figure 3). It is noteworthy that these two centrioles are morphologically dissimilar, as maturity markers like distal and subdistal appendages are exclusively found on the mature centriole, which has been assembled two cell cycles ago. The second centriole, which was assembled during the previous cell cycle, lacks these structures.

Pro-centriole assembly at the proximal end of both pre-existing centrioles is initiated at the G1/S-transition. Concomitantly with S phase entry, exactly one procentriole assembles at an orthogonal angle at the proximal end of each parental centriole (Alvey, 1985; Kochanski and Borisy, 1990; Kuriyama and Borisy, 1981; Paintrand *et al.*, 1992; Vorobjev and Chentsov Yu, 1982).

The pro-centrioles elongate during S and G2. Before the cell enters mitosis, centrosome size increases by the recruitment of additional γ-tubulin ring complexes (Palazzo *et al.*, 2000), the second parental centriole also acquires distal appendages and the loose connection tethering the two parental centrioles is severed through cell cycle specific activation of several kinases, including Nek2, Cdk1 and Plk1 (Berdnik and Knoblich, 2002; Blangy *et al.*, 1995; Fry *et al.*, 1998; Giet *et al.*, 1999; Glover *et al.*, 1995; Golsteyn *et al.*, 1995; Hannak *et al.*, 2001; Lane and Nigg, 1996; Sawin and Mitchison, 1995). Although the composition of this tethering structure is unknown, the separation event is thought to be regulated via the phosphorylation tatus of C-Nap1. This protein is specifically located at the proximal end of the parental centriole and probably provides docking sites for other linker proteins (Fry *et al.*, 1998; Mayor *et al.*, 2000), notably rootletin (Bahe *et al.*, 2005) and Cep68 (Graser *et al.*, 2007). The phosphorylation status of C-Nap1 is balanced via activation of the centrosomal kinase Nek2 and the antagonistic protein phosphatase PP1α which is inactivated at the beginning of mitosis (Meraldi and Nigg, 2001). Dephosphorylation of C-Nap1 leads to its displacement from the centrioles, allowing centrosome separation to occur through the action of plus and minus-end directed motor proteins. The centriole pair at each pole of the bipolar mitotic spindle looses its orthogonal orientation and disengages at the end of mitosis and the cell enters G1 phase with one centrosome harbouring two loosely associated centrioles.
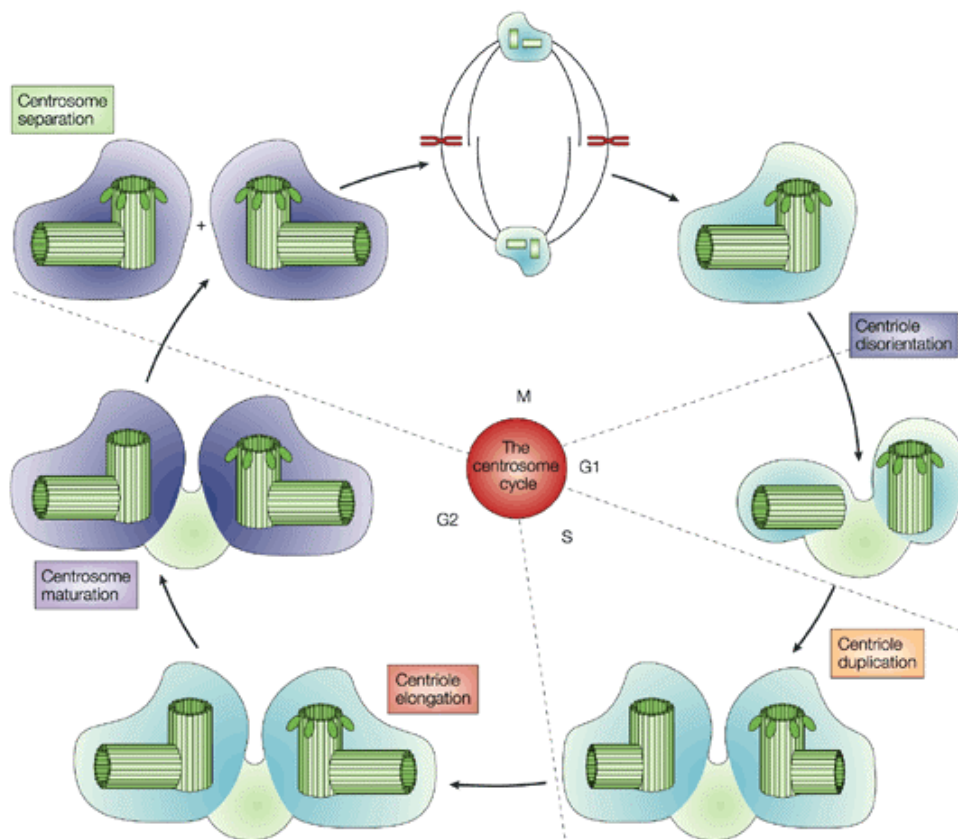
Figure 3. The centrosome cycle.

The centrosome duplication cycle can be subdivided into several discrete steps. 'Centriole duplication' is initiated as the cell enters S phase. 'Centriole elongation' takes place during S and G2 phase. Before the cell enters mitosis, the centrosome undergoes 'maturation' and with exit from mitosis, the parental and daughter centrioles loose their orthononal association – an event formerly referred to as 'Centriole disorienation', now termed 'Centriole disengagement' Now the two centrioles are licensed for a new round of duplication (Nigg, 2002).

Kinases involved in the regulation of centriole duplication

Several vertebrate kinases have been implicated in centriole duplication (Doxsey *et al.*, 2005), but the most definitive evidence has accumulated supporting a role for Cdk2 together with cyclin E and/or A in regulating centriole duplication (Matsumoto *et al.*, 1999; Meraldi *et al.*, 1999; Tsou and Stearns, 2006). Interestingly, abnormal centriole duplication has also been observed in Drosophila wing disc cells depleted of Cdk1 (Vidwans *et al.*, 2003). These cells not only show a prolonged S phase, but some daughter centrioles are characterized by an increase in length and most strikingly, in some of these cells, the parental centriole has acquired two daughter centrioles. However, a mechanistic understanding of Cdk requirement for centriole

duplication still needs to be achieved, and it remains possible that Cdk2 activity is necessary to advance cells into a permissive cell cycle stage, before centriole biogenesis can occur.

A screen for genes required for embryonic development of *C. elegans* uncovered Zyg-1, a centrosomal kinase required for all developmental stages (O'Connell *et al.*, 1998). Elegant genetic studies using reciprocal crosses between wild-type and mutant gametes revealed that Zyg-1 is essential for centriole duplication (O'Connell *et al.*, 2001). Independently, the protein kinase Plk4 (also known as Sak; (Fode *et al.*, 1994; Swallow *et al.*, 2005)) has been identified as a key regulator of centriole duplication in both *Drosophila* (Bettencourt-Dias *et al.*, 2005) and human cells (Habedanck *et al.*, 2005). Although the two kinases lack obvious sequence homology, it is plausible that Plk4 represents a functional homologue of *C. elegans* Zyg-1. When Plk4 was absent, centriole duplication was abolished and centrioles were progressively lost in both vertebrate and invertebrate cells. Moreover, the spermatids of *Drosophila* Sak/Plk4 mutants lacked basal bodies and were therefore unable to form flagella (Bettencourt-Dias *et al.*, 2005). When overexpressed in unfertilized eggs of *Drosophila,* Plk4 (Sak) induced the '*de novo'* formation of centrioles, demonstrating that this kinase is able to induce centriole biogenesis even in the absence of pre-existing centrioles (Peel *et al.*, 2007; Rodrigues-Martins *et al.*, 2007). Most strikingly, it has been shown that overexpression of Plk4 in human cell causes the recruitment of electron-dense material onto the proximal walls of parental centrioles, suggesting that Plk4 triggers multiple pro-centriole assembly via the enhanced recruitment of centriolar material (Habedanck *et al.*, 2005).

Maintenance of centrosome numbers

The question of how cells keep centriole numbers constant over successive cell divisions remains an intriguing yet unresolved issue. When considering the centrosome cycle from a purely conceptual perspective, two different regulatory mechanisms seem appealing (Figure 4) (Nigg, 2007). One mechanism ensures that only one progeny centriole forms at each parental centriole (copy number control) and it is tempting to speculate that Plk4 is the master regulator of copy number control.

The other control mechanism ensures that centrioles duplicate exactly once and only once during each cell cycle (cell cycle control), being negatively regulated by a licensing mechanism that prevents inappropriate centriole re-duplication during G2 and M phase and positively regulated by high Cdk2 activity driving pro-centriole assembly only during S phase. The licensing mechanism mentioned here will be discussed in more detail in the following section.

It is noteworthy that adherence to both rules is critical for the maintenance of constant centriole numbers, and deregulation of either one of the two control mechanisms is expected to give rise to aberrant centriole numbers and, consequently, to induce genomic instability.
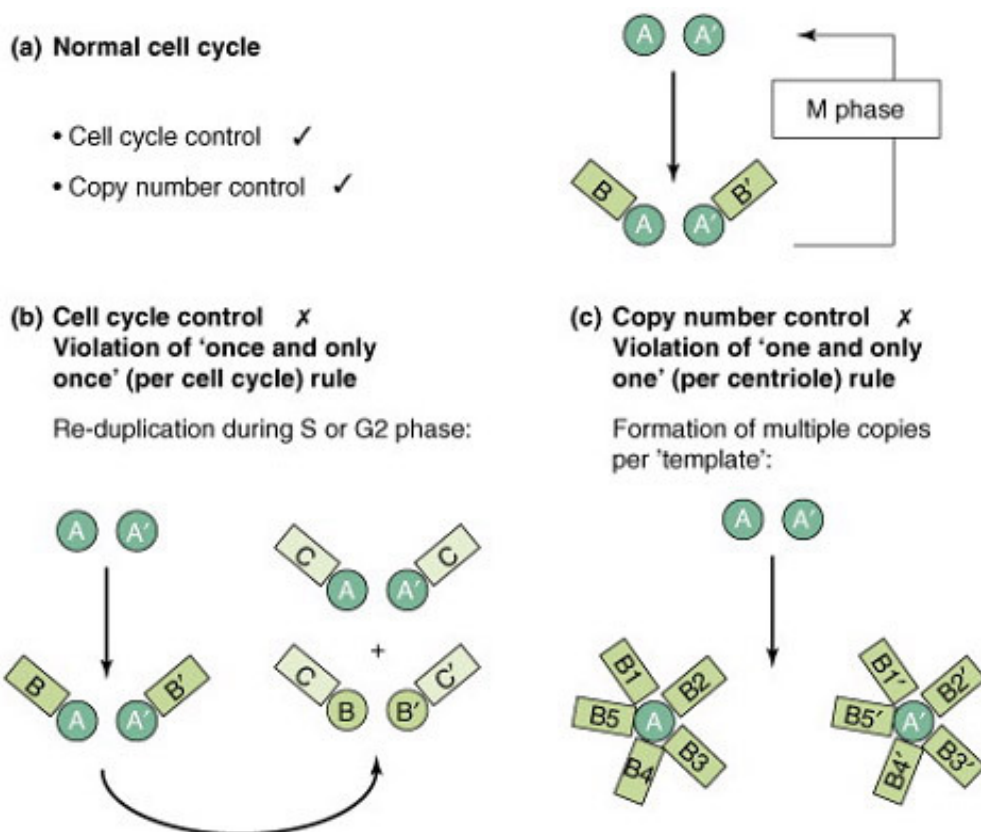
Figure 4. Two rules governing the centrosome cycle.
(a) Centriole duplication in a normal cell cycle involves two centrioles (A and A') giving rise to progeny (B and B'). This process is proposed to be controlled by two mechanisms. (b) The first mechanism imposes cell cycle control and ensures that centriole duplication takes place once and only once per cell cycle. Violation of this 'once and only once' per cell cycle rule results in re-duplication during S or G2 phase, leading to extra centrioles (C and C'). (c) The second mechanism imposes copy number control at each duplication event and limits the formation of pro-centrioles to one per pre-existing

centriole. Violation of this 'one and only one' per centriole rule results in the formation of multiple (pro-) centrioles (B1–B5 and B1'–B5') per template (Nigg, 2007).

Licensing of centriole duplication

Cell fusion studies done by Wong and Stearns proposed a centrosome-intrinsic mechanism that allows duplication in S phase but blocks centriole re-duplication during G2 phase of the cell cycle (Wong and Stearns, 2003). Together with detailed electron microscopic descriptions of the centriole duplication cycle done in the 70s and 80s, these data gave rise to the idea of a 'licensing' model. According to this model, the engagement (meaning the tight orthogonal association) of the new pro-centriole blocks further duplication until disengagement at the end of mitosis licenses the two centrioles for a new round of duplication.

New data obtained by Tsou and Stearns strongly support this 'licensing' model. By studying centriole disengagement and pro-centriole assembly in *Xenopus* egg extracts using purified human centrosomes, activation of the protease separase was found to be required for centriole disengagement. In turn, this event was shown to be critical for the subsequent assembly of new procentrioles (Tsou and Stearns, 2006). Before, separase was already well-known for its role in sister chromatid separation (Uhlmann *et al.*, 2000). At the metaphase to anaphase transition, the 'anaphase-promoting complex/cyclosome' (APC/C), an ubiquitin ligase, is activated and the separase inhibitors securin and cyclin B are targeted for degradation. Subsequently, centromeric cohesin is cleaved by active separase, allowing sister-chromatids to finally separate.

It remains to be determined whether separase acts directly on centrosomes, either by cleaving a centriolar 'glue' that links parental and daughter centrioles or acts indirectly on the centrosome, possibly through regulation of kinase and phosphatase activities that ultimately trigger centriole disengagement.

'De novo' centriole assembly pathways in mammalian cells

The molecular mechanism by which the parental centriole is able to coordinate the assembly of a single daughter centriole perpendicularly to its surface is still unclear. The formation of centrioles and basal bodies has been extensively studied by electron microscopy (Anderson and Brenner, 1971; Brinkley *et al.*, 1967; Chretien *et al.*, 1997; Dippell, 1968; Kuriyama and Borisy, 1981; Mizukami and Gall, 1966; Sorokin, 1968; Vorobjev and Chentsov Yu, 1982). These studies have suggested the existence of two fundamentally distinct assembly pathways. Many ciliated cells, such as those in vertebrate respiratory tracts, can have 200-300 cilia per cell (Figure 5A). It is well established that these large numbers of centrioles are predominantly generated via an acentriolar assembly pathway. These multiple centrioles form around fibrous granules in the cytoplasm termed 'deuterosomes' (Figure 5C). Simultaneously, a minor fraction of basal bodies is still assembled from pre-existing centrioles in these cells which are also capable of assembling multiple pro-centrioles simultaneously (Figure 5B). The simultaneous formation of multiple basal bodies by 'deuterosomes' was attributed to a '*de novo*' assembly mechanism, whereas the duplication of centrioles in proliferating cells was thought to require pre-existing centrioles as 'templates' for the formation of progeny (Beisson and Wright, 2003; Hagiwara *et al.*, 2004).

However, recent experiments have blurred the distinctions between these two pathways and it now appears that pre-existing centrioles act primarily as solid-state platforms to accelerate the assembly process (Khodjakov *et al.*, 2002; La Terra *et al.*, 2005; Rodrigues-Martins *et al.*, 2007; Uetake *et al.*, 2007). In particular, *'de novo'* formation of centrioles was shown to be inducible, at least in certain tumor-derived cell lines like HeLa (Figure 5D), provided that resident centrioles were first removed by laser ablation or microsurgery (La Terra *et al.*, 2005). In these studies, '*de novo* centriole assembly was observed to initiate with the formation of 2-10 centrin-positive aggregates during S phase. When these cells reached mitosis, all centrioles had acquired the typical canonical ultrastructure, were able to organize MTs and duplicate in the subsequent cell cycle. '*De novo'* centriole assembly has also been described in acentriolar cells in *Chlamomonas* and *Drosophila* (Marshall *et al.*, 2001; Peel *et al.*, 2007; Rodrigues-Martins *et al.*, 2007).

Taken together, these studies indicate that the presence of a single centriole is sufficient to inhibit *'de novo'* formation, and that *'de novo'* centriole formation takes place as the cells progress through S phase (La Terra *et al.*, 2005; Marshall *et al.*, 2001). Therefore, regulation of '*de novo'* centriole biogenesis seems similar to the canonical centriole cycle, albeit slower and unable to control the number of generated centrioles - while the presence of pre-existing centrioles restricts the numbers of new pro-centrioles to only one per template. How this 'copy number control' is implemented is presently not known, but the observed restriction, imposed by pre-existing centrioles, may suggest a process in which pro-centriole assembly in close proximity to a pre-existing centriole is kinetically favoured over '*de novo*' assembly in the cytoplasm.
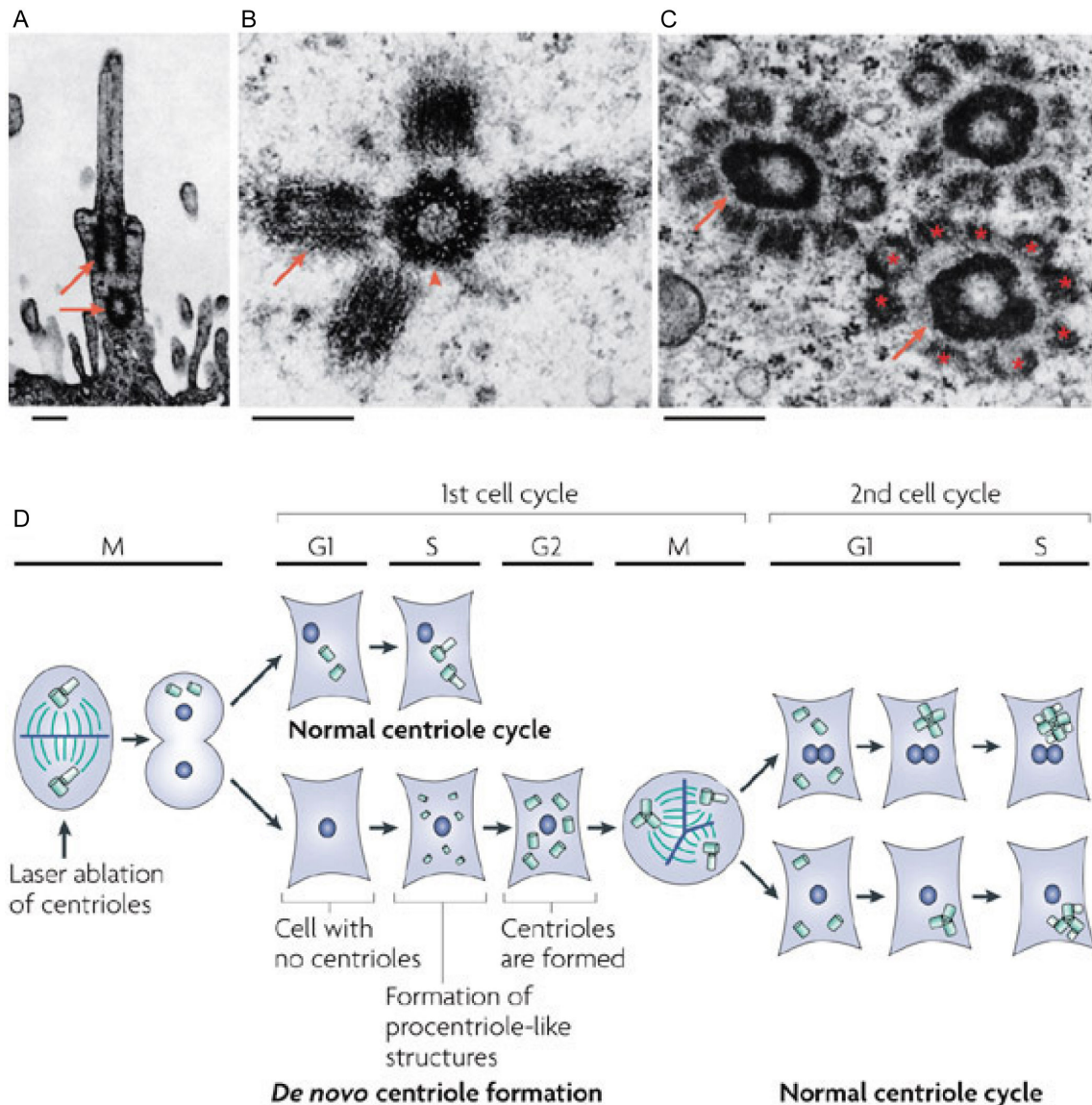
Figure 5. Atypical centriole assembly pathways.

(A) The formation of cilia in a monkey oviduct. One of the two centrioles/basal bodies (red arrows) forms the cilium. (B) Multiple nearly mature basal bodies (arrow) associate with the parental centriole (arrowhead) from a monkey oviduct. (C) Deuterosomes with multiple nascent procentrioles. Scale bar (A-C) 0.25µm. (D) Pedigree of a cell born without centrioles. In cells labelled with centrin-GFP, centrioles in one of the poles of a mitotic spindle were laser-ablated. This cell gives rise to one cell with normal centriole number and another that lacks centrioles. Both continue to progress through the cell cycle with normal kinetics. When the cell without centrioles enters S phase, multiple centrin-aggregates form. These pro-centriolar aggregates transform into morphologically complete centrioles by the time the cell enters mitosis. 'De novo' formed centrioles duplicate as the cell re-enters mitosis and normal centriole cycles resume (Bettencourt-Dias and Glover, 2007).

Templated centriole biogenesis in mammalian cells

A proposed templating model holds considerable appeal for explaining how centriole duplication is initiated by coordinated recruitment of centriolar proteins to the parental centriole wall (Delattre and Gonczy, 2004). Careful electron microscopic studies in mammalian cells have revealed a filamentous corona forming around the proximal walls of parental centrioles and electron-dense material protruding into the proximal half of the elongating centriole (Anderson and Brenner, 1971; Sorokin, 1968). Moreover, a characteristic fibrous structure displaying 9-fold symmetry (termed 'cartwheel') has been proposed to serve as a scaffold for the assembly of centriolar MTs (Figure 6) (Anderson and Brenner, 1971; Beisson and Wright, 2003; Cavalier-Smith, 1974). Interest in this putative scaffolding structure has been refreshed by the recent identification of a cartwheel-associated coiled-coil protein, Bld10p, that plays a crucial role in centriole/basal body assembly in *Chlamydomonas* (Matsuura *et al.*, 2004). Genetic studies in lower eukaryotes such as *Tetrahymena* (Stemm-Wolf *et al.*, 2005) have also convincingly established an essential role for the calcium-binding protein centrin in basal body duplication (reviewed in (Salisbury, 2007)).
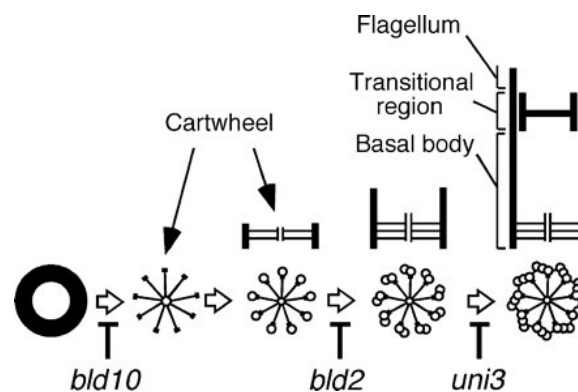
Figure 6. Possible roles of cartwheels and Bld10 in basal body formation.
Schematic diagramm showing the pathway of basal body formation. The bottom row shows the cross-sectional view of basal bodies at the proximal end. The top row shows the longitudinal cross section. The cartwheel appears in an early stage of the assembly process. Microtubules emerge from the cartwheel filament tips and elongate distally during maturation. Bld10p may function in cartwheel assembly, possibly as a component of the cartwheel itself. The black ring in the first step is an amorphous structure appearing at the first step of basal body assembly; for clarity it is omitted in the diagrams of subsequent steps (Matsuura *et al.*, 2004).

The role of centrins and Sfi1p in centrosome duplication

Some proteins essential for centriole duplication are highly conserved throughout evolution. Centrins are a family of small calcium-binding proteins most closely related to the Calmodulin superfamily. First identified in the flagella of green algae, centrins have turned out to be ubiquitous, widely conserved proteins that are closely associated with centriolar structures (or spindle pole bodies) from yeast to human.

The simple MTOC of budding yeast, the spindle pole body (SPB) is a tripartite structure consisting of an outer plaque that anchors γ-tubulin complexes and cytoplasmic MTs, a central plaque that is embedded in the nuclear envelope, and an inner plaque that anchors nuclear γ-tubulin and mitotic MTs (van Kreeveld Naone, 2004). Cdc31p, the centrin homologue in budding yeast, localizes to a specialized area of the nuclear envelope, called the half-bridge, which has a critical role during initiation of SPB duplication (Adams and Kilmartin, 1999). The assembly of a daughter SPB is initiated from a satellite structure at the distal end of the bridge, which forms a duplication plaque on the cytoplasmic side of the bridge (Adams and Kilmartin, 1999). The SPB is then inserted into the nuclear envelope and assembly is completed before the two SPBs separate by cleavage of the bridge, leaving a half-bridge with each new SPB.

Centrin (Cdc31p) has an essential function during SPB duplication as temperature-sensitive mutants arrest with a single large SPB (Byers, 1981; Winey *et al.*, 1991). Cdc31p interacts with three proteins in the half-bridge, Kar1p (Biggins and Rose, 1994; Spang *et al.*, 1995); Mps3p (Jaspersen *et al.*, 2002) and Sfi1p (Kilmartin, 2003) (Kilmartin, 2003). The latter one, Sfi1p, binds multiple centrin molecules along a series of 23 internal conserved repeats (Kilmartin, 2003; Salisbury, 2004). Genetic studies with temperature-sensitive mutants show a requirement for Sfi1p during SPB duplication, cell cycle progression and mitotic spindle assembly. (Anderson *et al.*, 2007; Ma *et al.*, 1999). Recent structural analyses of the Sfi1p-centrin complex and its asymmetric position within the SPB suggest a model for the initiation of SPB duplication (Figure 7), and provide a potential target for licensing this event (Jones and Winey, 2006). Immuno-electron microscopic (EM) localization of the Sfi1p N and C termini showed Sfi1p-centrin filaments spanning the length of the half-bridge with the N terminus localized at the SPB. This suggests that the half-bridge doubles in length by association of the Sfi1p C termini, thereby providing a new Sfi1p N

terminus to initiate SPB assembly (Li *et al.*, 2006). Moreover, the assembly of Sfi1p at the half-bridge might license the SPB for duplication and may itself be regulated via Cdk activity (Jones and Winey, 2006).
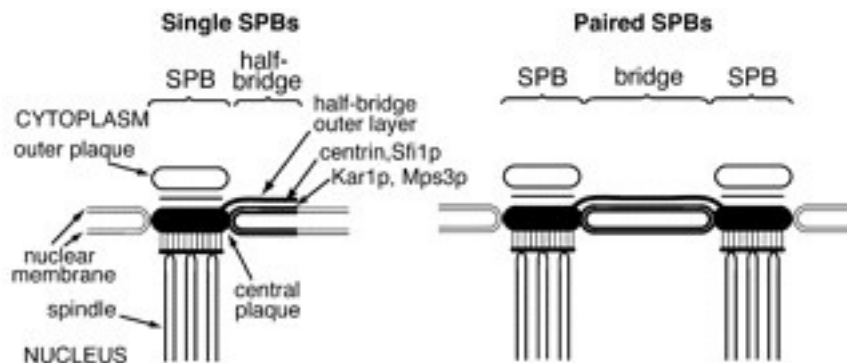
Figure 7. SPB duplication in Yeast.
Diagram of single and paired SPBs showing the location of half-bridge and bridge components. This model of SPB duplication suggests that the Sfi1p N terminus is bound to SPB, whereas the free C terminus recruits another Sfi1p molecule, and subsequently recruites other proteins to the free N terminus and initiates assembly of a new SPB (Li *et al.*, 2006).

Originally, centrins were identified as the major components of several types of calcium-sensitive contractile fibers, such as the nuclear-basal body connectors and the distal striated fibers in unicellular green algae (Huang *et al.*, 1988; Salisbury *et al.*, 1984). Several studies have revealed a role for centrin in the assembly of basal bodies and flagella in lower eukaryotes (reviewed in (Salisbury, 2007)). Although homologous proteins of Sfi1p and centrin are present in human centrosomes (Kilmartin, 2003), it is unclear whether their essential function during centriole/basal body duplication is conserved. However, it is well established that centrin is one of the first proteins to localize at sites of newly forming centrioles, both in the templated and the '*de novo*' assembly pathway (Figure 8) (Khodjakov *et al.*, 2002; Klink and Wolniak, 2001; La Terra *et al.*, 2005).
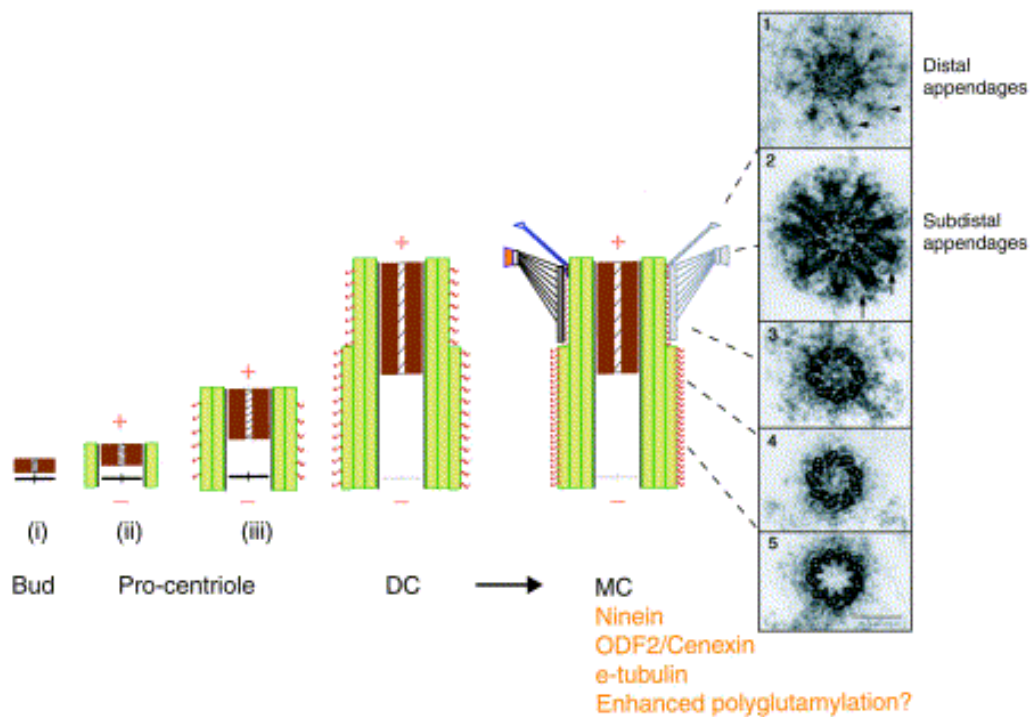
Figure 8. Centriole biogenesis in vertebrate cells.

Pro-centrioles are assembled from a centrin-containing bud (I, in brown) during S phase by growing singlet (ii), doublet (iii) and triplet microtubules (green) which are progressively polyglutamylated (red lines). They transform into fully differentiated daughter centrioles (DC) after centriole disengagement. They further transform into differentiated mother centrioles (MC) during the next cell cycle by aquiring appendages and maturation markers. The proximo-distal differentiation of the MC is demonstrated by serial sections on the right (Bornens, 2002).

Centriole biogenesis in *C. elegans*

The molecular mechanisms of centriole biogenesis in mammalian cells remains poorly understood, but substantial progress has recently been made in invertebrate organisms. In *Caenorhabditis elegans*, a protein kinase, Zyg-1 (O'Connell *et al.*, 2001) and four putative structural proteins, termed Spd-2, Sas-4, Sas-5 and Sas-6 are required for centriole duplication (Delattre *et al.*, 2004; Kemp *et al.*, 2004; Leidel *et al.*, 2005; Leidel and Gonczy, 2003; Pelletier *et al.*, 2004). Moreover, through elegant epistasis experiments and electron tomography, the five proteins could be shown to assemble sequentially on nascent pro-centrioles (Figure 9) (Delattre *et al.*, 2006; Pelletier *et al.*, 2006). After fertilization of the *C. elegans* embryo, Spd-2 was

found to be recruited first to parental centrioles, mediated by cyclin-dependent kinase-2 (Cdk2), and was then required for centriolar localization of the other four proteins. Zyg-1 accumulated next and in turn was required for the subsequent recruitment of Sas-5 and Sas-6. Sas-4 was recruited last. This assembly pathway could be further resolved by remarkable structural studies using electron tomography. These data revealed that upon recruitment of Sas-5 and Sas-6, centriole assembly was initiated by the formation of a central tube. Following the subsequent recruitment of Sas-4, centriolar MTs were then assembled onto the periphery of this central tube.

Sas-4 has been proposed to play a role in controlling centriole length by indirectly regulating protein recruitment and PCM size (Kirkham *et al.*, 2003; Leidel and Gonczy, 2005).
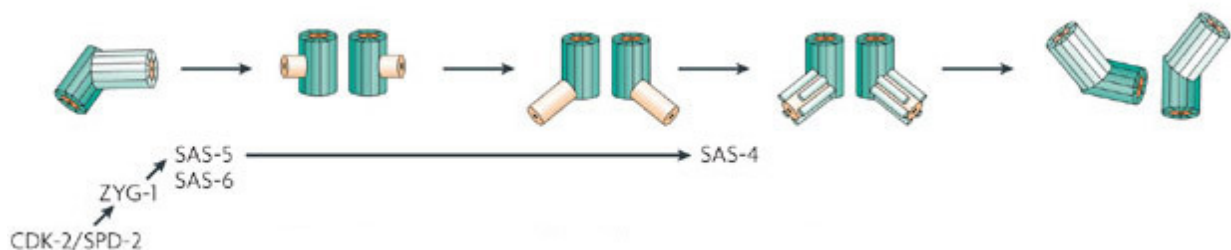
Figure 9. Centriole assembly in *C. elegans*.
Cyclin-dependent kinase-2 (Cdk2) is important for recruiting spindle-defective protein-2 (Spd-2) to the mother centriole. Spd-2 is necessary for the recruitment of Zyg-1, which in turn is important for the recruitment of the Sas-5/Sas-6-complex, which is required for the formation of the inner centriole tube. At a later step, the formation of this tube is essential for the binding of Sas-4, with subsequent production of the surrounding MTs (Bettencourt-Dias and Glover, 2007).

Interestingly, homologues of nematode Sas-4 and Sas-6 are also required for centriole biogenesis in *Drosophila* (Peel *et al.*, 2007; Rodrigues-Martins *et al.*, 2007). It is therefore tempting to speculate that fundamental aspects of centriole biogenesis have most likely been conserved during evolution.

Centriole biogenesis in human cells

As discussed above, Plk4 is a master regulator of centriole duplication in human cells and a possible functional analogue of Zyg-1. According to sequence analyses, Spd-2, Sas-4 and Sas-6 clearly have homologues in human cells, termed Cep192, CPAP (centrosomal P4.1-associated protein or CenpJ) and hSas-6, respectively (Andersen *et al.*, 2003; Hung *et al.*, 2000; Leidel *et al.*, 2005; Leidel and Gonczy, 2005). CPAP has been shown to interact with γ-tubulin and was found in a mass-spectrometric analysis of the centrosome (Andersen *et al.*, 2003; Hung *et al.*, 2000). At that time, it was not known whether CPAP, like Sas-4, is essential for centriole duplication in human cells. However, recent studies in human cells have demonstrated a key role for hSas-6 in this process, as depletion of hSas-6 inhibited centriole duplication whereas overexpression of hSas-6 induced centriole overduplication (Leidel *et al.*, 2005). Furthermore, Plk4 function was found to depend on hSas-6 and CP110 – as depletion of either protein blocked Plk4-induced centriole overduplication (Habedanck *et al.*, 2005). CP110 has been characterized as an *in-vitro* Cdk2 substrate and is required for centriole re-duplication in S phase arrested cells (Chen *et al.*, 2002).

The γ-TuRC, which is required for the nucleation of cytoplasmic MTs, has also been implicated in centriole duplication (Haren *et al.*, 2006; Luders *et al.*, 2006). While Nedd-1/GCP-WD is required for centrosomal localization of the γ-TuRC and maintenance of centriole numbers in human cells, a requirement for γ-tubulin has only been reported in lower eukaryotes (Ruiz *et al.*, 1999). Several other proteins and mechanisms, including Cdk2, CAMKII, SCF- and APC/C-dependent protein degradation have been suggested to play a role during centriole duplication (see Table 1).

Molecule	Organism	Assay	Phenotype	Refs
SAK/Plk4/ Zyg-1	Hs, Dm, Ce	RNAi; mutations Overexpression	No duplication; no re-duplication Amplification	(Bettencourt-Dias *et al.*, 2005); (Habedanck *et al.*, 2005); (Pelletier *et al.*, 2006); (Delattre *et al.*, 2006); (O'Connell *et al.*, 2001); (Rodrigues-Martins *et al.*, 2007); (Peel *et al.*, 2007)
Spd-2	Ce	RNAi; mutations	No duplication; no recruitment of PCM	(Pelletier *et al.*, 2004); (Kemp *et al.*, 2004)
Sas-6-Sas-5	Hs (only Sas-6), Ce	RNAi; mutations Overexpression	No duplication; no re-duplication Amplification	(Leidel *et al.*, 2005); (Dammermann *et al.*, 2004)
Sas-4	Dm, Ce	RNAi; mutations	No duplication	(Leidel and Gonczy, 2003); (Kirkham *et al.*, 2003); (Basto *et al.*, 2006)
Cdk2	Hs, Mm, Xl, Ce	Inhibition (dominant-negative, chemical); RNAi	Duplication can occur in its absence, no re-duplication; defective Spd-2 localization	(Cowan and Hyman, 2006); (Meraldi *et al.*, 1999); (Hinchcliffe *et al.*, 1999); (Duensing *et al.*, 2006)
Centrin/ Cdc31p	Hs, Sp,Sc, Cr, Pt	RNAi; mutations	No duplication (Hs, Sp, Sc); segregation of centrioles affected (Cr); geometry of duplication affected (Pt)	(Paoletti *et al.*, 2003); (Spang *et al.*, 1993); (Ruiz *et al.*, 2005); (Salisbury *et al.*, 2002); (Koblenz *et al.*, 2003)
SFI1	Hs, Sc	RNAi, mutations	No duplication	(Li *et al.*, 2006); (Kilmartin, 2003)
CP110	Hs	RNAi	No re-duplication	(Chen *et al.*, 2002)
Nucleophos-min	Hs	RNAi; inhibition of release from centrosome	Amplification; no duplication	(Budhu and Wang, 2005)
γ-tubulin	Hs, Dm, Ce, Pt, Tt	RNAi, mutations	No duplication (Ce, Hs, Tt); problems in centriolar structure, elongation and separation (Pt, Dm)	(Dammermann *et al.*, 2004); (Dutcher, 2004); (Haren *et al.*, 2006); (Ruiz *et al.*, 1999); (Raynaud-Messina *et al.*, 2004)
Δ-tubulin	Mm, Cr, Pt	Mutations	Doublets are formed (less cells with C-tubules)	(Dutcher, 2003)

ε-tubulin	Xl, Cr, Pt	Mutations; immunodepletion	Shorter centrioles, only singlets, no subsequent duplication; no duplication	(Dutcher, 2003); (Chang et al., 2003)
Bld10	Cr	Mutations	No duplication	(Matsuura et al., 2004)
Cep135	Hs	Inhibition, RNAi Overexpression	Disorganization of MTs Accumulation of particles	(Ohta et al., 2002)
CAMKII	Xl	Inhibition	Blocks early steps in duplication	(Sluder, 2004)
Skp1, Skp2, Cul1, Slimb (SCF-complex)	Mm, Xl, Sc, Dm	Mutations; inhibition	Blocks separation of M-D pairs; blocks re-duplication; increase in centrosome number	(Sluder, 2004); (Wojcik et al., 2000); (Murphy, 2003); (Delattre and Gonczy, 2004); (Fuchs et al., 2004)
p53	Hs	Mutations	Amplification	(Fukasawa et al., 1996) ; (Shinmura et al., 2007)
Separase	Xl	Inhibition	Blocks centriole disengagement	(Tsou and Stearns, 2006)

Table 1. Proteins involved in centriole duplication.

The term 'inhibition' is used here for inhibiting the function of a protein by dominant-negative mutants, chemical compounds or antibodies. 'Re-duplication' refers to centrosome amplification in S phase arrested cells. Ce, *Caenorhabditis elegans*; Cr, *Chlamydomonas reinhardtii*; D, daughter centriole; Dm, *Drosophila melanogaster*; Hs, *Homo sapiens*; M, mother centriole; Mm, *Mus musculus*; Pt *Paramecium tetraurelia*; PCM, pericentriolar material; Sc, *Saccharomyces cerevisiae*; Sp, *Saccharomyces pombe*; Tt, *Tetrahymena thermophila*; Xl, *Xenopus laevis* (Bettencourt-Dias and Glover, 2007).

Centrosome abnormalities and cancer

Theodor Bovery had already proposed a link between centrosome number, chromosome aneuploidy and tumorigenesis based on his observations of abnormal cell divisions in eggs of the nematode *Ascaris megalocephala*. He had observed that supernumerary centrosomes were accompanied by the formation of multipolar spindles and aberrant mitoses (Boveri, 1914; Goepfert, 2004). His proposal that centrosome aberrations might actively contribute to cancer development and

progression has gained renewed interest with the observation that several types of tumor cells exhibit centrosome amplification (Fukasawa *et al.*, 1996; Ghadimi *et al.*, 2000; Lingle *et al.*, 1998; Nigg, 2002; Pihan *et al.*, 1998). However, it remains to be solved whether deregulation of centrosome numbers in tumor cells precedes aneuploidy or whether centrosome amplification is a cause of mitotic errors induced by oncogenic transformation (Nigg, 2002).
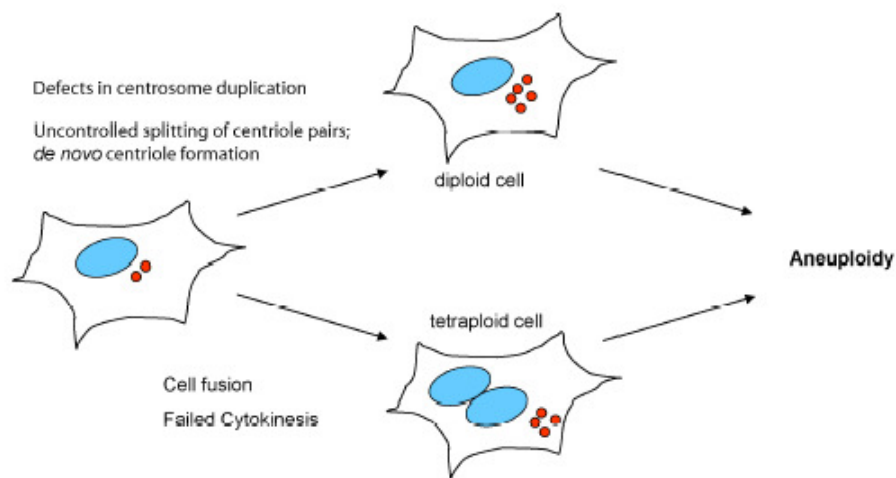
Figure 10. The origins of centrosome amplification.
A schematic diagram showing four pathways for acquiring extra copies of centrosomes. (adapted from (Goepfert, 2004))

In principle, there are four possible mechanisms that allow cells to accumulate supernumerary centrosomes (Figure 10). Additional centrosomes can arise via deregulation of the centriole duplication process, as it has been observed in S phase arrested transformed U2OS and CHO cells. Experimentally, centriole overduplication can be induced by overexpression of hSas-6, Plk4 or human papillomavirus oncoprotein E7 (Duensing et al., 2007a; Habedanck et al., 2005; Leidel et al., 2005). Similarly, multiple centrosomes can be generated '*de novo',* when the inhibitory pre-existing centriole is destroyed by laser ablation (Khodjakov *et al.*, 2002). Supernumerary MTOCs may also be obtained by splitting of centriole pairs or by centrosome fragmentation, induced by the overexpression of some PCM components (Oshimori *et al.*, 2006; Thein *et al.*, 2007). Regardless of the cause, all

these conditions lead to the generation of diploid or tetraploid cells harbouring abnormal centrosome numbers.

Excess centrosome numbers accompanied by polyploidy may result from either cell fusion or cell division failure. The origin of polyploidy may be unrelated to centrosome biology but nevertheless lead to centrosome amplification and result in tumorigenesis (Fujiwara *et al.*, 2005). Apart from numerical centrosome aberrations also structural aberrations effect centrosome function. Upregulated or downregulated microtubule nucleation capacity influences cell shape, polarity and motility of transformed tumor cells (Lingle *et al.*, 2002; Lingle and Salisbury, 2001).

Coalescence of excess centrosomes into two spindle poles in mitosis and into one MTOC during interphase has been reported in polyploid cells with amplified centrosomes (Brinkley, 2001; Rebacz *et al.*, 2007). This 'clustering' mechanism enables transformed cells to survive aneuploidy and to form progeny cells that might be a driving force during tumorigenic transformation and cancer development.

Although centrosome amplification can be cause or consequence of cancers, it is evident that there are several mechanisms existing in untransformed cells that tightly regulate centrosome numbers. Therefore, the centrosome itself or centrosomal related mechanisms e. g. controlling 'centrosomal clustering' may be potential targets of anti-cancer drugs, ideally inducing apoptosis very specifically only in transformed tumor cells.

AIMS OF THIS PROJECT

Plk4, and its potential functional homologue Zyg-1 have been identified as master regulators of centriole duplication in human cells, *Drosophila* and *C. elegans* (Bettencourt-Dias *et al.*, 2005; Habedanck *et al.*, 2005; O'Connell *et al.*, 2001). Furthermore, it was reported that Plk4 overexpression induces centriole overduplication via recruitment of excess electron-dense centriolar material onto the parental centrioles. The aim of this study was, first, to identify which centriolar proteins are excessively recruited upon Plk4 overexpression, second, to determine whether this protein recruitment indeed induces the assembly of complete centrioles and, based on this hypothesis, to analyze human centriole biogenesis at a molecular level. It remained to be solved whether the function of key proteins like Spd-2, Zyg-1, Sas-4 and Sas-6 is conserved from *C. elegans* to human and whether the potential cartwheel protein Bld10 has a functional human homologue. This study should also address the question of whether centrins and Sfi1p are as important for human centriole biogenesis as they are for SPB duplication in yeast.

RESULTS

In the first section, polyclonal antibodies specific for hSfi1, Cep135 and CPAP will be characterized. These antibodies were then used to perform initial biochemical analyses of the endogenous proteins in human cells. In the second section, Plk4-induced centriole biogenesis will be analyzed in human cells by diverse 'high-resolution based microscopic techniques', with a specific focus on the roles of Plk4, hSas-6, CPAP, Cep135, CP110, centrin and hSfi1 in centriole assembly. Following on these results, an additional function of CP110 in the maintenance of centriole morphology will be presented in the third section.

1. Initial biochemical characterization of the centrosomal proteins hSfi1, Cep135 and CPAP

Production of polyclonal anti-hSfi1 antibodies

Sequence analyses have identified potential Sfi1p homologues in various organisms including yeast, *Chlamydomonas* and human (Keller et al., 2005; Kilmartin, 2003). However, not much is known about the function of Sfi1 in human cells, except for its association with human centrin 2 and 3 (Kilmartin, 2003; Li *et al.*, 2006). In order to study the potential role of hSfi1 in human centriole duplication, a polyclonal rabbit antibody was raised against a C-terminal fragment of recombinant hSfi1 (aa 1101-1211, variant b). It has been reported that two splice variants of hSfi1p are expressed in human cells, differing only in the presence (variant a, 1242aa) or absence (variant b, 1211aa) of a short insertion of 31 amino acids at position 385 (Kilmartin, 2003). Therefore, the antigen used for generating the polyclonal antibody comprised a short coiled-coil region in the very C-terminal part and a short stretch of the more upstream located centrin-binding domain (Figure 11). Therefore, anti-hSfi1 antibodies target both hSfi1 isoforms.
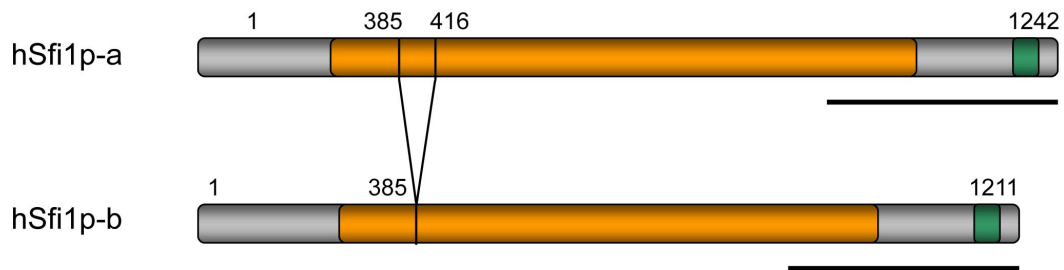
Figure 11. Schematic representation of human hSfi1 (variant a and b).
The centrally located centrin-binding domain is illustrated in orange. A short coiled-coil region has been identified at the very C terminus (green). Sequences used as antigens for antibody generation are indicated below in black.

Reactivity of this antibody was examined by Western blot analysis (Figure 12). Anti-hSfi1 antibodies recognized several bands in total lysates of U2OS, RPE-1, 293T and HeLaS3 cells. In agreement with the expected expression of two isoforms, a closely spaced double band at the size of ~120 kDa was recognized in isolated centrosomes purified from KE37 T-lymphoblastoid cells (Figure 12, arrow). Both hSfi1 isoforms could be specifically isolated from HeLaS3 cells via immunoprecipitation using purified anti-hSfi1 antibodies, demonstrating that additional bands detected in total cell lysates are most probably unspecific. Finally, antibody specificity was confirmed by siRNA. Depletion of hSfi1 in HeLaS3 cells using siRNA duplexes targeting both isoforms resulted in a complete loss of hSfi1 protein from total cell lysates.
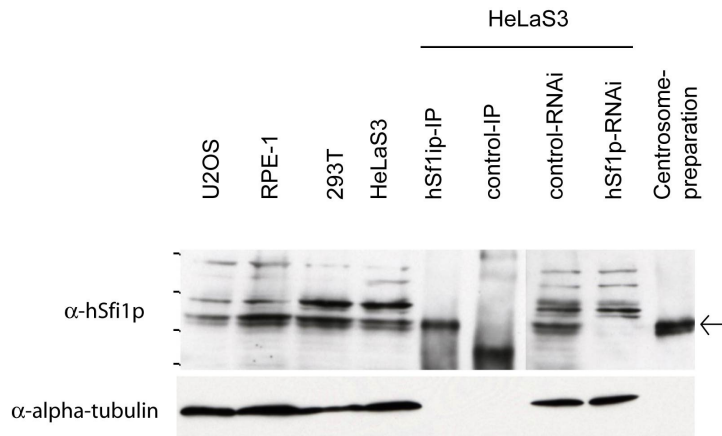
Figure 12. Specificity of anti-hSfi1 antibodies.

Purified antibodies directed against hSfi1 were tested on Western blots using total cell lysates of U2OS, RPE-1, 293T, HeLaS3 cells and centrosome preparations from KE37 cells. Antibody specificity was confirmed by efficient protein depletion upon siRNA treatment and by immunoprecipitation of endogenous hSfi1 from HeLaS3 cells. Blotting against α-tubulin illustrates equal loading. Marker bands indicate 250kDa, 150kDa, 100kDa and 75kDa.

Abundance of endogenous hSfi1 during the cell cycle

Subsequently, hSfi1 protein expression was analyzed throughout the cell cycle. Expression of hSfi1 mRNA and hSfi1 protein was determined in synchronized total lysates of HeLaS3 cells (Figure 13). As determined by qRT-PCR, hSfi1 mRNA levels were low during G1 and late S phase but peaked at the beginning of S phase and in mitosis, reaching a ~4-fold increase when compared to G1 (Figure 13A and B). Interestingly, the protein levels of hSfi1 when analyzed by Wester blot did not reflect this fluctuation (Figure 13C). Protein levels of both isoforms appeared constant during the cell cycle. It is also noteworthy that no obvious mobility shift could be detected for either isoform as the cells progressed through the cell cycle.
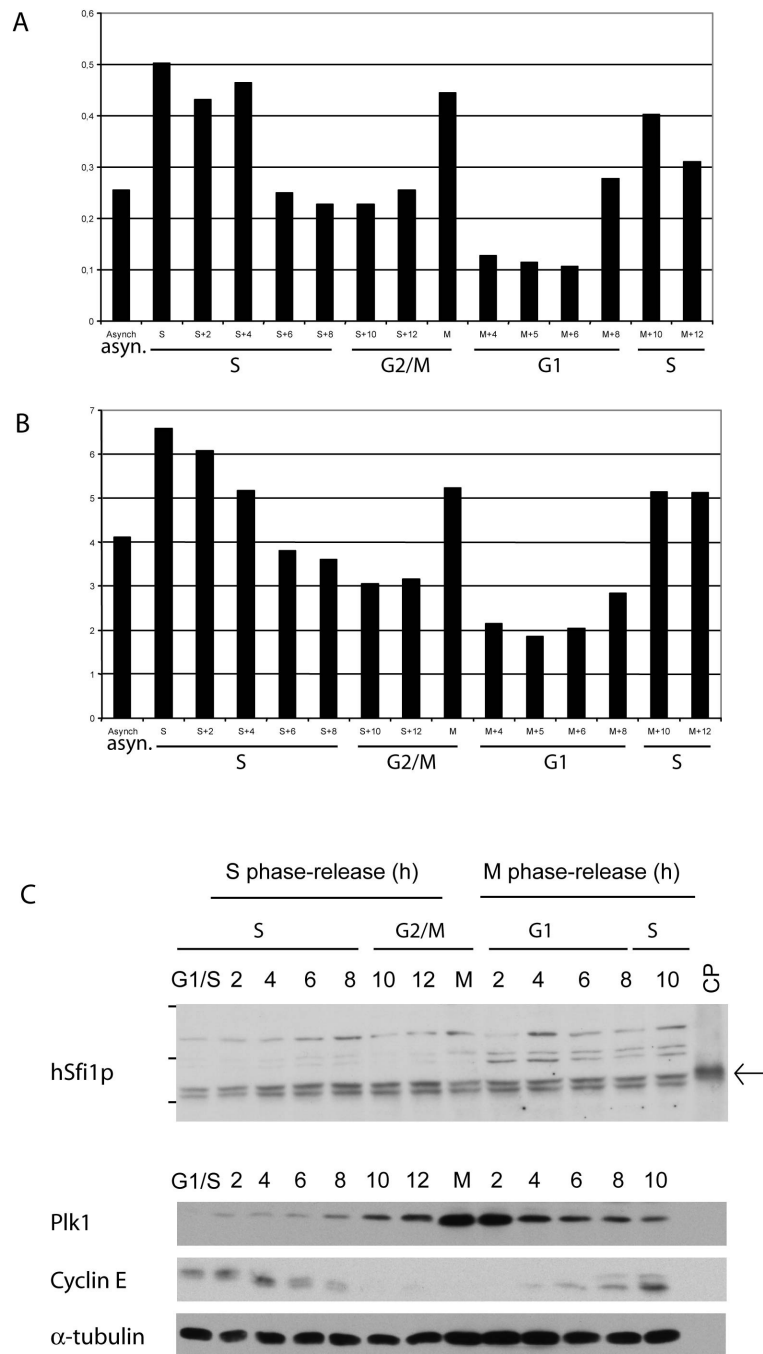
Figure 13. hSfi1 expression during the cell cycle.

(A, B) hSfi1 variant a (A) and variant b (B) mRNA levels across the cell cycle were determined in synchronized HeLaS3 cells, using qRT-PCR (see methods). (C) hSfi1 protein (arrow) levels throughout the cell cycle. HeLaS3 cells were arrested at the G1/S boundary by a double thymidine block or in M phase by a thymidine block followed by nocodazole treatment and release into fresh medium. Samples were harvested at the indicated time points and subjected to immunoblotting, using the antibodies indicated. CP: centrosome preparations from KE37 cells. Marker bands indicate 250kDa, 150kDa and 100kDa.

Identification of proteins interacting with hSfi1 and centrin

Whereas Spc110p has been identified as an interacting protein of Cdc31p and Sfi1p in yeast (Kilmartin, 2003), only very little is known about putative interaction partners for Sfi1 and centrins in human cells. HSfi1 and CP110, were both reported to interact with human centrin, while for hSfi1 there are no other interaction partners reported than centrin (Kilmartin, 2003; Tsang *et al.*, 2006).

In an unbiased approach to identify new centrosomal interaction partners, immunocomplexes were isolated from 293T cells using anti-hSfi1-and anti-centrin antibodies (20H5), respectively (Figure 14). These were separated by SDS-PAGE, stained with Coomassie Blue and analysed by mass-spectrometry (kindly performed by A. Ries, Max-Planck Institute of Biochemistry, Martinsried). Specific bands as well as some regions of unstained SDS-PAGE gel between prominently stained bands were investigated since these might contain low abundance proteins. As expected, endogenous hSfi1 was found to co-precipitate with both centrin 2 and 3, and vice versa. Additionally, both hSfi1 and centrins pulled down the DNA damage binding protein 1 DDB1 (Dualan *et al.*, 1995), ubiquitin and different ubiquitin-related proteins. HSfi1 co-precipitated with a hypothetical ubiquitin ligase (P534), and centrin with another hypothetical ubiquitin activating enzyme E1. Other proteins were specifically co-precipitated with one but not the other protein. SUMO-2, a small putative centrosomal protein (FLJ14346) and a protein termed FLJ34068 were found in hSfi1-precipitates only, while XPC (Araki *et al.*, 2001; Charbonnier *et al.*, 2006; Nishi *et al.*, 2005; Popescu *et al.*, 2003; Thompson *et al.*, 2006; Yang *et al.*, 2006) and Importin beta were exclusively found in immunoprecipitates performed with anti-centrin antibodies. Interestingly, FLJ34068 is highly similar to the regulatory subunit p65 of the protein phosphatase PP2A. Perhaps most strikingly, all components of the γ-tubulin ring complex (TuRC), namely γ-tubulin (GCP-1), GCP-2, -3, -4, -5, -6 could be identified in hSfi1 immunoprecipitates.
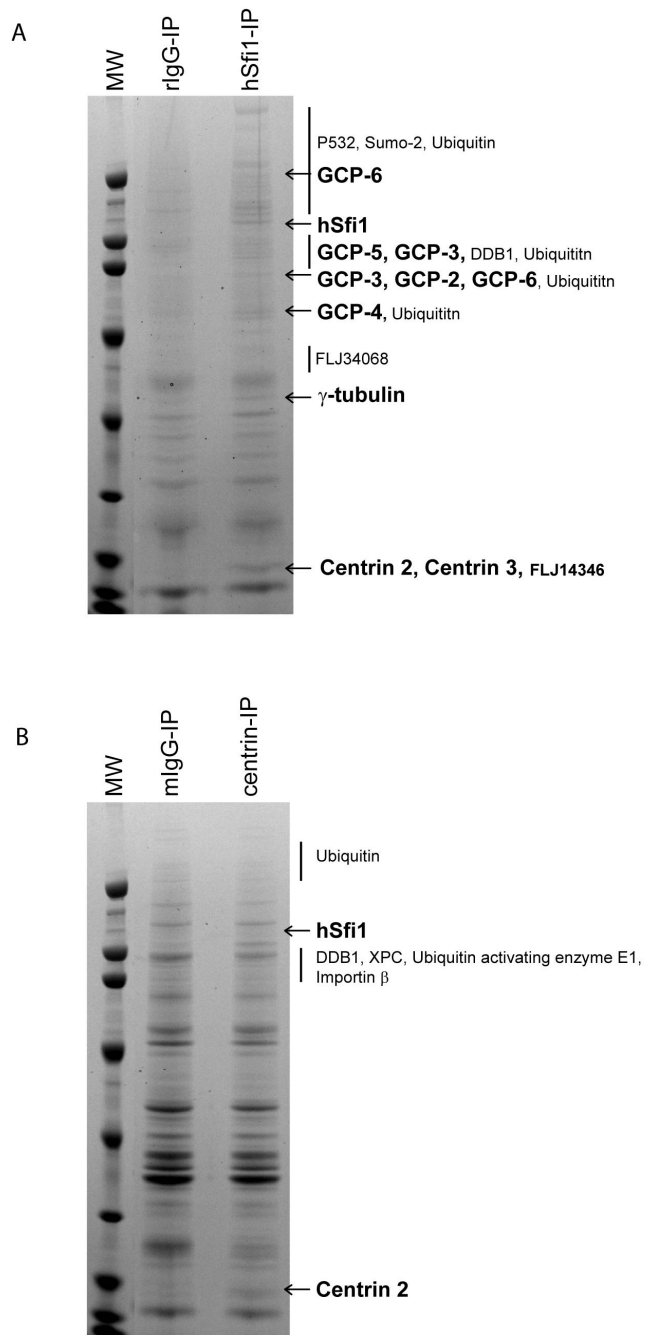
Figure 14. Mass-spectrometric analysis of hSfi1 and centrin-immunocomplexes.

Endogenous hSfi1 (A) and centrin (B) was immunoprecipitated with anti-hSfi1- and anti-centrin antibodies, respectively. After separation by SDS-PAGE and staining with Coomassie Blue, the bands and regions indicated were excised and analyzed by mass-spectrometry. Unspecific mouse and rabbit IgGs were used as controls. Marker bands (MW) indicate 205kDa, 116kDa, 97kDa, 66kDa, 45kDa, 29kDa and 20kDa.

Co-precipitation of hSfi1 with centrin 2/3 and γ-tubulin, GCP-2, -3, -4 were confirmed by Western blots (Figure 15). Further work will be required to investigate the potential physiological relevance of the interaction between hSfi1 and the γ-TuRC or a potential link to the ubiquitin-dependent degradation machinery.
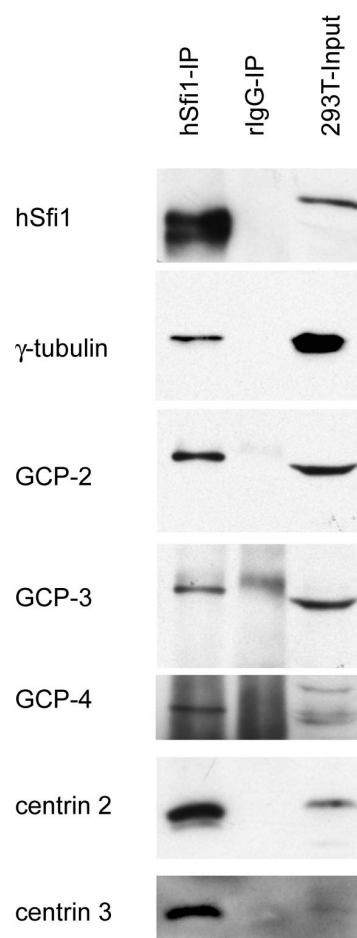
Figure15. Interaction of hSfi1 with γ-tubulin, GCP-2, -3, -4, centrin 2/3.
HSfi1 immunoprecipitates were isolated using anti-hSfi1 antibodies, separated by SDS-PAGE and analyzed by immunoblotting using the antibodies indicated. Unspecific rabbit IgGs were used as control.

Production of polyclonal anti-Cep135 and anti-CPAP antibodies

To study the centrosomal proteins Cep135 and CPAP in human cells, polyclonal antibodies were raised against C-terminal fragments of recombinant proteins (Figure 16). Antibody specificity was analyzed by Western blot analysis (Figure 17) and the abundance of endogenous Cep135 and CPAP was analyzed in a cell cycle profile (Figure 18 and 19).
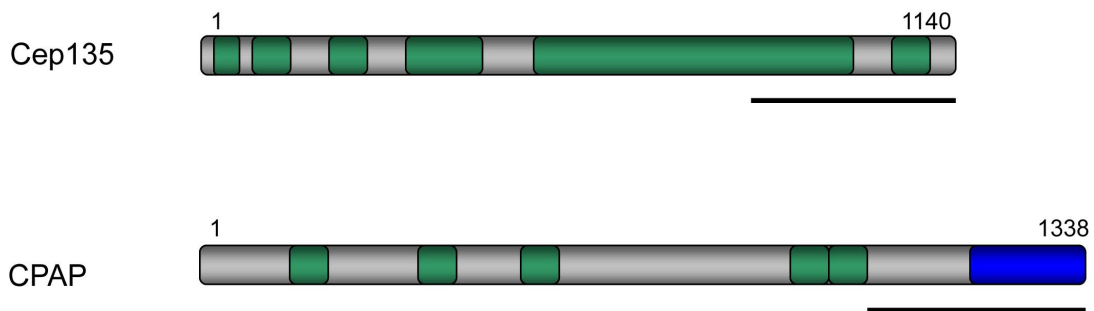
Figure 16. Schematic representation of human Cep135 and CPAP.
Coiled-coil regions are illustrated in green and a G-Box motive (CPAP, (Hung *et al.*, 2000)) is indicated in blue. Domains used as antigens for antibody generation are indicated below in black.

In agreement with the predicted protein size, anti-Cep135 antibodies recognized one major band of ~130 kDa in total lysates of U2OS, RPE-1, 293T and HeLaS3 cells and in isolated centrosomes (Figure 17). This band could also be detected in an immunoprecipitation of endogenous protein from HeLaS3 cells using anti-Cep135 antibodies (see lane 5). Interestingly, another minor band of ~90 kDa was additionally pulled down. It is tempting to speculate that this represents a shorter and less abundantly expressed isoform of Cep135 as this band can also be detected in isolated centrosomes. Finally, antibody specificity was confirmed by siRNA. The depletion of Cep135 in HeLaS3 cells resulted in a reduction of Cep135 protein levels (both the major and the minor band – data not shown) in total cell lysates.

Similarly, anti-CPAP antibodies recognized a band of ~160 kDa in total lysates of U2OS, RPE-1, 293T and HeLaS3 cells and in isolated centrosomes purified from KE37 cells. This band could also be detected in an immunoprecipitation of

endogenous protein from HeLaS3 cells using anti-CPAP antibodies. Unfortunately, detection of endogenous CPAP on cell lysates and the isolation of CPAP immunoprecipitates was less efficient than for Cep135. This might be due to low protein abundance or to limited accessibility of the antigenic region. Nevertheless, antibody specificity could be confirmed by siRNA, as the depletion of CPAP in HeLaS3 cells resulted in a loss of CPAP reactivity in total cell lysates. It is noteworthy, that additional bands of various sizes were pulled down in immunoprecipitates using anti-CPAP antibodies. It still needs further analysis if these bands are specifically recognized by anti-CPAP antibodies and therefore might represent different CPAP isoforms or degradation products, or, alternatively, CPAP associated proteins. Considering that anti-CPAP antibodies recognize a major unspecific band of ~ 80 kDa, that is absent in centrosome preparations but persists after CPAP-depletion, it is possible that anti-CPAP antibodies also react unspecifically in immunoprecipitations.
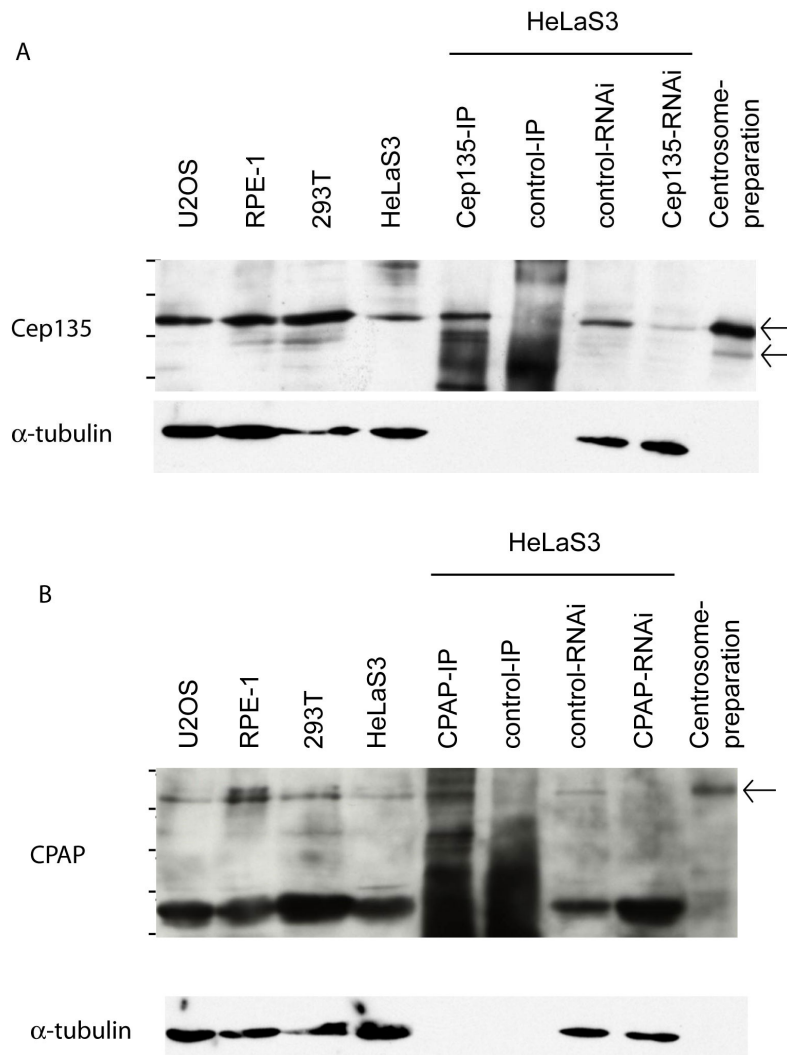
Figure 17. Specificity of Cep135 and CPAP antibodies.

Purified antibodies directed against Cep135 (A) and CPAP (B) were tested on Western blots using total cell lysates of U2OS, RPE-1, 293T, HeLaS3 cells and centrosome preparations from KE37 cells. Antibody specificity was confirmed by efficient protein depletion upon siRNA treatment and by immunoprecipitation of endogenous Cep135 or CPAP from HeLaS3 cells. Blotting against α-tubulin illustrates equal loading. Marker bands indicate 250kDa, 150kDa, 100 kDa, 75kDa (and 50kDa).

Abundance of endogenous Cep135 and CPAP during the cell cycle

Cep135 and CPAP protein expression during the cell cycle was analyzed in HeLaS3 cells, both at the RNA- and at the protein level. As determined by qRT-PCR and Western blotting, both Cep135 mRNA- and protein levels showed little change during the cell cycle (Figure 18).
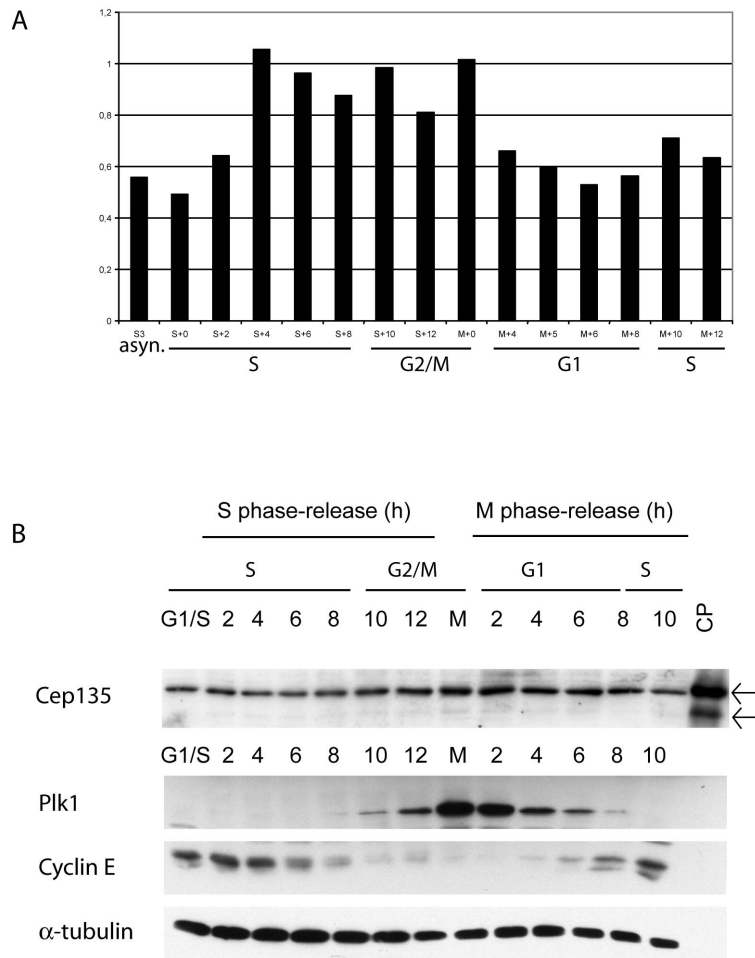
Figure 18. Cep135 expression during the cell cycle.
(A) Cep135 mRNA levels across the cell cycle were determined in synchronized HeLaS3 cells, using qRT-PCR (see methods). (B) Cep135 protein levels throughout the cell cycle. HeLaS3 cells were arrested at the G1/S boundary by a double thymidine block or in M phase by a thymidine block followed by nocodazole treatment and release into fresh medium. Samples were harvested at the indicated time points and subjected to immunoblotting, using the antibodies indicated.

CPAP mRNA levels showed moderate fluctuation during the cell cycle, peaking in early S phase and again in mitosis (Figure 19A). A slight increase in CPAP protein level upon entry into mitosis could also be observed on Western blots (Figure 19B). This slight increase was most obvious comparing the 10h- and 12h-samples after S phase release, where the total protein amounts are definitely comparable, whereas other mitotic samples appear to contain slightly more total

protein (see α-tubulin, loading control). Interestingly, CPAP appears to be slightly upshifted during mitosis and potential posttranslational modifications on CPAP are under current investigation in our lab.
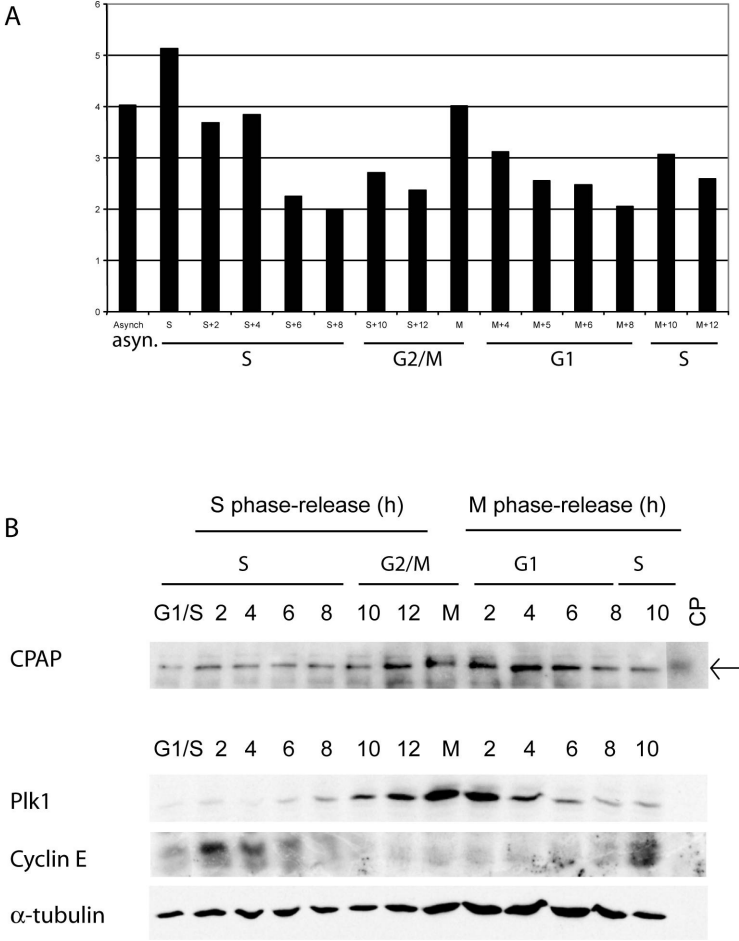
Figure 19. CPAP expression during the cell cycle.

(A) CPAP mRNA levels across the cell cycle were determined in synchronized HeLaS3 cells, using qRT-PCR (see methods). (B) CPAP protein levels throughout the cell cycle. HeLaS3 cells were arrested at the G1/S boundary by a double thymidine block or in M phase by a thymidine block followed by nocodazole treatment and release into fresh medium. Samples were harvested at the indicated time points and subjected to immunoblotting, using the antibodies indicated.

2. Plk4-induced centriole biogenesis in human cells

In the second and main section of this work, Plk4-induced centriole biogenesis will be described in detail by high-resolution immunofluorescence microscopy (IF) and electron microscopy (EM). This study focused specifically on the centriolar proteins hSas-6, CPAP, Cep135, γ-tubulin, CP110, centrin and hSfi1. Moreover, a new technique, termed 3dSIM, will be introduced as a powerful tool to study centriole assembly in future experiments.

Cell cycle regulation of Plk4-induced centriole biogenesis

Plk4 has been identified as a master regulator of centriole biogenesis in human cells and in *Drosophila* (Bettencourt-Dias *et al*., 2005; Habedanck *et al*., 2005). Most strikingly, excess Plk4 activity induced excessive recruitment of centriolar material to the parental centrioles (Habedanck *et al*., 2005).

To determine whether overexpression of Plk4 in human cells is capable of triggering the formation of multiple complete centrioles, we generated a cell line that allows the temporally controlled expression of this kinase and examined centriole formation during cell cycle progression. As centrin constitutes an excellent marker for centriole formation in human cells (Bornens, 2002; Paoletti *et al*., 1996), anti-centrin antibodies (Baron *et al*., 1992) were used to monitor centriole assembly in these experiments (Figure 20).

Already 16h after Plk4 induction, approximately 70% of asynchronously growing cells showed evidence of centriole amplification. They either displayed multiple scattered centrioles or multiple pro-centrioles arranged around each parental centriole, reminiscent of the petals of a flower (Figure 20A). Interestingly, flower-like structures could only be detected in Cyclin A-positive S and G2 phase cells (upper row), but not in Cyclin A-negative G1 cells, which instead contained multiple centrioles that appeared to be disengaged (lower row). Flower-like structures persisted during early stages of mitosis but then began to disassemble during late telophase (Figure 20B), consistent with the view that the disengagement of newly formed centrioles from parental centrioles occurs during exit from mitosis (Tsou and Stearns, 2006). These data demonstrate that overexpression of Plk4 induces the assembly of multiple pro-centrioles during S phase. These then elongate during G2

and persist in an engaged state with their parental centrioles until disengagement at the end of mitosis causes centriole scattering.
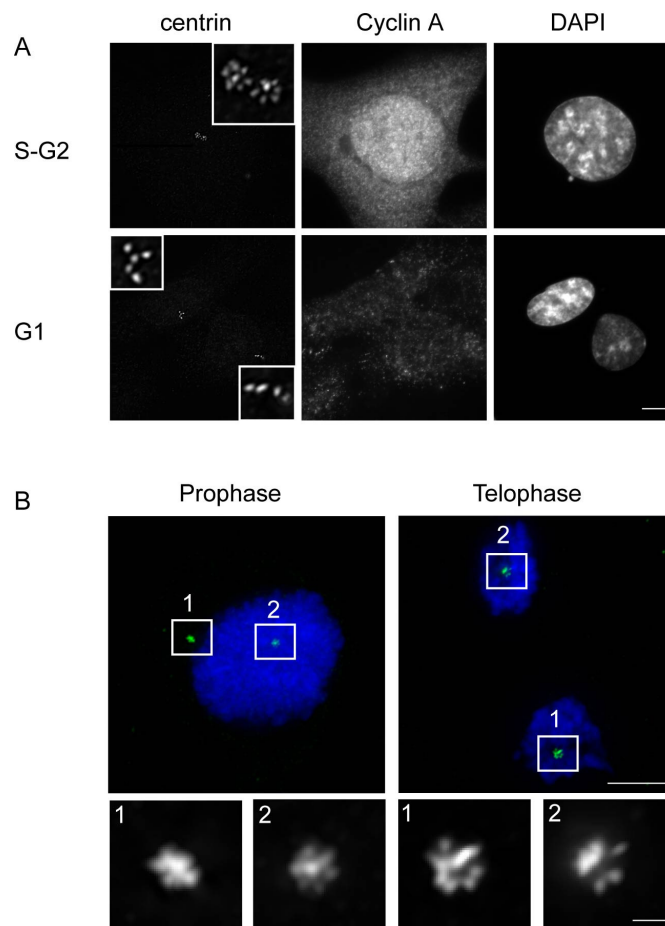
Figure 20. Plk4-induced centriole biogenesis during cell cycle progression.
Myc-Plk4 expression was induced for 16h in asynchronously growing U2OS cells before they were fixed and analyzed by immunofluorescence microscopy, using the antibodies indicated. (A) Interphase cells co-stained for centrin (20H5) and Cyclin A to indicate cell cycle position, and DNA (DAPI). Note that Cyclin A-positive cells (in S or G2 phase; upper row) show multiple centrioles in a flower-like arrangement, whereas Cyclin A-negative cells (in G1; lower row) show scattered (disengaged) centrioles. Insets show enlarged views of centriole 'flowers' and clusters, respectively. (B) Mitotic cells co-stained for centrin (rabbit antibody) and DNA (DAPI). Upper panels show overviews of representative prophase and telophase cells; lower panels show higher magnifications of the two poles in each cell to visualize flower-like structures. Scale bars indicate 10μM and 1μM (higher magnifications).

Simultaneous assembly of multiple pro-centrioles in G1/S

We next asked whether the ability of Plk4 to induce the formation of multiple centrioles is regulated during the cell cycle and whether multiple pro-centrioles develop simultaneously or sequentially. After release from a nocodazole block in M phase, cells had to be incubated for 10-12 hours before flower-like structures could be seen (data not shown). In contrast, cells that were synchronized and held at the G1/S transition by aphidicolin responded to Plk4 induction by 'flower' formation within 1-3 hours (Figure 21A). This indicates that cells need to reach a permissive cell cycle window (G1/S transition and early S phase) before they can respond to Plk4 activity. When using centrin staining as a marker for centriole assembly, the first visible evidence for Plk4-induced pro-centriole formation was the formation of a halo (or ring) around each parental centriole (see Figure 21B, 1h-Halo). Within these halos, a more intensely staining region could occasionally be discerned, suggesting that the one pro-centriole existing already at the onset of these experiments persisted on the parental centrioles. Halo formation could be seen in a significant fraction of cells already after 1 hour of Plk4 induction and was essentially complete after 3 hours (Figure 21A). At later times, each halo progressively resolved into a number of discrete nascent pro-centrioles. These new pro-centrioles appeared with very similar kinetics, indicating that they formed nearly simultaneously. A quantitative analysis of flower-like structures 16 hours after Plk4 induction revealed that most of them contained 6 centrin-positive pro-centrioles, although some variation in number could be seen (Figure 21B). The limited spatial resolution of these experiments masks the exact events occurring during the conversion of a halo structure to individualized pro-centrioles, but analysis of the radial spacing of nascent pro-centrioles indicates that these structures formed randomly with regard to the circumference of the parental centriole (Figure 21B).
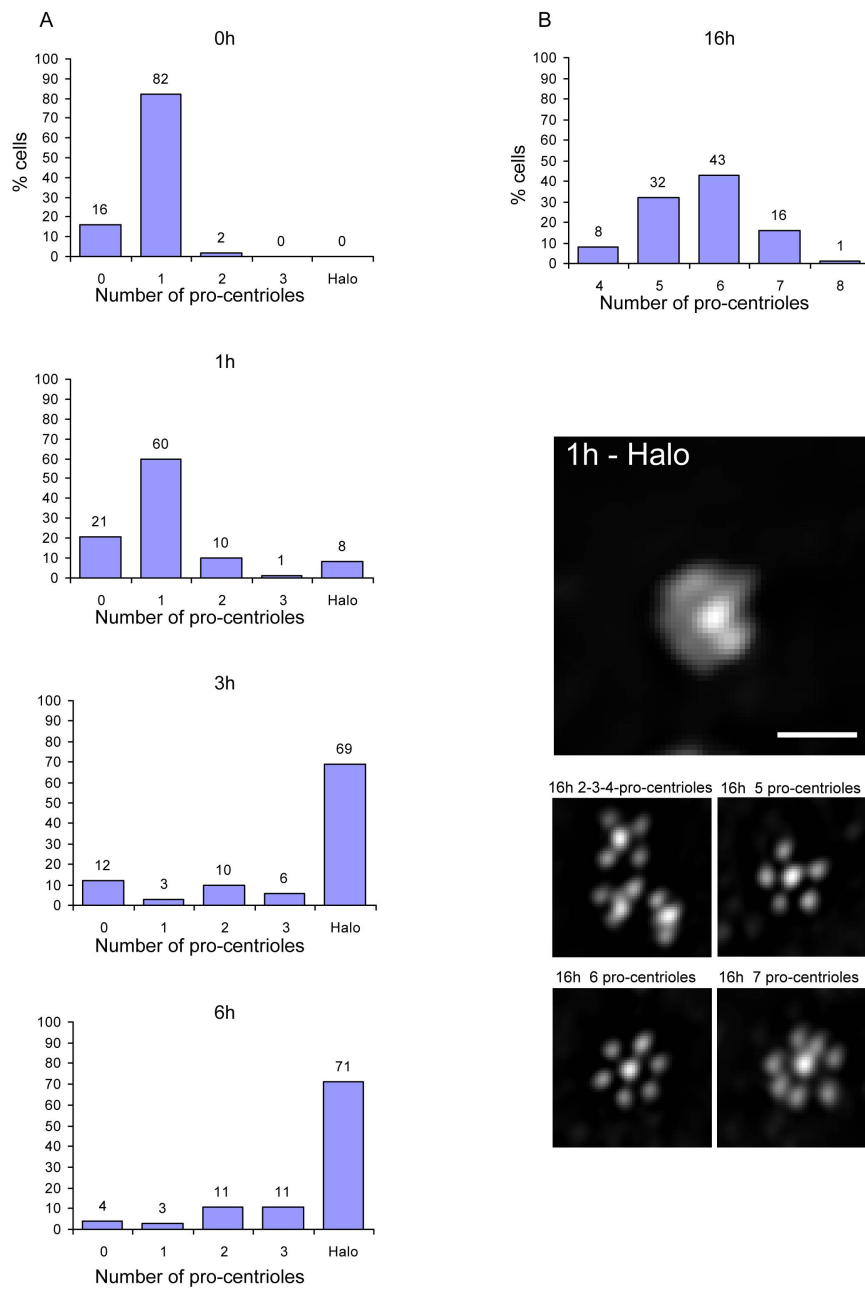
Figure 21. Multiple pro-centrioles form simultaneously in S phase.

Cells were synchronized by aphidicolin treatment for 24h before Myc-Plk4 expression was induced for 1h, 3h, 6h (A) and 16h (B) and pro-centriole formation was visualized using anti-centrin 2 staining. Histograms in A and B summarize, for each indicated time point, the percentages of cells showing a halo surrounding each parental centriole or the indicated numbers of pro-centrioles, respectively. At each time point 100 cells were analyzed. Centrin stainings (B) are shown to illustrate the appearance of a typical halo (1h) as well as flower-like structures with 2-7 pro-centrioles (16h). Note that the flower-like structures harbouring 2, 3 and 4 centrioles were taken from a cell that fortuitously contained 3 parental centrioles. Scale bars denote 1µM.

Identification of key proteins in centriole assembly

Our ability to control centriole biogenesis by induction of Plk4 provided a unique opportunity for studying the assembly process in time and space. To identify centrosomal proteins required for Plk4-induced centriole biogenesis, we first depleted nearly 30 candidate proteins (Andersen *et al.*, 2003) by siRNA before inducing Plk4 expression and examining (pro-)centriole formation by immunofluorescence microscopy (Figure 22). To discriminate between pro-centriolar intermediates and mature centrioles, all cells were co-stained with antibodies against centrin 2 and polyglutamylated tubulin, as markers for nascent centrioles and stable MTs typical of mature centrioles, respectively (Bornens, 2002). Results illustrated in histogramm A show the percentage of Plk4-induced centriole 'flowers'. Compared to control (GL2-treated) cells, a drastic ($\geq$ 50 %) reduction in the formation of flower-like centriole structures was seen upon depletion of hSas-6, CPAP, Cep135, and CP110. To the extent that antibodies were available, successful depletion was assessed by immunofluorescence microscopy (black bars). In all other cases, qRT-PCR was used to determine transcript levels (grey bars). These analyses indicated that different transcripts were depleted to different levels (see Table 2). Therefore, it is possible that additional proteins required for centriole biogenesis have escaped detection in the above screen. For example, it is surprising that the above analysis revealed no requirement for Cep192 in centriole duplication, even though a putative invertebrate homologue of this protein (Spd-2 of *Caenorhabditis elegans*) is clearly required for initial centriole duplication after fertilization (Kemp *et al.*, 2004; Pelletier *et al.*, 2004). Whether this implies that human Cep192 is not required for centriole duplication in somatic cells or whether this negative result reflects incomplete depletion remains to be addressed in future studies. Taken together, this siRNA screen identified hSas-6, CPAP (the putative homologue of *C. elegans* Sas-4), Cep135 and CP110 as being indispensable for centriole biogenesis.
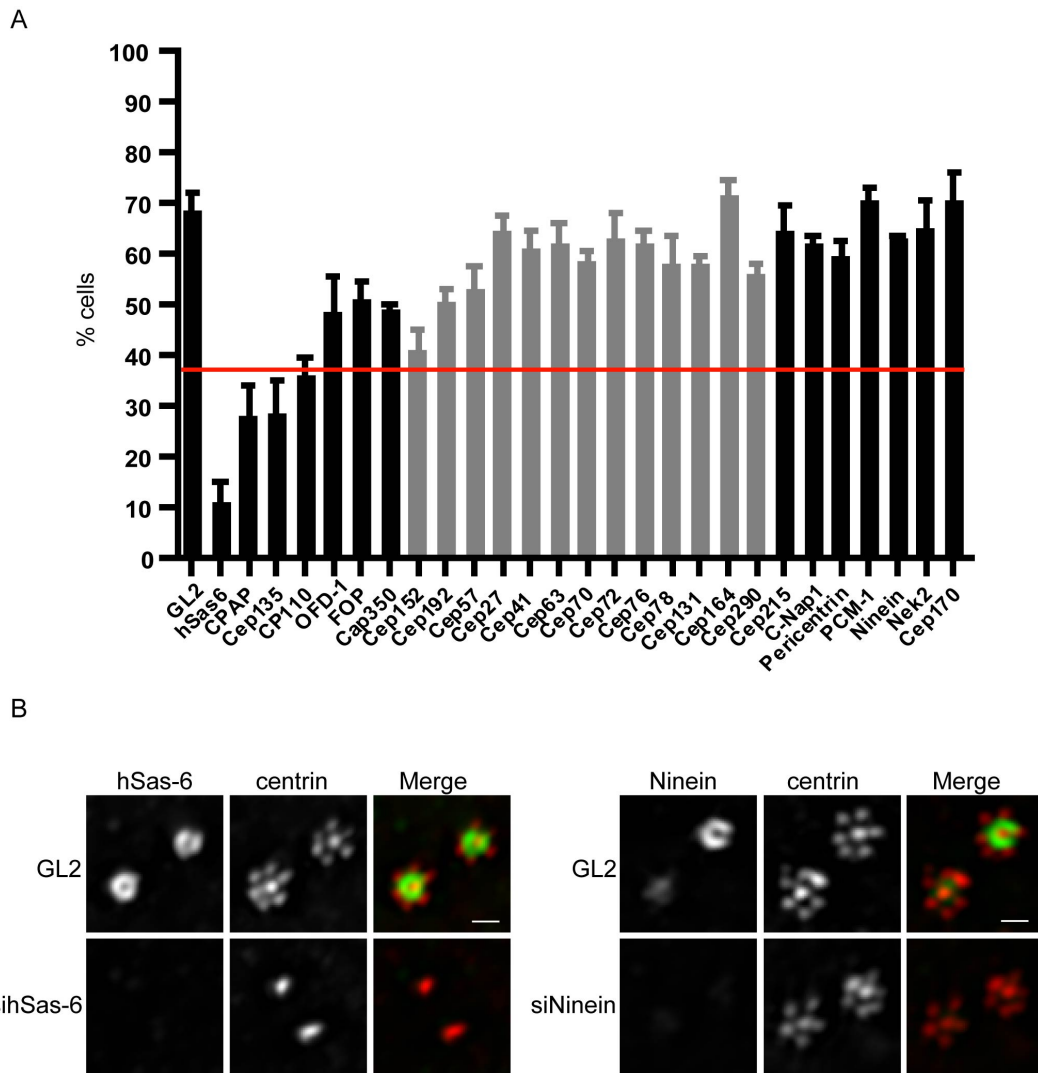
Figure 22. siRNA screen for proteins involved in centriole biogenesis.
U2OS cells were treated for 48 hours with siRNA duplexes targeting the indicated centrosomal proteins, before Myc-Plk4 overexpression was induced for 16h and cells were analyzed by immunofluorescence microscopy. (A.) Histogram illustrating the percentages of cells showing Plk4-induced centriole 'flowers'. Results are from 3 independent experiments (n=100, each), bars indicate standard deviations. (B) Two representative examples of the results shown. Note that anti-centrin staining revealed strong inhibition of pro-centriole formation upon depletion of hSas-6, whereas depletion of ninein did not affect pro-centriole formation. Scale bar 1µM.

Localization of key proteins in centriole assembly

High-resolution immunofluorescence microscopy was then used to determine at what stages the above proteins contribute to centriole assembly. Following induction of Plk4, nascent flower-like structures as well as disengaged multiple centrioles were stained with antibodies against Plk4, Cep135, hSas-6, CPAP, and CP110 as well as α- and γ-tubulin. Simultaneously, centrin staining was used to visualize both pro-centrioles and mature centrioles (Paoletti *et al.*, 1996). As summarized in Figure 23, different proteins displayed strikingly different localization patterns.
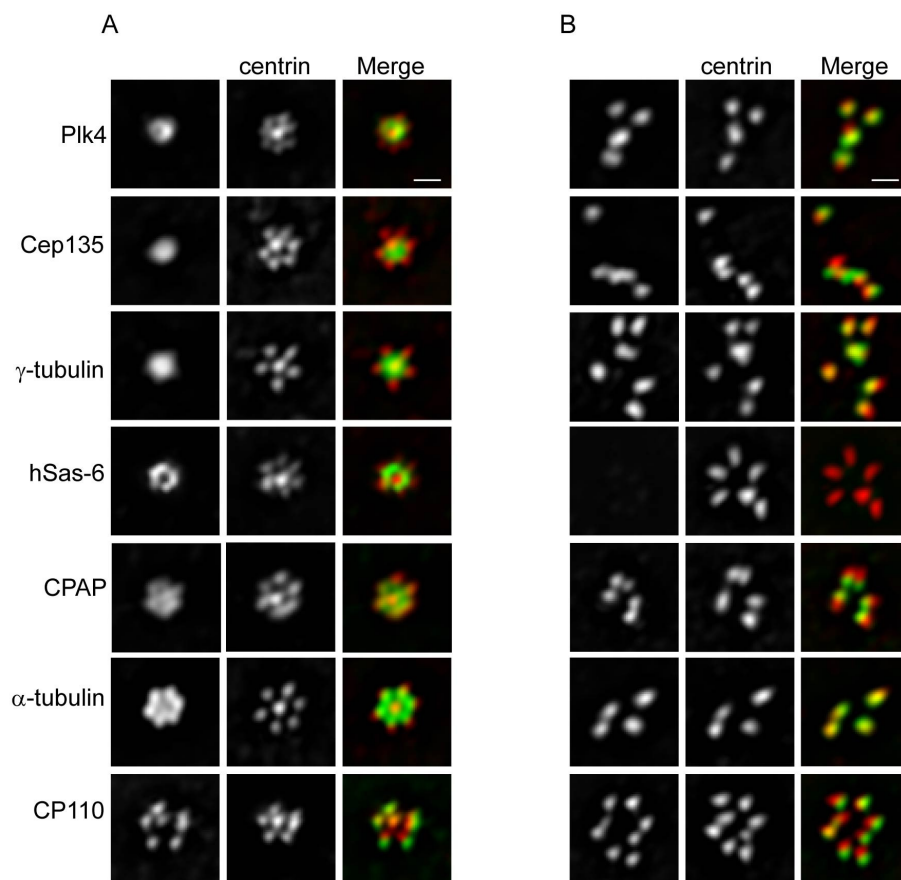
Figure 23. Localization of proteins identified as essential for centriole biogenesis.
Assembly of multiple pro-centrioles was triggered by 16h Myc-Plk4 induction in U2OS cells. All cells were stained for centrin (red) to identify both parental centrioles and pro-centrioles and co-stained for the indicated proteins (green). Panel A shows multiple pro-centrioles arranged in typical flower-like structures around parental centrioles (centres), whereas panel B shows centriole clusters after disengagement. Scale bar 1 µM.

Within the flower-like structures observed 16h after Plk4 induction (Figure 23A), Plk4 accumulated in a ring-like pattern around the parental centrioles (see also Figure 25), and similar localizations were seen for Cep135, γ-tubulin and hSas-6 (Figure 23A). However, compared to Plk4, Cep135 appeared to form a more compact structure, suggesting that it concentrates also within the lumen of the parental centriole (see below). In the case of hSas-6, the ring structure was not as smooth as that seen with Plk4, suggesting that hSas-6 does not decorate the surface of the parental centriolar cylinder but rather associates with nascent pro-centrioles. Staining for CPAP, α-tubulin and CP110, revealed star-like structures overlapping the nascent pro-centrioles, but, again, subtle differences were apparent. Compared to the localization of centrin, anti-CPAP antibodies clearly stained both the parental centriole and the proximal ends of nascent pro-centrioles, whereas α-tubulin was seen all along the length of the centrioles and CP110 could be detected primarily on the distal ends. Analysis of the multiple, Plk4-induced centrioles occurring in dispersed clusters (Figure 23B) revealed that Plk4, Cep135, CPAP, γ-tubulin, α-tubulin and CP110 all co-localized with centrin-positive disengaged centrioles. In stark contrast, hSas-6 was undetectable on G1 phase centrioles (Figure 23B), indicating that this protein is transiently recruited to nascent pro-centrioles but subsequently displaced or degraded, possibly during centriole disengagement.
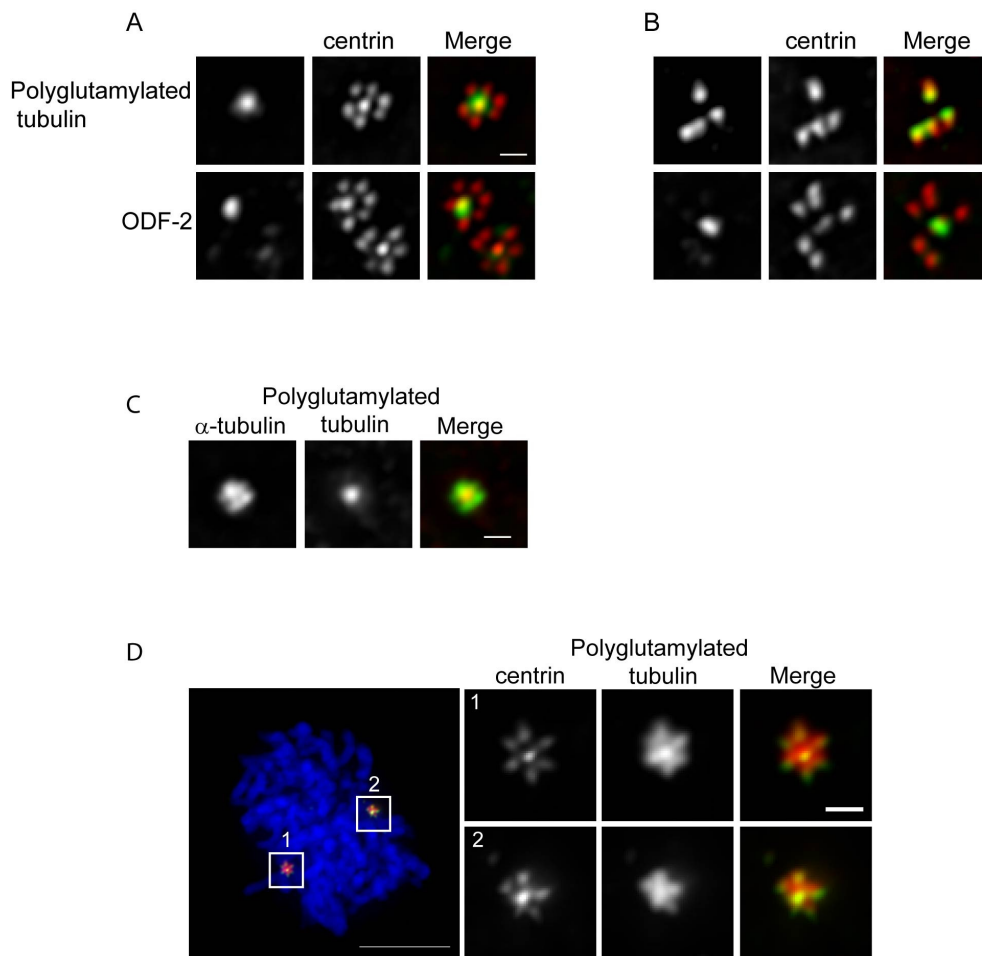
Figure 24. Localization of maturation markers on centriolar structures.

Assembly of multiple pro-centrioles was triggered by 16h Myc-Plk4-induction in asynchronous U2OS cells. (A, B) Cells were stained for centrin (red) to identify both parental centrioles and pro-centrioles and co-stained for the indicated proteins (green). Panel A shows multiple pro-centrioles arranged in typical flower-like structures around parental centrioles (centres), whereas panel B shows centriole clusters after disengagement. (C) Interphase cell showing a nascent Plk4-induced flower-like structure. Note that the newly formed centrioles (the 'petals' on the flower) are already positive for α-tubulin but still negative for GT335. (D) Prometaphase cell showing flower-like structures at both spindle poles. The left panel shows an overview, including DAPI staining, whereas the panels on the right show higher magnifications to illustrate the arrangement of centrioles at the two poles. Scale bar 1 µM.

To examine the acquisition of centriole maturity markers during Plk4-induced centriole biogenesis, we also stained early flower-like structures and late disengaged centrioles for polyglutamylated tubulin, a marker for stabilized centriolar MTs (Bobinnec *et al.*, 1998) and ODF-2, a marker for centriole maturation (Ishikawa *et al.*, 2005). As demonstrated by staining with GT335 antibody (Wolff *et al.*, 1992), only parental centrioles were polyglutamylated during early centriole biogenesis, whereas the newly assembled tubulin of nascent pro-centrioles lacked this modification (Figure 24A and C). Likewise, ODF-2, a component of centriolar appendages (Ishikawa *et al.*, 2005), could only be detected on one of the two parental centrioles, identifying it thereby as the fully mature parent (Figure 24A). At later stages, all centrioles in flower-like structures of mitotic cells (Figure 24D) and in centriole clusters of G1 phase cells (Figure 24B) stained positive for GT335, indicating that these centrioles were composed of polyglutamylated, stabilized MTs. In contrast, ODF-2 staining remained confined to only one centriole, the former parent, even in G1 cells with multiple disengaged centrioles (Figure 24B). This is consistent with the expectation that newly formed centrioles acquire appendages only during final maturation, which occurs in late G2 of next cell cycle (Bornens, 2002). Taken together, the above analysis demonstrates that overexpression of Plk4 induces the simultaneous formation of multiple complete centrioles.

Delineation of a centriole assembly pathway
The above results suggested that Plk4 localizes early on the proximal walls of parental centrioles, and then triggers the subsequent recruitment of essential centriolar proteins which assemble the nascent pro-centrioles. To corroborate this conclusion, we used siRNA to deplete individual proteins implicated in centriole biogenesis and then monitored pro-centriole formation in response to Plk4 induction. This approach made it possible to establish dependencies amongst individual proteins and visualize assembly intermediates.

Following depletion of either hSas-6, CPAP, Cep135, γ-tubulin or CP110, Plk4 still accumulated around the parental centrioles, exactly as it did in GL2-treated controls (Figure 25). This demonstrates that Plk4 localization does not depend on

any of the above proteins and supports the view that this kinase acts high up in a regulatory hierarchy.
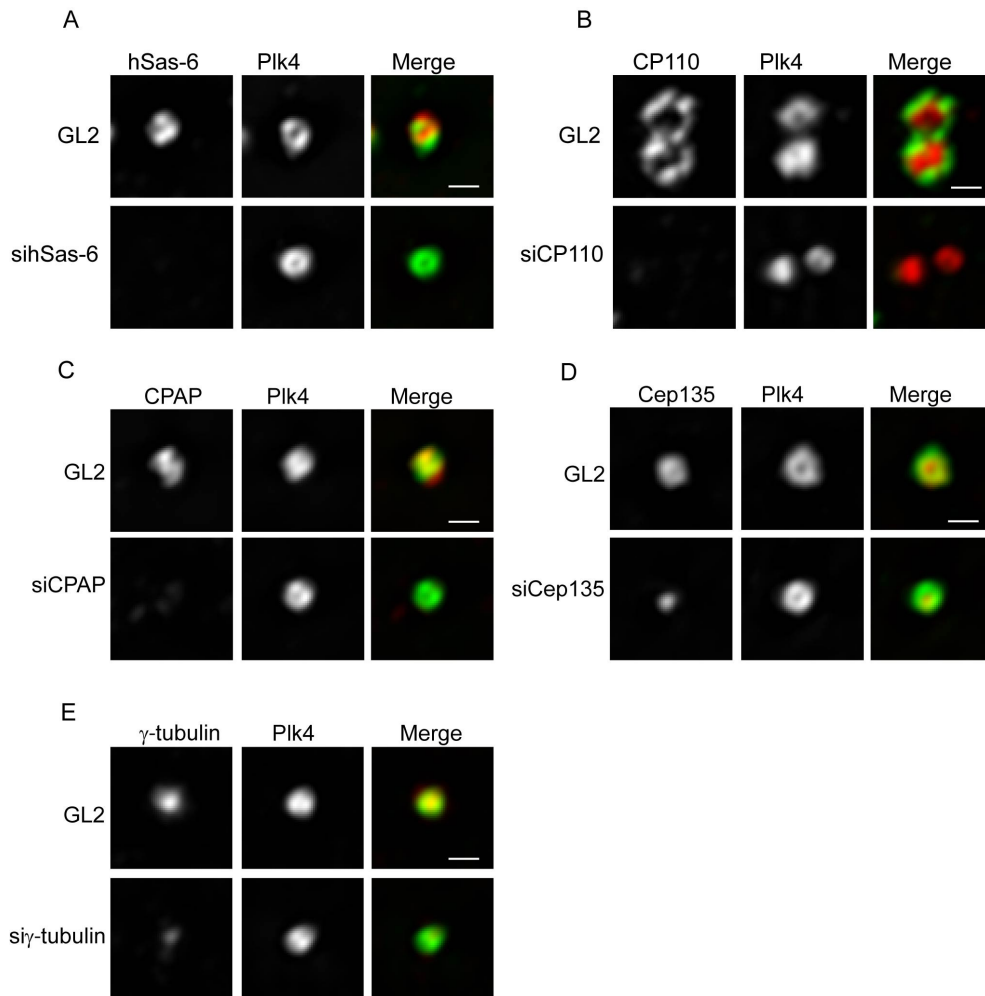
Figure 25. Delineation of a centriole assembly pathway.
U2OS cells were transfected for 72h with siRNA duplexes targeting hSas-6 (A), CP110 (B), CPAP (C), Cep135 (D), γ-tubulin (E) or GL2 for control. Then, Myc-Plk4 was induced for 16h in the continued presence of siRNA duplexes and cells were processed for immunofluorescence microscopy, using anti-Myc antibodies. Scale bar 1μM.

In contrast, the depletion of hSas-6 completely suppressed the Plk4-induced assembly of pro-centrioles and, as a consequence, all other proteins remained restricted to parental centrioles (Figure 26A and data not shown). Likewise, centriole

biogenesis was completely suppressed in response to depletion of CPAP (Figure 26C, left panels). Some hSas-6 staining of parental centrioles could be seen in such cells, but since hSas-6 is not present within the lumen of parental centrioles (see Figures 23 and 30), we presume that this signal reflects residual hSas-6 associated with the centriolar surface. Most interestingly, pro-centriole formation also failed upon depletion of CP110, as visualized by centrin staining (Figure 26B, left panels), but in this case, ring-like structures clearly stained positive for hSas-6 (Figure 26B, right panels). This indicates that pro-centriole formation was blocked downstream of hSas-6 recruitment.

Similarly, centriole biogenesis was completely suppressed in response to depletion of Cep135 or γ-tubulin (Figure 26C, middle and right panels). Taken together, these data indicate that hSas-6, CPAP, Cep135 and γ-tubulin are recruited early after Plk4 induction to form nascent pro-centrioles. The four proteins were mutually dependent on each other and similarly required for further development of pro-centrioles, at least within the temporal and spatial resolution of these experiments. In contrast, CP110 clearly functions at a later stage.
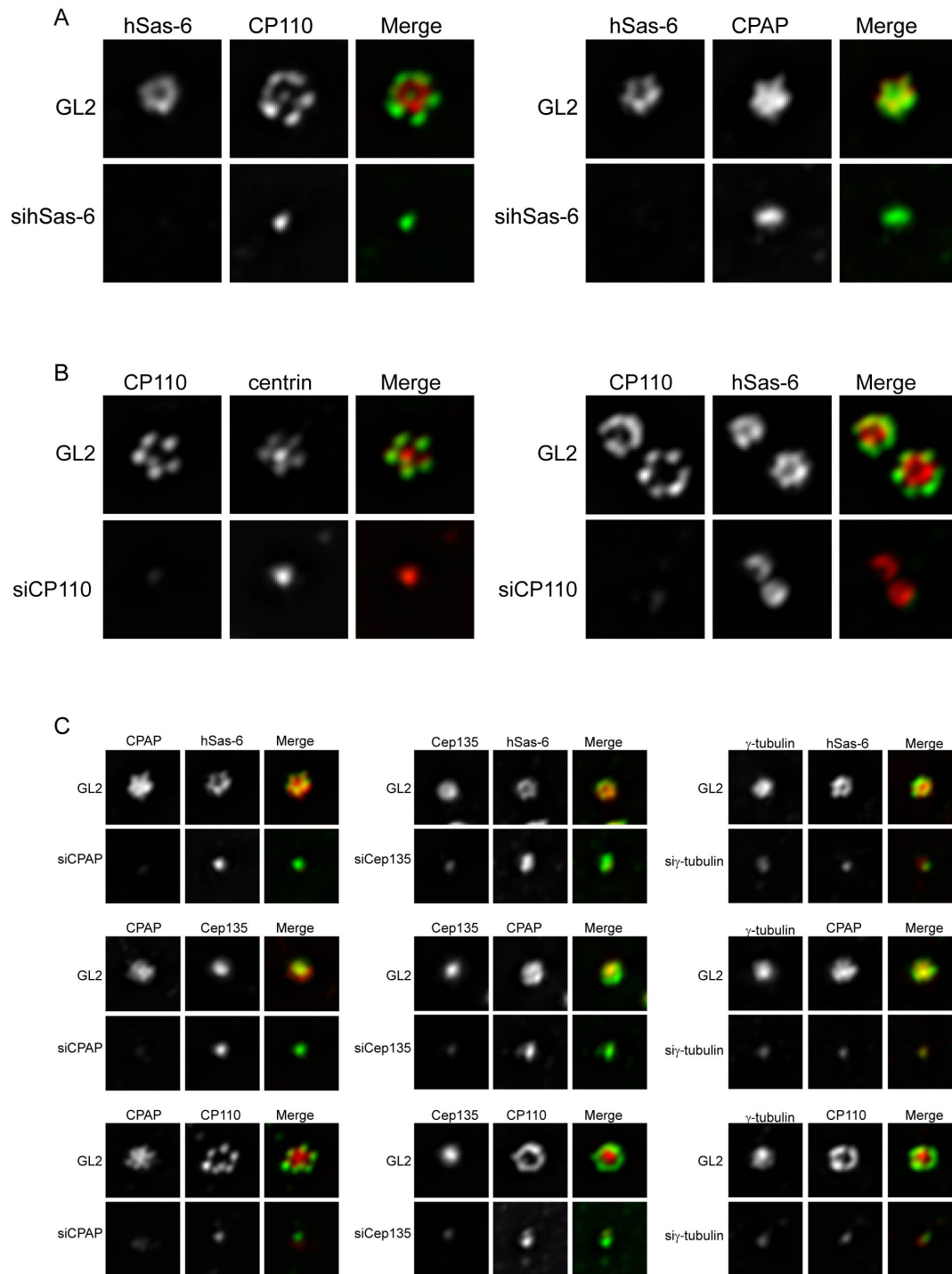
Figure 26. Delineation of a centriole assembly pathway.

U2OS cells were transfected for 72h with siRNA duplexes targeting hSas-6 (A), CP110 (B), CPAP (C), Cep135 (C), γ-tubulin (C) or GL2 for control. Then, Myc-Plk4 was induced for 16h in the continued presence of siRNA duplexes and cells were processed for immunofluorescence microscopy, using the antibodies indicated. Scale bar 1μM. (A) Depletion of hSas-6 completely abolishes centriole assembly. (B) Depletion of CP110 abolishes centriole assembly after hSas-6 has been recruited. (C) Pro-centriole biogenesis is blocked in CPAP-, Cep135- and γ-tubulin-depleted cells.

The role of centrin and hSfi1 in human centriole biogenesis

It has been reported that centrin 2 and 3 are expressed ubiquitously in somatic cells, whereas centrins 1 and 4 are restricted to multiciliated and flagellated cells (Gavet *et al.*, 2003; Hart *et al.*, 1999; Laoukili *et al.*, 2000; Middendorp *et al.*, 1997). Centrin 4 has been identified in mouse and it is noteworthy that only centrin 1, 2 and 3 are found the the human genome, whereas no centrin 4 protein has ever been reported in the literature nor could be found by any database analysis. To rule out the possibility that centrin 1 might be expressed in human U2OS cells, we performed RT-RNA with primers able to discriminate between centrin isoforms. Cells were induced for Plk4 expression and expression of centrins 1, 2, 3 and Myc-Plk4 in parallel was examined. As expected, solely expression of centrin 2 and 3 could be detected in Plk4-induced U2OS cells (Figure 27).
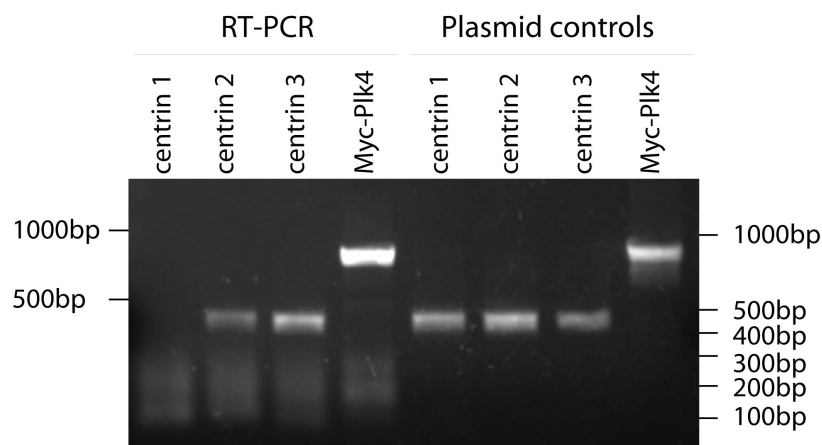
Figure 27. Centrin expression in Plk4-transgenic U2OS cells.
RT-PCR experiments with primers able to discriminate between centrin isoforms were used to examine the expression of centrins 1, 2 and 3 in U2OS cells induced for Plk4 expression. Myc-Plk4 levels were examined in parallel. Lanes on the right show corresponding plasmid controls.

To study the effect of centrin depletion on Plk4-induced pro-centriole formation, we focused on the two isoforms centrin 2 and 3 and protein depletion was achieved by 72h treatments of cells with siRNA duplexes targeting centrins 2 and 3 (Figure 28). Considering that centrin 2 was previously reported to be required for centriole duplication in human cells (Salisbury *et al.*, 2002), we were surprised to find

that induction of Plk4 in cells depleted of centrins 2 and 3 still induced both the formation of α-tubulin-positive pro-centrioles and, at later times, multiple disengaged centrioles, indistinguishable from controls (Figure 28A). Furthermore, centrin depletion produced no detectable adverse effects on the recruitment of CPAP, Cep135 or CP110 to nascent pro-centrioles (Figure 28B). Efficient depletion was confirmed using an antibody (20H5; (Baron *et al.*, 1992) known to detect both centrins 2 and 3 (Middendorp *et al.*, 1997; Paoletti *et al.*, 1996). With regard to a possible compensatory role of other centrin isoforms, we emphasize that no human centrin 4 gene has yet been identified and RT-PCR revealed no evidence for expression of centrin 1 in the cells studied here (Figure 27).
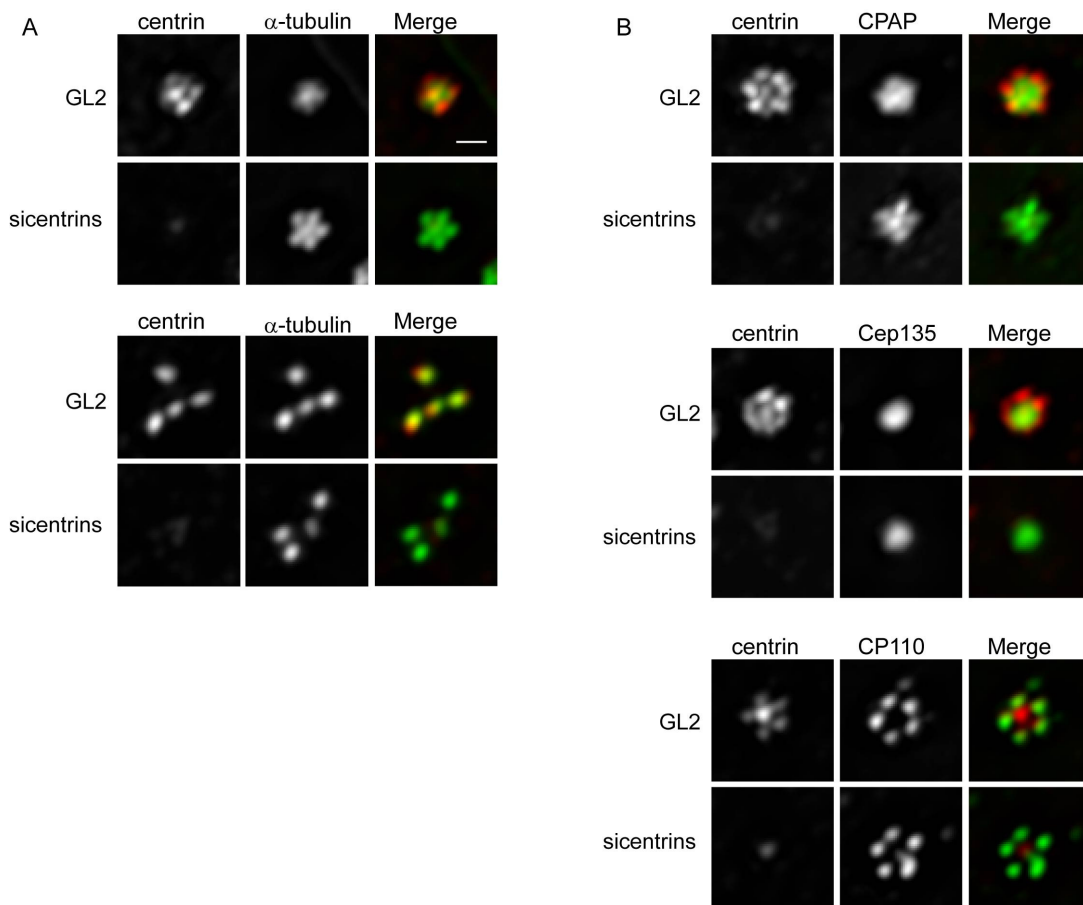
Figure 28. Formation of multiple centrioles in centrin-depleted cells.
U2OS cells were treated as described in the legend to Figure 25, using siRNA duplexes targeting both centrin 2 and 3, or GL2 for control. Co-stainings were performed using the anti-centrin 2/3 reagent 20H5 and the antibodies indicated. Scale bar 1μM.

Likewise, deletion of the centrin-binding protein hSfi1 did not abolish centriole assembly, as illustrated by hSfi1 and α-tubulin co-staining (Figure 29). Interestingly, hSfi1 depletion did abolish the incorporation of centrin into the newly forming pro-centrioles, as indicated clearly by co-staining of hSfi1-depleted cells with centrin and α-tubulin (lower panels).
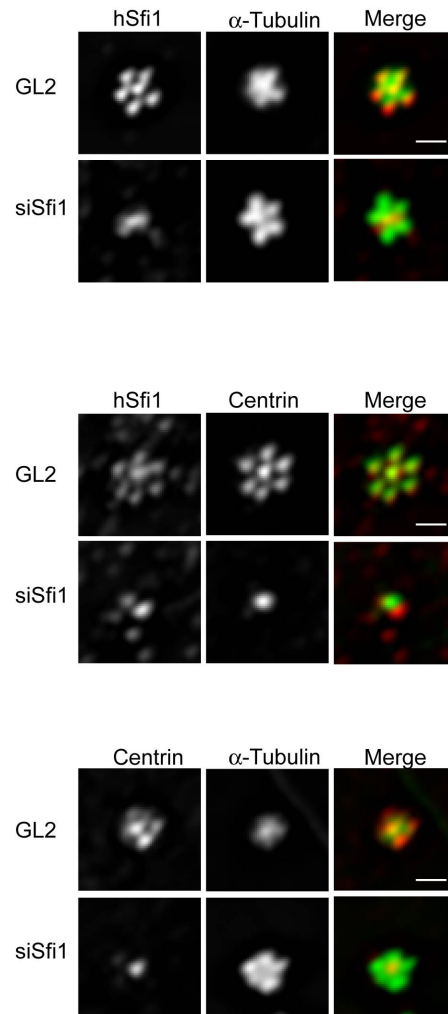
Figure 29. Formation of multiple centrioles in hSfi1-depleted cells.
U2OS cells were treated as described in the legend to Figure 25, using siRNA duplexes targeting hSfi1, or GL2 for control. Co-stainings were performed using the anti-hSfi1, anti-centrin 2/3 reagent 20H5 and anti-α-tubulin antibodies. Scale bar 1µM.

Taken together, although centrins and hSfi1 associate with nascent pro-centrioles early during assembly, our data provide no evidence to indicate that they are required for Plk4-induced centriole biogenesis. Furthermore, these data demonstrate that hSfi1 is required for proper centrin incorporation into the assembling pro-centriole. Although the centrin scaffolding protein hSfi1 seems to be dispensable for centriole biogenesis, it might serve as a docking site for other centriolar or pericentriolar components as we can not rule out the possibility that hSfi1-depleted centrioles display altered ultrastructural morphology. A detailed ultrastructural analysis of hSfi1-depleted centrioles will definitely require electron microscopy.

Analysis of centriole biogenesis by immuno-electron microscopy

In a final series of experiments, immuno-electron microscopy was used to obtain more definitive insight into the localization of key proteins implicated in centriole biogenesis. As summarized in Figure 23, Plk4, hSas-6, CPAP, Cep135, CP110 and centrin 2 could be localized to distinct structures during early stages of pro-centriole assembly. Unfortunately, hSfi1 could not be visualized using the paraformaldehyd-based fixation method. Myc-tagged Plk4 could be seen on the outer wall of parental centrioles and at the interface between parental and nascent pro-centrioles (Figure 30A). A similar localization was also observed for endogenous hSas-6, although hSas-6 appeared to be associated more prominently with the nascent pro-centriole (Figure 30B and C). In contrast, CPAP and Cep135 were concentrated within the proximal lumen of both parental centrioles and pro-centrioles (Figure 30D and E). In particular, antibodies against Cep135 produced strong luminal staining within the proximal ends of centrioles as well as weaker staining along the centriolar surface (Figure 30E, right hand panel). Such a staining pattern might be expected for a protein that forms part of a putative cartwheel structure (Anderson and Brenner, 1971; Cavalier-Smith, 1974). CP110 showed yet another, clearly distinct localization pattern. This protein was detected on the distal ends of both parental centrioles and nascent pro-centrioles (Figure 30F). Of particular interest, CP110 associated early with nascent pro-centrioles and then decorated the distal tips of all centrioles, regardless of their elongation state. This indicates that CP110 assembles into a cap-

like structure early during pro-centriole formation and then remains on the distal end during centriole elongation, implying that α-/β-tubulin dimers are most likely inserted underneath a CP110 cap. Finally, centrin was seen within the lumen of both pro-centrioles and parental centrioles (Figure 30G), consistent with previous results (La Terra *et al.*, 2005; Paoletti *et al.*, 1996) and confirming that this protein constitutes a genuine marker for both nascent centrioles and mature centrioles.
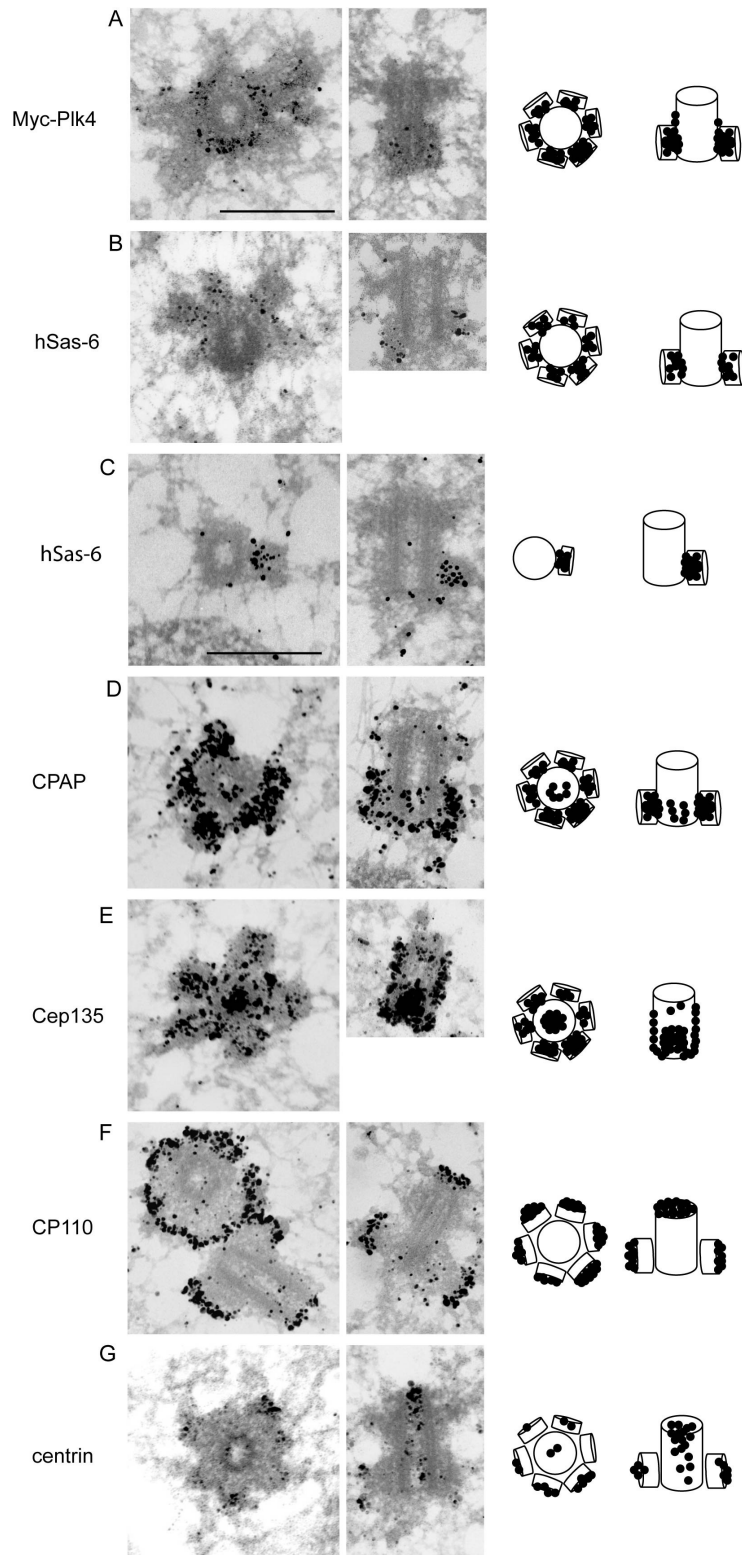
Figure 30. Analysis of centriole biogenesis by immuno-electron microscopy.

Myc-Plk4 was induced (all samples except 'C') in U2OS cells for 16h before cells were processed for immuno-electron microscopy, using antibodies against the indicated proteins and anti-Myc antibodies for visualization of Myc-Plk4, followed by gold-labelled secondary α-rabbit or α-mouse antibodies. Schemes on the right indicate the localization of the individual proteins for clarity. Note that in panel C,

U2OS cells (carrying the Plk4 transgene) were processed for immuno-electron microscopy without induction of Plk4 expression and endogenous hSas-6 was then stained with anti-hSas-6 antibody. Scale bar 0.5µm.

Analysis of centriole biogenesis by 3dSIM (structured illumination microscopy)

Using state-of-the-art widefield deconvolution microscopy (see MATERIALS & METHODS), we have been able to examine protein interdependencies at a relatively high subcellular resolution. However, the limitation of this technique becomes obvious in our inability to examine detailed events happening at the very beginning of centriole assembly. Thus, it was not possible to distinguish if a protein is present only within the centriole lumen or on the surface of the parental centriole. Similarly, we were not able to discriminate between immunofluorescence signals at the proximal surface of the parental centriole and signals within the proximal region of the emerging pro-centrioles. Therefore, a higher spatial resolution would definitely be desirable in order to examine the exact localization of the proximal proteins hSas-6, CPAP, Cep135 and γ-tubulin and to gain more insight into their individual functions during centriole biogenesis.

The fundamental limitation of conventional light microscopy is the diffraction limit (or Abbe limit) of resolution, that is, the smallest distance at which two distinct microscopic structures can be resolved. This limitation has its roots in the physical properties of light and the biological limitations of the human eye. As a result, objects that lie closer than 200-350 nm apart, can no longer be distinguished, but instead appear merged together. This limit does not apply for electron microscopy, but the increase of resolution frequently comes together with a loss of structure preservation and labeling specificity, due to limiting sample preparation methods. Recently a number of techniques have been developed to overcome this fundamental limitation, such as 4-Pi, STED or PALM microscopy (for review see (Hell, 2007).

In collaboration with L. Schermelleh (Department of Biology II, Ludwig Maximilians University Munich (LMU)), we could apply a novel microscopy technique, 3-dimensional structured illumination (3dSIM), to visualize Plk4-induced centriolar structures with subdiffraction limit resolution. The 3dSIM technology was developed and implemented in a custom-built microscope (termed OMX) in the laboratory of J.

W. Sedat (University of California, San Francisco). It extends the principle of structured illumination (Gustafsson, 2000) to three dimensions, thus improving the resolution by a factor of two beyond the diffraction limit in lateral (xy, ~100 nm) and axial (z, ~250 nm) direction and, at the same time, retaining all advantages of light microscopy. Notably, 3dSIM is currently the only extended-resolution imaging technique that allows detection of multiple wavelengths in the same sample, using standard fluorescent dyes and conventional slide preparation. So far, it has been used to study nuclear pore complexes and chromatin-related structures in human cells (Schermelleh *et al.*, manuscript submitted).

In an initial series of experiments, Plk4-induced centriole biogenesis was examined using anti-Plk4, anti-centrin 2 and anti-α-tubulin antibodies. Co-immunostaining of Plk4 and centrin 2 clearly illustrates the accumulation of Plk4 around the proximal end of the centriole, while centrin can be detected within the distal centriole lumen and on the assembling pro-centrioles (Figure 31A). High-resolution 3dSIM images thus clearly confirm the localizations determined by light and electron microscopy (Figures 23 and 30).

Similarly informative was a co-staining of Plk4 and α-tubulin (Figure 31B). Both the parental and the pro-centriolar structures could be resolved as hollow microtubule-based cylinders, separated from one another by the PCM. Plk4 could be detected around the parental centriole exactly at the sites where the new pro-centrioles emerge. An additional weak Plk4-staining could also be detected inside the centriole lumen. Therefore, these images not only confirmed already existing EM-data (Figure 30), but also demonstrate that Plk4 localizes exactly to sites where pro-centriole assembly is initiated, rather than forming a ring-like structure. In contrast to previous EM-data, the problem of missing antibody-staining because of sample preparation or staining method is reduced here. Furthermore, this image clearly illustrates the spatial constraints that apply onto the newly emerging centrioles. Obviously, six equally distributed pro-centrioles completely fill out the radial surface provided by the parental centriole. This is consistent with our observation that most of the Plk4-induced centriolar structures contain 6 pro-centrioles.

Co-immunostaining of centrin 2 and α-tubulin in disengaged centrioles illustrates that centrin is not only present in the distal region of the centriole, but can be detected along the whole length of the centriole lumen (Figure 31C).

Taken together, the advantages of 3dSIM have become obvious. As all images taken by 3dSIM are multi-color 3D image stacks - obtained by methanol fixation and with the use of standard fluorescent dyes – artefacts, caused by sample preparation and demanding fixation methods, can to our knowledge largely be excluded.

Therefore, 3dSIM represents a valuable method to bridge the gap between conventional light microscopy and electron microscopy and is a powerful new tool to study processes like centriole assembly within the cellular environment.
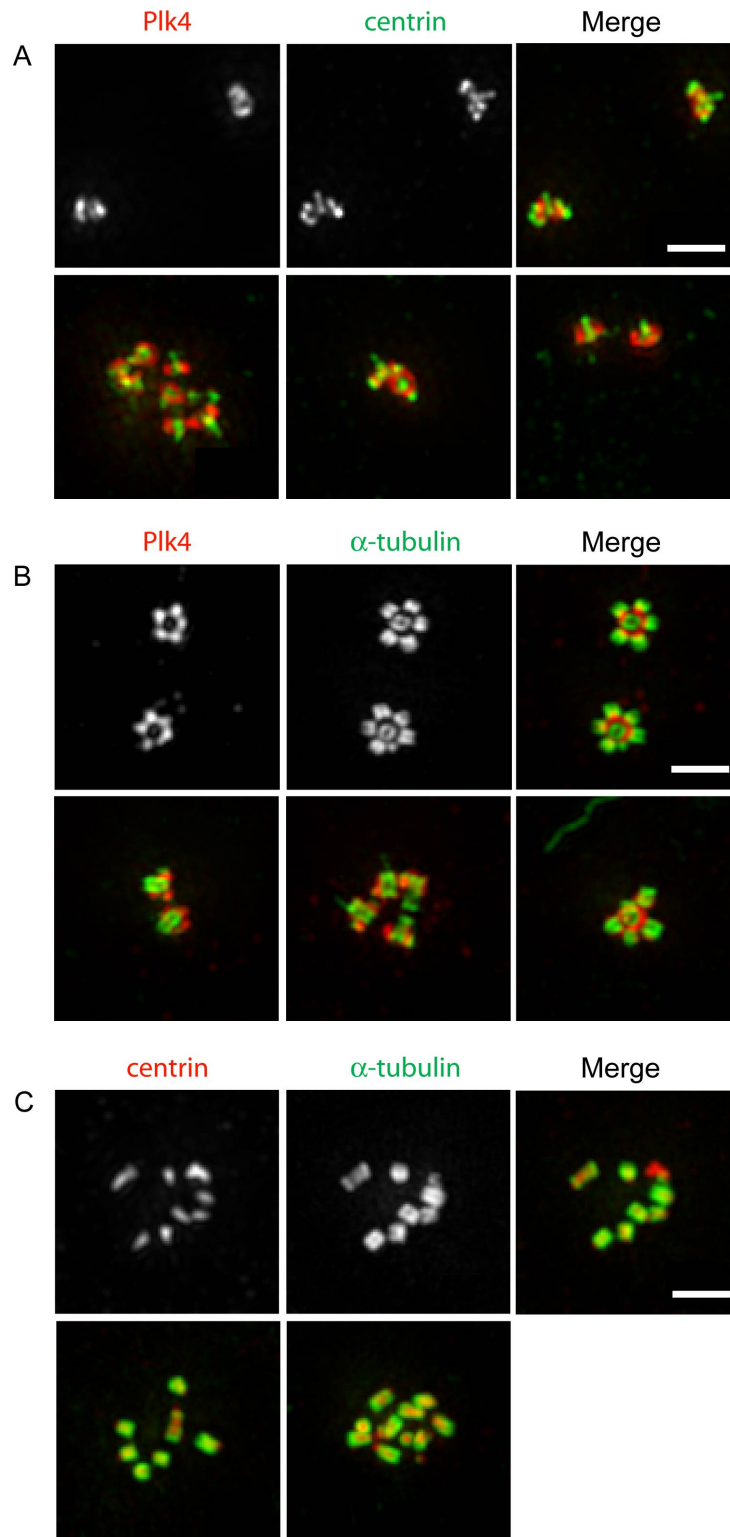
Figure 31. 3dSIM imaging of Plk4-induced centriolar structures.

Myc-Plk4 was induced in U2OS cells for 16h before cells were processed for IF-microscopy, using antibodies against the indicated proteins. Lower rows show additional merged images. Maximum intensity projections of 3d image stacks are shown. Scale bar 1 µm. All images presented here were kindly taken and processed by L. Schermelleh.

3. Maintenance of proper centriole morphology requires the distal capping protein CP110

As demonstrated earlier (Figure 22 and 26), depletion of hSas-6, CPAP, Cep135, γ-tubulin or CP110 abolishes Plk4-induced centriole biogenesis. Furthermore, these results demonstrated that depletion of any of the proximal centriolar proteins (hSas-6, CPAP, Cep135, γ-tubulin) induced an earlier block in the assembly process than depletion of the distal capping protein CP110 did.

Here, we demonstrate that, additionally to this block of pro-centriole assembly, loss of CP110 specifically caused very characteristic morphological alterations at mature centrioles. Immunofluorescence staining of α-tubulin visualized microtubule-based fiber-like extensions emanating from CP110-depleted centrioles (Figure 32). Interestingly, a very similar phenotype has also been observed in γ-tubulin-depleted cells (data not shown, preliminary results).
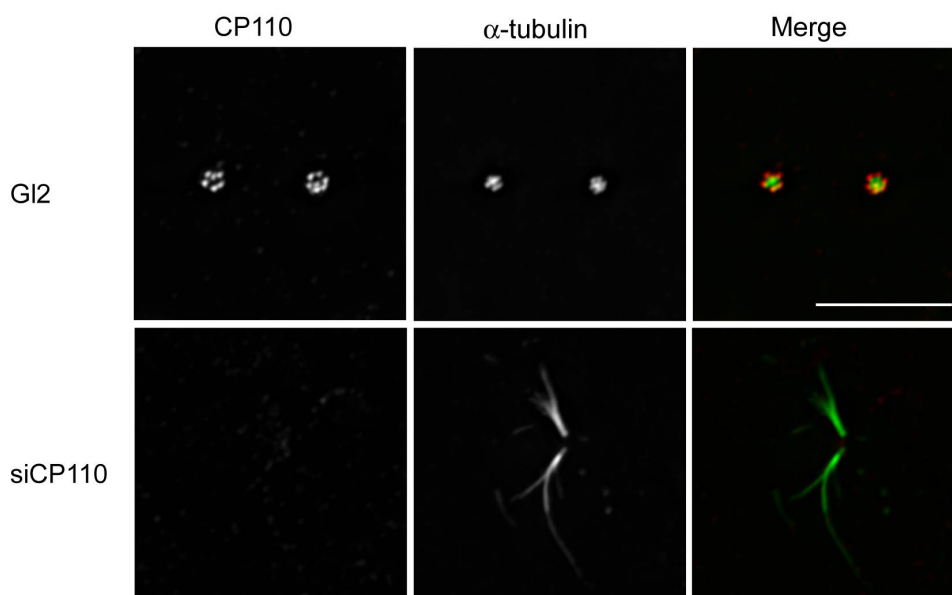
Figure 32. Microtubule-based fiber-like extensions emanating from CP110-depleted centrioles. U2OS cells were transfected for 72h with siRNA duplexes targeting CP110 or GL2 for control. Then, Myc-Plk4 was induced for 16h in the continued presence of siRNA duplexes and cells were processed for immunofluorescence microscopy, using anti-CP110 and anti-α-tubulin antibodies. Scale bar 1µM.

This phenotype could be reproduced in U2OS and HeLaS3 cells (data not shown), independently of Plk4-overexpression. To analyze these fiber-like extensions further, CP110-depleted cells were co-stained with α-tubulin and the proximal centriolar protein hSas-6. As reported earlier (Figures 23 and 30), hSas-6 can be detected at the proximal region of duplicating centrioles and in the interphase between parental centriole and pro-centriole later on. Upon CP110-depletion, hSas-6 localization was unaltered (Figure 33). Microtubule-extensions appeared to emanate from both the parental centriole and the assembling pro-centriole – indicated by images showing a hSas-6-positive interphase region where two microtubule-extensions originate from. Similarly, some fibrous structures emanating from all the petals of Plk4-induced flowers could be detected in CP110-depleted Myc-Plk4-U2OS cells (data not shown). However, fibres emanating from all petals were only rarely seen, as efficient CP110 depletion abolishes Plk4-induced flower assembly. Nevertheless, in some cells residual CP110-levels might allow initial pro-centriolar flower assembly, but might then not be functional enough to allow assembly and maintainance of stable centriolar capping structures.

According to this morphological alterations in CP110-depleted cells, it is very tempting to hypothesize that CP110 is recruited early during centriole biogenesis, forms a capping structure at the very distal centriole end and then persists throughout centriolar development and maturation. This distal capping structure appears to be required to ensure proper centriole morphology probably by prohibiting addition of α/β-tubulin dimers to the distal centriole end. Careful examination of these structures by immunofluorescence staining for several centriolar marker proteins and electron microscopy or 3dSIM will reveal more about the nature and composition of these microtubule-based fiber-like centriole extensions. Further studies will also be required to elucidate whether the role of CP110 in pro-centriole assembly and centriole capping can be attributed to two independent functions. It is also possible that the loss of a basic structural CP110 function produces both the duplication block and the abnormal centriole morphology, depending on the 'developmental stage' of the centriole.
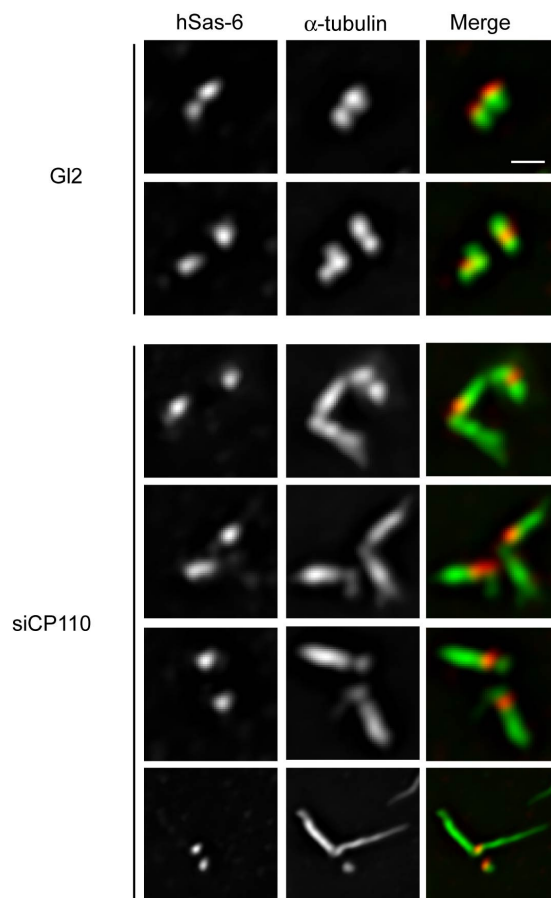
Figure 33. MT-extensions emanating from distal ends of parental centrioles and pro-centrioles in normal U2OS cells.

U2OS cells were transfected for 72h with siRNA duplexes targeting CP110 or GL2 for control. Then, cells were processed for immunofluorescence microscopy, using anti-α-tubulin to visualize MT-extensions and anti-hSas-6 to visualize the proximal centriole region. Scale bar 1μM.

DISCUSSION

Here we have shown that overexpression of Plk4 in human cells induces the near-simultaneous formation of multiple complete centrioles within a single S phase. Independently, *Drosophila* Plk4/Sak was reported to induce large numbers of centrioles even in a cell type (the unfertilized egg) that lacks a pre-existing centriole (Peel *et al.*, 2007; Rodrigues-Martins *et al.*, 2007). These studies thus identify Plk4 as a key regulator of centriole biogenesis and strengthen the notion that pre-existing centrioles represent 'solid-state platforms' to facilitate centriole formation rather than genuine 'templates' (Nigg, 2007).

Cell cycle control of Plk4-induced flower-like centriole structures

Our analyses of synchronized cells revealed that Plk4 induced pro-centriole formation rapidly, provided that cells had reached a cell cycle stage permissive for centriole formation. This requirement falls in line with previous studies indicating that centrosome duplication depends on traverse of G1/S, as reflected by phosphorylation of the retinoblastoma protein, activation of the E2F transcription factor and activation of Cdk2 in a complex with cyclin E and/or A (Cowan and Hyman, 2006; Hinchcliffe *et al.*, 1999; Lacey *et al.*, 1999; Matsumoto *et al.*, 1999; Meraldi *et al.*, 1999). In response to Plk4 activation, nascent pro-centrioles initially grew off each parental centriole in an arrangement reminiscent of petals on a flower. Interestingly, these flower-like structures remained intact throughout S and G2 phase as well as most of M phase before they began to disassemble in late telophase, consistent with the proposal that centriole disengagement is triggered by Separase activity (Tsou and Stearns, 2006). At present, there is no information on the dimensions of the first 'seed' structures that form on the surface of parental centrioles. Thus, it is interesting that the cylinders of parental centrioles most frequently supported the formation of six pro-centrioles, most likely reflecting steric constraints imposed by the dimensions of nascent precursor structures and their vicinity to the 'solid-state assembly platform'.

Identification of proteins required for centriole biogenesis

To identify human centrosomal proteins required for centriole biogenesis, we carried out a siRNA-based phenotypic screen. This approach positively identified hSas-6, CPAP, CP110, Cep135 and γ-tubulin as indispensable for centriole formation. A requirement for hSas-6 and CPAP in centriole formation was expected in view of previous studies in invertebrates (Basto *et al.*, 2006; Leidel *et al.*, 2005; Leidel and Gonczy, 2003; Peel *et al.*, 2007; Rodrigues-Martins *et al.*, 2007). Likewise, γ-tubulin had previously been shown to be required for basal body formation in the ciliate *Paramecium* (Ruiz *et al.*, 1999) and structural similarity has been noted between Cep135 and Bld10, a component of a putative cartwheel structure implicated in basal body formation in *Chlamydomonas* (Matsuura *et al.*, 2004). In the case of CP110, no invertebrate or protozoan homologue has previously been described. However, human CP110 was originally identified as a Cdk2 substrate required for centrosome over-duplication in S phase arrested cells (Chen *et al.*, 2002). So, to the extent that homologues of the various proteins studied here exist in invertebrates or protozoans, these are likely to play functionally analogous roles.

At first glance, it may appear surprising that depletion of both centrins known to be expressed in U2OS cells (centrins 2 and 3) and the centrin-binding protein hSfi1 did not detectably interfere with Plk4-induced centriole biogenesis. The yeast centrin homologue Cdc31p is clearly required for spindle pole body duplication in *Saccharomyces cerevisiae* (Paoletti *et al.*, 2003; Spang *et al.*, 1995) and a previous siRNA study had proposed an essential role for mammalian centrin 2 in centrosome duplication (Salisbury *et al.*, 2002). As with all siRNA experiments, we cannot rigorously exclude that residual, albeit undetectable, centrin protein may have conferred some functionality in our experiments. However, we emphasize that there is presently no genetic evidence to support a role for centrin-related proteins in centriole duplication in *Drosophila* or *C. elegans* (Azimzadeh, 2004), and studies in *Paramecium* indicate that centrins are required for basal body positioning rather than biogenesis (Ruiz *et al.*, 2005).

Our data also provide new data about the centrin-binding protein hSfi1p. As expected from data obtained in yeast, the human homologue of Sfi1p exactly co-localizes with its binding partner centrin at the distal end of parental centrioles and procentrioles. While centriole assembly was unaltered in hSfi1-depleted cells, centrin

incorporation was clearly abolished. A strong interdependency between centrin and its scaffolding protein hSfi1 was confirmed biochemically, as centrin 2 and 3 were found in endogenous hSfi1 immunoprecipitations.

However, despite its role in SPB duplication, the yeast Sfi1p homologue has also been implicated in cell cycle progression and assembly of the mitotic spindle. While in some conditional mutants of Sfi1p, binding of Cdc31p and SPB duplication was blocked, other conditional mutants of Sfi1p where binding to Cdc31p seemed unaffected, arrested with duplicated but unseparated spindle poles (Anderson *et al.*, 2007; Strawn and True, 2006). There is a growing body of evidence that, additional to its role in the initiation of SPB duplication, Sfi1p might also function in bridge splitting and in separation of the duplicated SPBs (Anderson *et al.*, 2007; Li *et al.*, 2006). So far, there is not much known about separation of the SPB bridge, but interestingly, Cdc4 an F-box component of the ubiquitin ligase known as SCF, has been implicated in the process (Mathias *et al.*, 1996). This suggests the possibility that an SCF substrate needs to be degraded, by ubiquitin-mediated proteolysis, for bridge separation to occur (Anderson *et al.*, 2007). Consistent with this hypothesis is the observation that increased activity of the mitotic motor protein Cin8p is capable to suppress Sfi1p-mutants, thereby allowing duplicated SPBs to separate (Anderson *et al.*, 2007).

Although Sfi1p function in centrosome duplication does not seem to be conserved in higher eukaryotes, its function in SPB separation and spindle assembly might be conserved throughout evolution. In this context, a specific interaction of hSfi1 with all members of the γ-TuRC might indicate a new physiological function for hSfi1 in centrosome separation and mitotic spindle assembly. Interestingly, hSfi1 additionally coprecipitated ubiquitin and ubiquitin-related proteins. Furthermore, Sfi1p has been identified as a *in vitro* Cdk1-substrate in yeast (Ubersax *et al.*, 2003) and the human homologue harbours multiple (~20) destruction boxes (D-boxes, (http://elm.eu.org)) identified by the server 'ELM – Functional sites in Proteins') – indicating that Sfi1p might be targeted for ubiquitin-mediated degradation.

Delineation of a centriole assembly pathway in human cells

We have used siRNA approaches to establish mutual dependencies between individual proteins implicated in centriole biogenesis and, in parallel, studied their localization by both high resolution fluorescence and immuno-electron microscopy. The results of these studies afford a comprehensive view of the centriole assembly pathway, as summarized schematically in Figure 34. Following activation of Plk4 on the surface of the parental centriole cylinder, we observed the rapid recruitment of hSas-6, CPAP, Cep135 and γ-tubulin. Whether these proteins are recruited at exactly the same time could not be resolved. However, they are unlikely to form a single complex because hSas-6 was recruited exclusively to the nascent pro-centrioles, whereas CPAP and Cep135 could be seen within the proximal lumen of both parental and pro-centrioles (Figure 30) and similar intra-luminal localization has also been described for γ-tubulin (Fuller *et al.*, 1995). Whereas γ-tubulin is likely to nucleate centriolar MTs, CPAP and Cep135 probably play scaffolding roles in early centriole biogenesis. Once incorporated, these three proteins remained associated with centrioles. In contrast, hSas-6 was lost from centrioles, presumably in the course of centriole disengagement, either through displacement or degradation. Finally, the time of assembly and localization of CP110 indicates that centrioles do not grow by tubulin addition to distal tips, but rather by insertion of tubulin underneath a CP110-containing cap.

Formation of a centriolar 'seed'   MT nucleation   Centriole elongation   Centriole stabilization
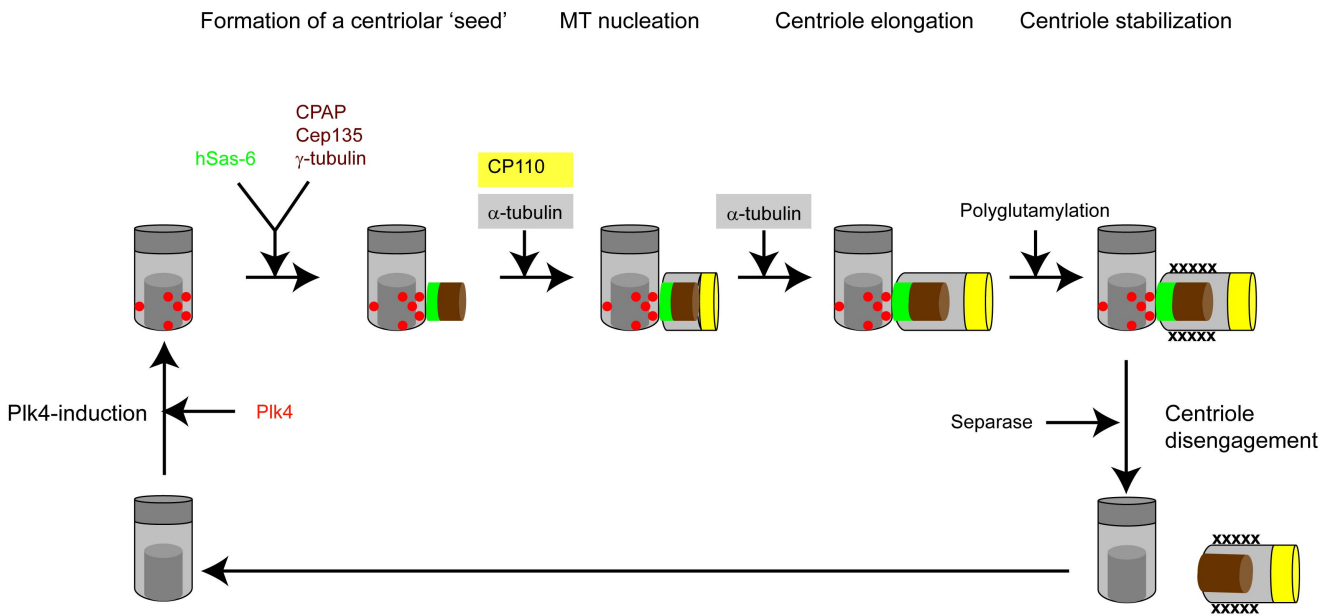
Figure 34. Model of centriole assembly in human cells.

This scheme summarizes the salient features of the centriole assembly pathway that emerge from our siRNA and immuno-electron microscopy studies. Nascent pro-centriolar structures are depicted coding Plk4 in red, hSas-6 in green, CPAP, Cep135 and γ-tubulin in brown, α-tubulin in grey and CP110 in yellow. Polyglutamylation is indicated by x. For simplicity the parental centriole is depicted in grey, polyglutamylation on the parental centriole is omitted and only one nascent pro-centriole is shown. For detailed explanation see main text.

Collectively, these findings strengthen the view that centriole and basal body formation are governed by an evolutionarily conserved mechanism (Delattre *et al.*, 2006). However, some of the proteins described here do not have obvious homologues in invertebrates and, conversely, Sas-5 has so far been identified only in nematodes (Delattre *et al.*, 2004). Thus, a better understanding of centriole biogenesis will undoubtedly benefit from the continued study of the underlying mechanism in multiple organisms.

Abnormal centriole morphology in CP110-depleted cells

This work also reports the identification and very initial examination of the morphological abnormalities induced on existing centrioles by CP110 depletion. Just recently, an elaborate study done by the Dynlacht lab (Spektor *et al.*, 2007) was published, reporting that CP110 and a newly identified interacting protein, Cep97, collaborate to suppress ciliogenesis in cycling cells. The authors found the previously uncharacerized protein Cep97 to interact and co-localize with CP110. Moreover, centriolar localization of both proteins was interdependent, suggesting that Cep97 and CP110 are coordinately recruited to the centrosome. Depletion of Cep97 by siRNA resulted in the formation of abnormal mitotic spindles and cytokinesis defects – as had previously been reported for CP110-depleted cells (Tsang *et al.*, 2006). Most strikingly, depletion of Cep97 or CP110 in cycling U2OS cells induced formation of long filamentous structures emanating from the distal ends of centrioles (Figure 35; reproduced from Spektor *et al.*, 2007)). As these filaments could be positively stained for centriolar proteins (like centrin and polyglutamylated tubulin) as well as for ciliary marker proteins (like polaris, polycystin-2 (PC-2) and acetylated tubulin), the authors assumed, that these filamentous structures represent inappropriately assembled primary cilia. In line with this hypothesis, protein expression levels of both proteins in serum starved T98G cells were found to be low.

Although assembly of a primary cilium can be induced by serum starvation in some cells, this has never been observed in U2OS. Therefore, the authors performed similar experiments in RPE-1 and mouse 3T3 cell – both capable to grow a primary cilium upon starvation – and observed a similar increase of ciliary markers in cycling cells. Further experiments performed in U2OS cells showed that expression of dominant negative Cep97 mutants mislocalized CP110 from the centrosome and gave also rise to filamentous structures resembling cilia. Finally, ectopic expression of CP110 strikingly suppressed primary cilia formation in serum-starved 3T3 cells.
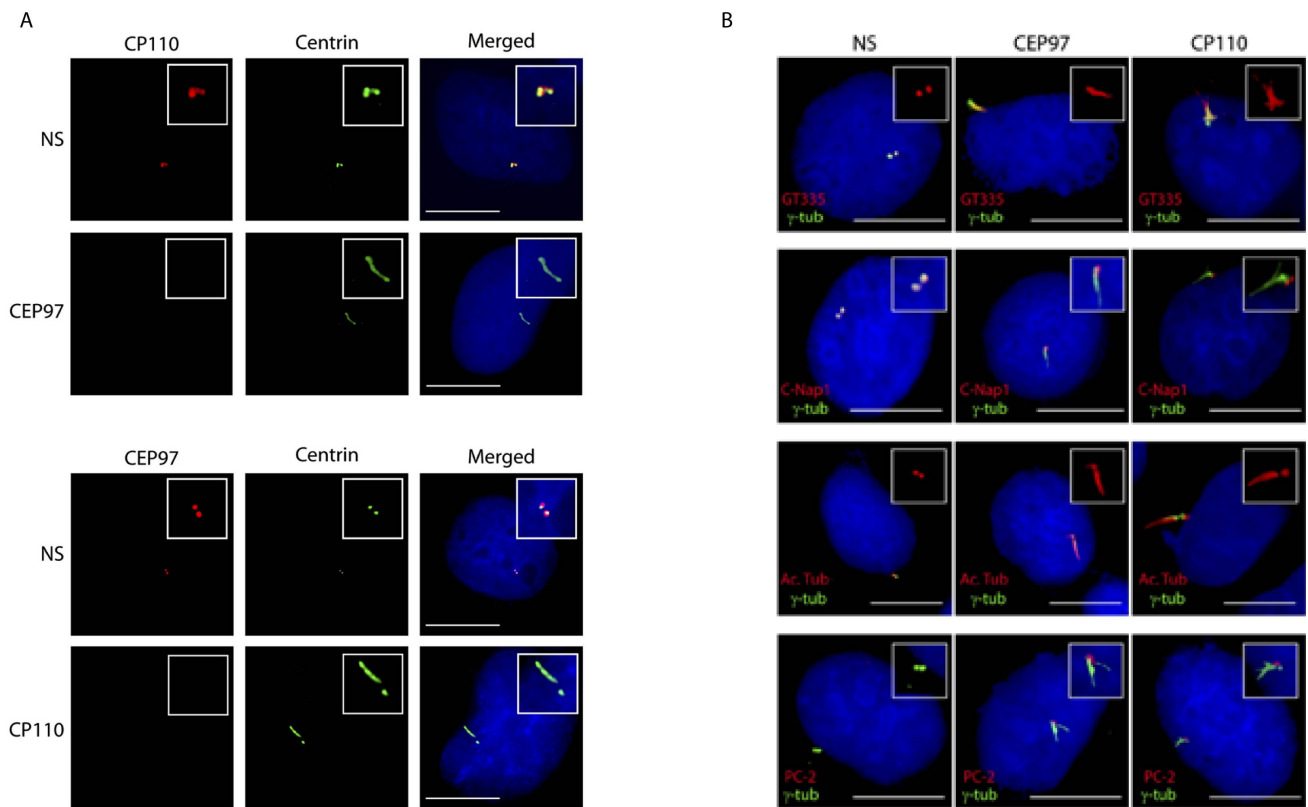
Figure 35. Fiber-like extensions are positive for ciliary marker proteins.
U2OS cells were transfected with siRNA duplexes targeting CP110 , Cep97 or 'NS' for control and stained with the indicated antibodies (top). Note that CP110 depletion results in disappearance of Cep97 from centrosomes and vice versa. Note also that fiber-like extensions are positive for centrin (A), polyglutamylated and acetylated tubulin (Ac. Tub, B) and polycystin-2 (PC-2, B) but negative for C-Nap1 (B). (Reproduced from Spektor *et al.*, 2007).

Taken together, the striking localization of CP110 at the centriolar distal end and the morphological alterations caused by CP110 depletion indicate that the distal capping protein CP110 has to be removed from the centriole in order to allow elongation of centriolar MTs at the distal end during ciliogenesis.

Dynlacht and co-workers interpreted these microtubule-based centriolar extensions as primary cilia and imply that the absence of CP110 and Cep97 triggers the molecular mechanism of ciliogenesis in cycling somatic U2OS cells. Although this is possible, another interpretation seems more appealing to us. In particular, we consider it likely that the observed filamentous structures emanating from the

centrioles emerge simply via inappropriate addition of α/β-tubulin dimers onto the accessible centriole ends, rather than representing the assembly of genuine functional cilia. In support of this view, it is known that α/β-tubulin heterodimers do assemble onto isolated centrioles *in-vitro* (Gould and Borisy, 1977) (Figure 36A, reproduced from Gould and Borisy, 1977). A phenotype very reminiscent of CP110 depletion has been reported in taxol-treated cells (Figure 36B, reproduced from (Raynaud-Messina et al., 2004)) and in mitotic cells depleted of γ-tubulin (Figure 36C, reproduced from Kuriyama *et al.*, 1986) (Kuriyama *et al.*, 1986; Raynaud-Messina et al., 2004). In these cells, centriolar microtubules are extremely elongated at their distal ends and they are even capable of forming an abnormal pseudo-spindle (Raynaud-Messina *et al.*, 2004). Although our preliminary data of γ-tubulin-depleted interphase cells suggest that abnormal MT elongation occurs in a cell cycle independent manner, protection of centriolar MT ends by capping proteins and pericentriolar material might be of special importance during mitosis as the microtubule turnover at the centrosome is extremely high during this phase. It has been suggested already more than 40 years ago that regulatory proteins might block the distal ends of centrioles and thereby prevent centriolar elongation until a cell cycle regulated and very specific axonemal program triggers ciliogenesis in quiescent cells (Krishan and Buck, 1965; Raynaud-Messina *et al.*, 2004).

In future studies, it will be important to determine whether this 'centriole elongation' phenotype can specifically be attributed to the absence of CP110 and Cep97. Depletion or mislocalization of other centrosomal proteins might alter centriole morphology in a similar way, thereby producing similar phenotypes – as preliminary results suggest for γ-tubulin. Finally, only functional analyses of these hypothetical ciliary structures and careful ultrastructural examination by 3dSIM or electron microscopy will determine whether these structures are indeed functional and morphologically normal primary cilia or simply abnormally elongated centriolar microtubules.
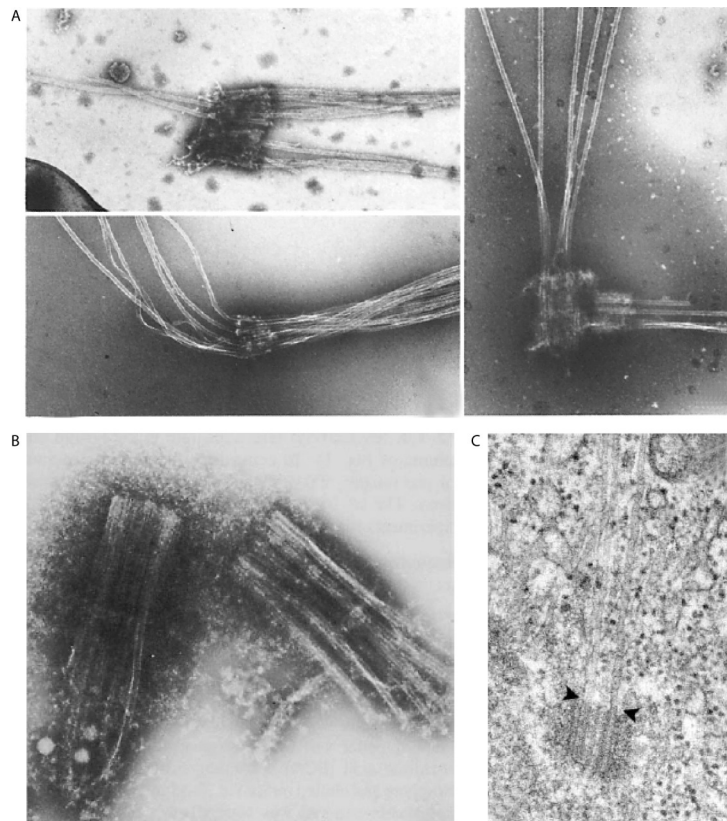
Figure 36. Electron micrographs showing abnormal elongation of distal centriolar MTs.

(A) Purified interphase centrioles after incubation with tubulin in polymerization buffer. Tubulin has polymerized onto a centriole pair (left, top), a pro-centriole (left, bottom), and a centriole/pro-centriole pair (right). In each case growth onto the distal end is favored (taken from (Gould and Borisy, 1977). (B) Whole-mount electron micrograph of centrioles isolated from taxol-treated cells. In most cases, microtubules were outgrowing from all of the triplet microtubules of centrioles (taken from (Raynaud-Messina et al., 2004). (C) Elongation of the centriole microtubules. The spindle microtubules resulted at least partly from the elongation of the distal ends of centriolar microtubules (arrowheads) (taken from (Kuriyama et al., 1986).

Copy number control and centriole amplification in tumor cells

The Plk4-induced flower-structures described here emphasize that parental centrioles are competent to support the simultaneous formation of multiple centrioles, extending previous observations (Anderson and Brenner, 1971; Duensing et al., 2007b; Vidwans et al., 2003). This clearly indicates that tight regulation of Plk4 activity is critical for controlling centriole numbers ('copy number control' (Nigg,

76

2007)) and raises the question of what mechanisms normally limit pro-centriole formation to one copy per pre-existing centriole? On the premise that parental centrioles constitute solid-state platforms to facilitate assembly rather than genuine 'templates', one plausible scenario would be that Plk4 marks potential assembly sites on the parental centriole cylinder by phosphorylating yet to be identified substrates. Plk4 activity is expected to be balanced by a counter-acting phosphatase and it will be crucial to determine whether mitogenic signalling and cell cycle cues operate through activation of Plk4, inhibition of the antagonistic phosphatase, or both. Next, a protein (hSas-6?) or protein complex present in limiting amounts might be recruited to a site marked by Plk4, thereby forming a 'seed' for a nascent pro-centriole. Under normal conditions, stabilization of a first seed (chosen at random) could constitute a rate-limiting step, whereas subsequent expansion of the nascent pro-centriolar structure would occur very rapidly, thereby consuming limiting material and preventing the utilization of secondary sites (akin to crystal growth). In response to excess Plk4 activity, however, multiple seeds can be stabilized simultaneously, leading to the concurrent formation of multiple pro-centrioles, as described here. Interestingly, formation of multiple pro-centrioles can apparently occur also on parental centrioles that already harbour one pro-centriole (Figure 21B). Live cell imaging will be required to determine whether the one pre-existing pro-centriole dissociates before the formation of multiple pro-centrioles, or whether new pro-centrioles form next to the pre-existing one. In either case, the data show that excess Plk4 overrides an S phase control that normally limits pro-centriole formation to one per parental centriole (Nigg, 2007).

Simultaneous formation of multiple centrioles could represent one important mechanism for rapid centrosome amplification in tumor cells (Duensing et al., 2007b). Thus, it will be interesting to examine how frequently Plk4 and/or other positive regulators of centriole biogenesis are upregulated in tumors. At first glance it may seem paradoxical that Plk4^{+/-} mice are prone to form tumors comprising supernumerary centrosomes (Ko *et al.*, 2005), since reduced levels of Plk4 are known to impair rather than enhance centrosome formation (Bettencourt-Dias *et al.*, 2005; Habedanck *et al.*, 2005). However, the centrosome amplification seen in Plk4^{+/-} cells may be explained by the cell division failures that occur upon depletion of Plk4, possibly as a consequence of abnormal spindle formation (Habedanck *et al.*, 2005).

With the identification of Plk4 as a key regulator of centriole biogenesis the stage is now set for studying its cell cycle regulation in both normal cells and tumor cells. Moreover, a key challenge for the future will be to identify the physiological substrates of this kinase.

MATERIALS & METHODS

Chemicals and materials

All chemicals were purchased from Merck, Sigma-Aldrich Chemical Company (Sigma, St Louis, MO), Fluka-Biochemika, Switzerland, or Roth, unless otherwise stated. Components of growth media for *E. coli* and yeast were from Difco Laboratories or Merck. The Minigel system was purchased from Bio-Rad and the Hoefer SemiPHor Blotting system from Pharmacia-Biotech. Tabletop centrifuges were from Eppendorf.

Sequence analysis

For identifying motifs and domains, hSfi1, CPAP and Cep135 protein sequences were analysed using ScanProsite (Gattiker *et al.*, 2002) whereas coiled-coil domains were scored using the COILS program (Lupas *et al.*, 1991). All programs were accessed from by web interface on www.expasy.ch.

Plasmid constructions

All cloning procedures were performed according to standard techniques as described in Molecular Cloning, A Laboratory Manual, 2nd editition, Sambrook, J.,Fritsch, E.F., Maniatis, T., Cold Spring Harbor Laboratory Press 1989 and Current Protocols in Molecular Biology, Wiley, 1999. Restriction enzyme reactions were carried out as specified by the suppliers (NEB) and ligation reactions were done using T4 DNA Ligase (NEB). Extraction of DNA from agarose gels and preparation of plasmid DNA was performed using kits from QIAGEN according to the manufacturer's instructions. For PCR reactions, the Pfu DNA polymerase PCR System was used as recommended by the manufacturer (Promega) and reactions were carried out in a RoboCycler Gradient 96 (Stratagene). All PCR products were checked by sequencing at Medigenomix (Martinsried, Germany).

hSfi1

Polymerase chain reaction was used to amplify full-length human hSfi1 from KIAA0542 clone (from Kazusa DNA Research Institute). The cDNA was then subcloned into the cloning vector pcDNA-TOPO4 (pCJW45.0, Table 4a). The

construct was verified by sequencing. For expression of recombinant hSfi1 fragments, bp 3394-3726 were PCR amplified, inserted into the cloning vector pcDNA-TOPO4 (Jk14, Table 4a) and confirmed by sequencing. The construct was subcloned into the expression vector pMalpFN (JK15, Table 4a). Maltose-binding protein (MBP)-tagged C-terminal hSfi1 (aa 1101-1211) was expressed in *E.coli* strain BL21(DE3) and purified under denaturing conditions using standard protocols (QIAexpressionist system, Qiagen). MBP was cleaved off using Precision Protease (Roche) according to the manufacturers protocol. The almost identical hSfi1 fragment (aa 1100-1211) construct was subcloned into the expression vector pGEX-5X-2 (Strategen, JK40, Table 4a), GST-tagged C-terminal hSfi1 (aa 1100-1211) was expressed in *E.coli* strain BL21(DE3) and purified under denaturing conditions using standard protocols (QIAexpressionist system, Qiagen).

Cep135

Polymerase chain reaction was used to amplify an incomplete cDNA of human Cep135 from the KIAA0635 clone (from Kazusa DNA Research Institute). The cDNA was then subcloned into a mammalian expression vector providing a C-terminal myc-tag (pCJW206, Table 4a). The construct was verified by sequencing. For expression of a recombinant Cep135 fragment (bp 2236-3654) were PCR amplified, inserted into the cloning vector pcDNA-TOPO4 (JK67, Table 4a) and confirmed by sequencing. The construct was subcloned into the expression vectors pET28b+ (Novagene, JK68, Table 4a) and pGEX-5X-2 (Stratagene, JK69, Table 4a). His6- and GST-tagged C-terminal Cep135 was expressed in *E.coli* strain BL21(DE3) and purified under denaturing conditions using standard protocols (QIAexpressionist system, Qiagen).

CPAP

Plasmids encoding CPAP (Hung *et al.*, 2000) were kindly provided by Dr. T. Tang (Institute of Biomedical Sciences, Academia Sinica, Taipei 115, Taiwan). For expression of a recombinant CPAP fragment, bp 3211-4011 were PCR amplified, inserted into the cloning vector pBSIISK (JK64, Table 4a) and confirmed by sequencing. The construct was subcloned into the expression vectors pET28b+ (Novagene, JK65, Table 4a) and pGEX-5X-2 (Stratagene, JK66, Table 4a). His6- and GST-tagged C-terminal CPAP was expressed in *E.coli* strain BL21(DE3) and

purified under denaturing conditions using standard protocols (QIAexpressionist system, Qiagen).

Antibody Production

Polyclonal antibodies were raised against hSfi1 (aa 1101-1211), Cep135 (aa 648-1145) and CPAP (aa 1071-1337) (all Charles River Laboratories, Romans, France). Antibodies were affinity-purified using GST-tagged antigens bound to Affigel (Biorad) according to standard protocols.

Cell culture and transfections.

All cells were grown at 37°C in a 5% CO2 atmosphere. HeLa, U2OS or HEK293T cells were cultured in Dulbecco's modified Eagle's medium (DMEM), supplemented with 10% heat-inactivated fetal calf serum and penicillin-streptomycin (100 i.u./ml and 100µg/ml, respectively, Gibco-BRL, Karlsruhe, Germany). HTERT-RPE1 cells were cultured in DMEM Nutrient Mixture F-12 Ham (Sigma, München, Germany) supplemented with 10% FCS (as above), penicillin-streptomycin (as above), 1% glutamine (PAN Biotech, Aidenbach, Germany; 200mM), and 0.35 % sodium bicarbonate (Sigma, Munich, Germany).

The tetracyclin-inducible cell-line expressing Myc-tagged Plk4 was kindly provided by J. Westendorf (Department of Cell Biology, Max-Planck-Institute for Biochemistry, D-82152 Martinsried). It was generated by transfection of U2OS-Trex cells (Invitrogen). Stable transformants were established by selection for 2 weeks with 1 mg ml^{-1} G418 (Invitrogen) and 50µg ml^{-1} hygromycin (Merck, Darmstadt, Germany). U2OS-cells were cultured as described previously (Habedanck *et al.*, 2005) and Myc-Plk4 expression was induced by the addition of 1µg ml^{-1} of tetracyclin.

siRNA-mediated protein depletion

Centrosomal proteins were depleted using siRNA duplex oligonucleotides (Dharmacon Research Inc, Lafayette, CO and Qiagen, Hilden, Germany) siRNA target sequences are listed in Table 2. An oligoduplex targeting luciferase was used as control (GL2, (Elbashir *et al.*, 2001). Transfections were performed using

Oligofectamin (Life Technologies, Karlsruhe, Germany) according to standard protocols.

Cell extracts, immunoblotting and immunoprecipitations

For immunblotting experiments, total cell extracts were washed once in PBS and lysed directly in gel sample buffer. For immunoprecipitations, total cell extracts of HEK293T or HeLaS3 cells were prepared by washing cells once in PBS, prior to lysis for 10 min (4°C) in (Co-) IP buffer (150 mM NaCl, 50 mM Tris-HCl pH8.0, 1% NP-40, 1 mM PMSF, protease inhibitor cocktail tablets (Roche)). Lysates were cleared by centrifuging for 15 min at 16,000xg, 4°C and incubated with prot-G beads bearing anti-10µg hSfi1, CPAP, Cep135 antibodies (see Table 3) for 2h at 4°C. Immunocomplexes bound to beads were then washed thrice with Co-IP wash buffer.

Immunoprecipitated proteins were eluted into Laemmli buffer, boiled for 8 min and separated by SDS-PAGE. Extracts were boiled for 5 min, and proteins resolved by SDS-PAGE. Immunoblotting was performed by electrophoretic transfer onto nitrocellulose membranes using a Semi-Phor blotting apparatus (Hoefer Scientific Instruments, San Francisco, CA). Proteins were visualized by Ponceau S staining, before blocking the membranes for one hour with blocking buffer (5% low-fat dried milk in 1x PBS + 0.1% Tween-20). Antibody incubations were carried out for 1-16h in blocking buffer, and bound IgGs were visualized using HRP conjugated goat anti-mouse or anti-rabbit antibodies (Jackson Immunoresearch). Signals were detected by enhanced chemiluminescence using ECL Supersignal reagents (Pierce Chemical Co.).

Cell cycle profiles of protein levels

To monitor the levels of hSfi1, Cep135 and CPAP expression during cell cycle progression, HeLaS3 cells were arrested at the G1/S boundary by double thymidine block or in mitosis by thymidine nocodazole treatment and released into fresh medium. Samples harvested at the indicated time points were subjected to immunoblotting analyses with the indicated antibodies.

Immunofluorescence (IF) microscopy

To maximize visualization of centrioles, cytoplasmic MTs were depolymerised by a 1h cold treatment (4℃) before cells were permeabilized and fixed by incubation for 30s in PBS, 0.5% Triton X-100, followed by 10min methanol (-20°C). After thouroughly washing in PBS, cells were incubated with primary antibodies (see Table 3) in blocking buffer (3% BSA, PBS) for 1 hour at room temperature, followed by staining with Alexa-Fluor conjugated goat secondary antibodies (Molecular probes). Secondary antibodies were Alexa-Fluor-488/-555-conjugated IgGs (1:1000, Molecular Probes). DNA was stained with 4,6-diamidino-2-phenylindole (DAPI; 0.2 µg/ml). Coverslips were mounted onto glass slides using mounting medium (phenylenediamine in 90% glycerol) and analysed using a Deltavision microscope on a Nikon TE200 base (Applied Precision, Issaquah, WA) equipped with an APOPLAN x100/1.4 n.a. oil-immersion objective. Serial optical sections obtained 0.2 µm apart along the Z-axis were processed using a deconvolution algorithm and projected into one picture using Softworx (Applied Precision). Exposure times and settings for image processing (deconvolution) were constant for all samples to be compared within any given experiment. Images were opened in Adobe Photoshop CS and then sized and placed in figures using Adobe Illustrator CS2 (Adobe Systems).

Immuno-electron microscopy (EM)

Electron microscopy was kindly performed by Y-D Stierhof (ZMBP, University of Tübingen, Germany). For electron microscopy, cells were grown on coverslips, fixed with 4% paraformaldehyd for 10 min, permeabilized with PBS+0.5% Triton X-100 for 2 min. Blocking and primary antibody incubations were performed as described for IF microscopy, followed by goat anti-mouse and anti-rabbit IgG-Nanogold (1:50 Nanoprobes) for 50 min.

Cells were further fixed with 2.5% glutaraldehyd in PBS for 60 min, washed with distilled water, and Nanogold was silver-enhanced with HQ Silver (Nanoprobes) for 8.5 min or with silver lactate/gum arabicum for 40-45 min (Stierhof *et al.*, 1991). After thouroughly washing with distilled water, cells were postfixed with 1% aqueousuranyl acetate, dehydrated in ethanol and embedded in epoxy resin (EPON®; Shell Chemical Co.). After polymerisation, the EPON® layer containing the cells was separated from the coverslip by dipping into liquid nitrogen. Ultrathin

sections were cut in parallel to the monolayer and stained with aqueous uranyl acetate and lead citrate.

Mass-spectrometry

Proteins isolated by co-immunoprecipitation with endogenous hSfi1 were kindly analysed by A. Ries and Dr. Roman Körner (Max-Planck Institute of Biochemistry, Martinsried, Germany) as previously described (Sauer *et al.*, 2005). Briefly, Coomassie Blue stained protein bands were in-gel digested (Shevchenko et al., 1996) by trypsin (Promega, sequencing grade). Peptides were desalted and concentrated using C18 extraction tips, and analysed with a CAPLC nano HPLC system (Waters, Milford) coupled to a Q-TOF mass spectrometer (Q-ToF, Ultima, Micromass, London, UK). Data were searched against the Mass Spectrometry Protein Sequence Database (MSDB, cscfserve. hh.med.ic.ac.uk/msdb.html) or the human International Protein Index database (www.ebi.ac.uk/IPI/IPIhelp.html) using in-house Mascot version 1.7 (www.matrixscience.com). Proteins identified by two or more peptides with a combined peptide score higher than 50 or by one single peptide with a score higher than 60 were considered significant, whereas all lower-scoring proteins were either included or discarded after inspection of individual spectra.

Centrosome preparations

Human centrosomes were purified from the T-lymphocyte KE-37 cell line according to the protocols reported in Andersen *et al.* (2003) and Moudjou and Bornens (1994).

RT-PCR

RNA purification was carried out using the QIAGEN RNeasy Mini Kit, according to the manufacturer`s protocol. Fragments of centrins 1, 2, 3 and Myc-Plk4 were amplified from isolated RNA using the Titan One Tube RT-PCR System (Roche) with isoform-specific primers. Control PCRs were performed using corresponding plasmid DNAs as templates. The following primers were used (5'-3'):

Centrin 1: CCCAGCGCTGCCTCCACCGGC, CTCCTCGTTCACTTCGCCG
Centrin 2: GCAAACATGGCATCAAGTTCTC, TTGCTCACTGACCTCTCCA
Centrin 3: GTGAGCTTGTAGTGGA, CTCTTGGTTTATTTCTCCA

Myc-Plk4: GGAGGACCTGAACCTGGAG,
CCTCGAGTCAACATAAAGGATGGTCCAAT

Quantitative Real-Time-PCR (qRT-PCR)

Quantitative Real-Time-PCR was kindly performed by P. Descombes (Genomics Platform, Univ. of Geneva) and Sebastien Lavoie (Department of Cell Biology, Max-Planck-Institute for Biochemistry, D-82152 Martinsried). To analyze expression levels of hSfi1, Cep135 and CPAP genes across the cell cycle, total RNA was extracted from HeLa S3 cells at different time points after release from a double thymidine block or a thymidine-nocodazole block using an Rneasy Mini Kit (QIAGEN, Hilden, Germany). For the analysis of siRNA efficiency, total RNA of HeLa S3 cells treated for 72 h with siRNA oligonucleotide duplexes targeting centrosomal protein genes (Table 2) was extracted. cDNAs were synthesized from the RNA samples using random hexamers and Superscript II reverse transcriptase (Invitrogen, Carlsbad, CA) following the manufacturer's instructions. PCR reactions contained cDNA, Power SYBR Green Master Mix (Applied Biosystems) and 300 nM of forward and reverse primers. Primers were designed with Primer Express Software (Applied Biosystems) and amplified fragment corresponded to an exon–exon junction. All primer sequences are available on request. qRT-PCR was carried out in optical 384-well plates and fluorescence was quantified with a Prism 7900 HT sequence detection system (Applied Biosystems). Samples were analyzed in triplicate and the raw data consisted of PCR cycle numbers required to reach a fluorescence threshold (Ct). Raw Ct values were obtained using SDS 2.0 (Applied Biosystems). The relative expression level of target genes was normalized according to geNorm (Vandesompele et al., 2002) using EEF1A1 (eukaryotic translation elongation factor a-1) and GusB (beta glucuronidase) genes as references to determine the normalization factor. The thermal profile recommended by Applied Biosystems was used for amplification (50°C for 2 min, 95°C for 10 min, 40 cycles of 95°C for 15 s and 60°C for 1 min). To verify the specificity of amplification, a melting curve analysis was included according to the thermal profile suggested by the manufacturer (95°C for 15 s, 60°C for 15 s, and 95°C for 15 s). The generated data were analyzed with SDS 2.2 software (Applied Biosystems). qRT-PCR results are listed in Table 2.

3dSIM image acquisition

3dSI microscopy was kindly performed by L. Schermelleh (Department of Biology II, LMU Munich). The custom-built microscope platform, termed "OMX" (Optical Microscope, eXperimental) has been developed in the laboratory of J. W. Sedat (UCSF) and will be described in detail in Schermelleh *et al.* (manuscript submitted). In brief, light from one of three lasers (405 nm, 488 nm, or 532 nm) is passed through a holographic diffuser before being coupled to a multimode fiberoptic cable, which focuses the light onto a diffraction grating. The grating splits the incident light into multiple orders, the innermost three of which (orders 0, +1, -1) interfere in the image plane to produce a sinusoidal pattern with a line spacing of approximately 0.2 µm. The pattern was made to illuminate sequential planes of the sample by moving the stage in the z-direction with a step size of 0.125 µm. For each z-section, 5 phases of the sinusoidal pattern were recorded sequentially by translating the diffraction grating between exposures. Three z-stacks are recorded one after the other in this manner with three angular orientations of the diffraction grating, 60° apart. The objective used was 100x, 1.4 NA, oil-immersion (Olympus). Emitted light from the sample passes through a set of four dichroic mirrors, which direct light based on its wavelength into four independently controlled EMCCD cameras (512x512 pixel with size of 8x8 µm, Andor, Inc). For multifluorescence experiments the color channels were recorded sequentially. Exposure times were between 100-500 ms, yielding typically 1,000 to 10,000 counts in a raw image of 16-bit dynamic range. To avoid extensive bleaching, a 300 ms pause was added between each exposure. Alignment of color channels was performed by custom Python scripts applying translation, rotation, and both isotropic and anisotropic scaling, using alignment parameters obtained from measurements with 100 nm multi-wavelength fluorescent beads (Molecular Probes) taken with the same camera setup as the biological samples. Raw images were saved to disk and processed with a dedicated algorithm (L. Shao, PhD thesis, UCSF) to reconstruct high-resolution information. Images were opened in Adobe Photoshop CS and then sized and placed in figures using Adobe Illustrator CS2 (Adobe Systems).

ABBREVIATIONS

All units are abbreviated according to the International Unit System.

AA: amino acid(s)

ATP: adenosine 5´-triphosphate

BSA: bovine serum albumin

DAPI: 4´,6-diamidino-2-phenylindole

DTT: dithiothreitol

ECL: enhanced chemiluminescence

EDTA: ethylenedinitrilotetraacetic acid

EGFP: enhanced green fluorescent protein

EM: electron microscopy

FCS: Fetal calf serum

GFP: green fluorescent protein

HCl: hydrochloric acid

HEPES: N-2-Hydroxyethylpiperazine-N`-2-ethane sulfonic acid

IgG: Immunoglobulin G

IP: Immunoprecipitation

IPTG: isopropyl-beta-D-thiogalactopyranoside

mAb: monoclonal antibody

MTOC: microtubule organising centre

PBS: Phosphate-buffered saline

PCR: Polymerase chain reaction

Plk4: Polo-like kinase 4

PMSF: phenylmethylsulfonyl fluoride

RNA: Ribonucleic Acid

RT: room temperature

SAK: Snk/Fnk akin kinase

SDS-PAGE: Sodium dodecylsulfate polyacrylamid gelelectrophoresis

siRNA: small interference Ribonucleic Acid

SPB: Spindle Pole Body

WT: wild-type

Table 2: List of siRNA oligos

Gene	Target sequence	Oligo	qRT-PCR (residual transcript)
hSas-6	5'-AAGCACGTTAATCAGCTACAA-3'	363	(Leidel *et al.*, 2005)
CPAP	5'-CCCAATGGAACTCGAAAGGAA-3'	251	IF (+++)
CPAP	5'-AAGGAAGATTGCACCAGTCAA-3'	250	IF (+++)
Cep135	5'-AAGCAGATTGAGCTAAGAGAA-3'	275	IF (++)
Cep135	5'-AAAGCTTATTGCTCATTTAAA-3'	274	IF (++)
CP110:	5'-TAGACTTATGCAGACAGATAA-3'	291	IF (++)
CP110	5'-CCCGAAATTATGCCAAAGTTA-3'	290	IF (++)
OFD-1	5'-CTCAGACAAGTTCGACATTTA-3'		IF (+)
FOP	5'-AAGTGATCAGGCGCTGTCAAC-3'	201	(Yan *et al.*, 2006)
Cap350	5'-ATGAACGATATCAGTGCTATA-3'	377	(Yan *et al.*, 2006)
C-Nap-1	5'-CTGGAAGAGCGTCTAACTGAT-3'	239	(Bahe *et al.*, 2005)
Pericentrin	5'-AAGCAGCTGAGCTGAAGGAGA-3'	236	(Dammermann and Merdes, 2002)
PCM-1	5'-AATCAGCTTCGTGATTCTCAG-3	405	(Dammermann and Merdes, 2002)
Ninein	5'-GCGGAGCTCT CTGAAGTTAAA-3'	299	IF (++)
Nek-2	5'-TTACGAGGATGTTAAACTTAA-3'	253	IF (+)
Cep170	5'-GAAGGAATCCTCCAAGTCA-3'	37/38	(Guarguaglini *et al.*, 2005)
Cep152	5'-GCGGATCCAACTGGAAATCTA-3'	277	28%
Cep192	5'-AACAGT GAATGTGCAAGTAAA-3'	281	33%
Cep57	5'-AGCCATCAAGGTCTAATGGAA-3'	259	13 %
Cep27	5'-CTGAAGAAAGTTATCTTTATA-3'	255	14 %
Cep41	5'-CACTGGTAACAG-TATGACTAA-3'	257	23%
Cep63	5'-CAACGCTTGAT TTATCAGCAA-3'	260	12%
Cep70	5'-GAAGATCGCATTGTCACTCAA-3'	265	12%
Cep72	5'-AGAGCTATGT-ATGATAATTAA-3'	266	50%
Cep76	5'-CTCGGTATTATAGGGCCAATA-3'	268	15%
Cep78	5'-CAGTTGTGTAAAG CTCTTAAA-3'	270	10%
Cep131	5'-CCCACTCAGCCCGGAACAATA-3'	272	11%
Cep164	5'-ACCACTGGGAATAGAAGACAA-3'	278	5%

Cep290	5'-TAGCCTCGAAAG-ACTAGTTAA-3'	285	23%
Cep215	5'-GTGGAAGATCTCCTAACTAAA-3'	283	17%
γ-tubulin	5'-AAGGAGGACATGTTCAAGGAA-3'		(Luders *et al.*, 2006)
centrin 2	5'-AAGAGCAAAAGCAGGAGATCC-3'	218	(Salisbury *et al.*, 2002)
centrin 3	5'-CTGGTGACATTT AAAGAATTA-3'	360	IF (++)

Table 2. siRNA screen for proteins involved in centriole biogenesis.

siRNA oligonucleotides: IF* or qRT-PCR (residual transcript):

*IF indicates that extent of depletion could be assessed by immunofluorescence microscopy: +++ nearly complete depletion (undetectable); ++ very good depletion (50-80%); + ca. 50 % depletion. Oligonucleotide duplexes were purchased from Dharmacon Research Inc., Layfayette, CO and Qiagen, Hilden, Germany.

Table 3: List of Antibodies

Number	Antigen	Made in	Dilution	Comment	Distributor/reference
R1	HSfi1	Rabbit	1:200	Affinity purified	This work
R2	HSfi1	Rabbit	n.d.	Affinity purified, unspecific	This work
738	Cep135	Rabbit	1:1000	Affinity purified	Kleylein-Sohn *et al.*, 2007
719	Cep135	Rabbit	1:1000	Serum	This work
729	CPAP	Rabbit	1:500(IF) 1:200(WB)	Affinity purified	Kleylein-Sohn *et al.*, 2007
730	CPAP	Rabbit	1:500(IF) 1:200(WB)	Affinity purified	This work
91-390	HSas-6	Mouse	Undiluted (IF)	Hybridoma supernatant	Kleylein-Sohn *et al.*, 2007-Kindly provided by M.LeClech
95-381	CPAP	Mouse	undiluted (IF)	Hybridoma supernatant	Kleylein-Sohn *et al.*, 2007-Kindly provided by M.LeClech
20H5	Centrin	Mouse	1:3000	Affinity purified	Kindly provided by J.Salisbury (Salisbury *et al.*, 2002)
R66/67	Centrin 2	Rabbit	1:500	Affinity purified	Kleylein-Sohn *et al.*, 2007
	ODF-2	Rabbit	1:1000	Affinity purified	Ishikawa *et al.*, 2005

R28	Cyclin A	Rabbit	1:500	Affinity purified	Maridor et al., 1993
36-298-4	Plk1	Mouse	1:3	Hybridoma tissue culture supernatant	Yamaguchi et al., 2005
DM1A	α-tubulin	Mouse	1:5000	FITC-Coupled	Sigma
GTU-88	γ-tubulin	Mouse	1:1000		Sigma
GT335	Poly-glutamylated tubulin	Mouse	1:1000	Affinity purified	Kindly provided by B. Edde
9E10	Myc	Mouse	undiluted (IF)	Hybridoma tissue culture supernatant	Evan et al., 1985
HE-12	Cyclin E	Mouse	1:5	Hybridoma tissue culture supernatant	Kindly provided by J.Bartek (Danish Cancer Society, Copenhagen
519-689	Plk4	Rabbit	1:500	Affinity purified	Kindly provided by J. Westendorf
-	CP110	Rabbit	1:500	Affinity purified	Kindly provided by B.Dynlacht (Chen et al., 2002)

Table 4: List of Plasmids and Primers

Table 4a: Plasmids

Plasmids pCSM45.0 and pCSM7.1 were generated by C. Wilkinson.

Name	Gene	Species	Insert	Vector	Tag
pCSM45.0	Sfi1	human	1-1211	pcDNA4-Topo	-
JK14	Sfi1	human	aa 1101-1211	pcDNA4-Topo	-
JK15	Sfi1	human	aa 1101-1211	pMalpFN	MBP
JK36	Sfi1	human	aa 1100-1211	pBS	-
JK40	Sfi1	human	aa 1100-1211	pGEX-5X-2	GST
pCSM7.1	Cep135	human	aa 295-1140	pEGFP-C1	GFP
JK67	Cep135	human	aa 648-1140	pcDNA4-Topo	-
JK68	Cep135	human	aa 648-1140	pCJW227	HIS
JK69	Cep135	human	aa 648-1140	pGEX-5X-2	GST
JK64	CPAP	human	aa 1070-1338	pBS	-
JK65	CPAP	human	aa 1070-1338	PCJW227	HIS
JK66	CPAP	human	aa 1070-1338	pGEX-5X-2	GST

Table 4b: Primers

Primer-name	Sequence (5' – 3')	Plasmids
M2245	TTGGCCGGCCTGACCGACTGCAGCCGGAGGTCAGCCCAGCAG	JK14, JK15
M2246	TTGCGGCCGCCTAGTGGTGGTGGTGGTGGTGGCACAGGGCCTG CCGCAGGGCCT	JK14, JK15
M2746	GGATCCCCTTCTCAGCCACCAGGGCTGGGCC	JK36, JK40
M2307	CTCGAGGCACAGGGCCTGCCGCAGGGCCT	JK36, JK40
M3560	GAGAAGTGAGCTTGTAGTGGACAAAAC	JK67, JK68,
M3610	GGGATCCCCGCTCAAAAATTTAGCCATGTGG	JK67, JK68,
M3350	GGGATCCCCCTTGCGAACACATCTGTTCG	JK64, JK65,
M3354	CGTCGACCAGCTCCGTGTCCATTGACACATTAC	JK64, JK65,

ACKNOWLEDGEMENTS

REFERENCES

Adams, I.R., and Kilmartin, J.V. (1999). Localization of core spindle pole body (SPB) components during SPB duplication in Saccharomyces cerevisiae. The Journal of cell biology *145*, 809-823.

Alvey, P.L. (1985). An investigation of the centriole cycle using 3T3 and CHO cells. Journal of cell science *78*, 147-162.

Andersen, J.S., Wilkinson, C.J., Mayor, T., Mortensen, P., Nigg, E.A., and Mann, M. (2003). Proteomic characterization of the human centrosome by protein correlation profiling. Nature *426*, 570-574.

Anderson, R.G., and Brenner, R.M. (1971). The formation of basal bodies (centrioles) in the Rhesus monkey oviduct. J Cell Biol *50*, 10-34.

Anderson, V.E., Prudden, J., Prochnik, S., Giddings, T.H., Jr., and Hardwick, K.G. (2007). Novel sfi1 alleles uncover additional functions for Sfi1p in bipolar spindle assembly and function. Molecular biology of the cell *18*, 2047-2056.

Araki, M., Masutani, C., Takemura, M., Uchida, A., Sugasawa, K., Kondoh, J., Ohkuma, Y., and Hanaoka, F. (2001). Centrosome protein centrin 2/caltractin 1 is part of the xeroderma pigmentosum group C complex that initiates global genome nucleotide excision repair. The Journal of biological chemistry *276*, 18665-18672.

Azimzadeh, J.a.B., M. (2004). The Centrosome in Evolution, In 'Centrosomes in Development and Disease'. E.A.Nigg, editor. Weinheim: Wiley-VCH. pp. 93-122.

Badano, J.L., Mitsuma, N., Beales, P.L., and Katsanis, N. (2006). The Ciliopathies: An Emerging Class of Human Genetic Disorders. Annu Rev Genomics Hum Genet *7*, 125-148.

Bahe, S., Stierhof, Y.D., Wilkinson, C.J., Leiss, F., and Nigg, E.A. (2005). Rootletin forms centriole-associated filaments and functions in centrosome cohesion. J Cell Biol *171*, 27-33.

Balczon, R., Bao, L., and Zimmer, W.E. (1994). PCM-1, A 228-kD centrosome autoantigen with a distinct cell cycle distribution. The Journal of cell biology *124*, 783-793.

Baron, A.T., Greenwood, T.M., Bazinet, C.W., and Salisbury, J.L. (1992). Centrin is a component of the pericentriolar lattice. Biol Cell *76*, 383-388.

Basto, R., Lau, J., Vinogradova, T., Gardiol, A., Woods, C.G., Khodjakov, A., and Raff, J.W. (2006). Flies without centrioles. Cell *125*, 1375-1386.

Beales, P.L., Bland, E., Tobin, J.L., Bacchelli, C., Tuysuz, B., Hill, J., Rix, S., Pearson, C.G., Kai, M., Hartley, J.*, et al.* (2007). IFT80, which encodes a conserved intraflagellar transport protein, is mutated in Jeune asphyxiating thoracic dystrophy. Nature genetics *39*, 727-729.

Beisson, J., and Wright, M. (2003). Basal body/centriole assembly and continuity. Curr Opin Cell Biol *15*, 96-104.

Berdnik, D., and Knoblich, J.A. (2002). Drosophila Aurora-A is required for centrosome maturation and actin-dependent asymmetric protein localization during mitosis. Curr Biol *12*, 640-647.

Bettencourt-Dias, M., and Glover, D.M. (2007). Centrosome biogenesis and function: centrosomics brings new understanding. Nature reviews *8*, 451-463.

Bettencourt-Dias, M., Rodrigues-Martins, A., Carpenter, L., Riparbelli, M., Lehmann, L., Gatt, M.K., Carmo, N., Balloux, F., Callaini, G., and Glover, D.M. (2005). SAK/PLK4 is required for centriole duplication and flagella development. Curr Biol *15*, 2199-2207.

Biggins, S., and Rose, M.D. (1994). Direct interaction between yeast spindle pole body components: Kar1p is required for Cdc31p localization to the spindle pole body. The Journal of cell biology *125*, 843-852.

Blangy, A., Lane, H.A., d'Herin, P., Harper, M., Kress, M., and Nigg, E.A. (1995). Phosphorylation by p34cdc2 regulates spindle association of human Eg5, a kinesin-related motor essential for bipolar spindle formation in vivo. Cell *83*, 1159-1169.

Blow, J.J., and Dutta, A. (2005). Preventing re-replication of chromosomal DNA. Nature reviews *6*, 476-486.

Bobinnec, Y., Moudjou, M., Fouquet, J.P., Desbruyeres, E., Edde, B., and Bornens, M. (1998). Glutamylation of centriole and cytoplasmic tubulin in proliferating non-neuronal cells. Cell Motil Cytoskeleton *39*, 223-232.

Bond, J., Roberts, E., Springell, K., Lizarraga, S.B., Scott, S., Higgins, J., Hampshire, D.J., Morrison, E.E., Leal, G.F., Silva, E.O.*, et al.* (2005). A centrosomal mechanism involving CDK5RAP2 and CENPJ controls brain size. Nature genetics *37*, 353-355.

Bornens, M. (2002). Centrosome composition and microtubule anchoring mechanisms. Curr Opin Cell Biol *14*, 25-34.

Boveri, T. (1914). Zur Frage der Entstehung maligner Tumoren. (English Translation: The Origin of Malignant Tumors, Williams and Wilkins, Baltimore, Maryland, 1929).

Brinkley, B.R. (2001). Managing the centrosome numbers game: from chaos to stability in cancer cell division. Trends Cell Biol *11*, 18-21.

Brinkley, B.R., Stubblefield, E., and Hsu, T.C. (1967). The effects of colcemid inhibition and reversal on the fine structure of the mitotic apparatus of Chinese hamster cells in vitro. J Ultrastruct Res *19*, 1-18.

Budhu, A.S., and Wang, X.W. (2005). Loading and unloading: orchestrating centrosome duplication and spindle assembly by Ran/Crm1. Cell cycle (Georgetown, Tex *4*, 1510-1514.

Byers, B. (1981). Multiple roles of the spindle pole body in the life cycle of Saccharomyces cerevisiae. Molecular Genetics in Yeast, edited by D. von Wettstein, J. Friis, M. Kiellandbrandt and A. Stenderup. Munksgaard, Copenhagen. pp. 119-133.

Carroll, P.E., Okuda, M., Horn, H.F., Biddinger, P., Stambrook, P.J., Gleich, L.L., Li, Y.Q., Tarapore, P., and Fukasawa, K. (1999). Centrosome hyperamplification in human cancer: chromosome instability induced by p53 mutation and/or Mdm2 overexpression. Oncogene *18*, 1935-1944.

Cavalier-Smith, T. (1974). Basal body and flagellar development during the vegetative cell cycle and the sexual cycle of Chlamydomonas reinhardii. J Cell Sci *16*, 529-556.

Chang, P., Giddings, T.H., Jr., Winey, M., and Stearns, T. (2003). Epsilon-tubulin is required for centriole duplication and microtubule organization. Nature cell biology *5*, 71-76.

Charbonnier, J.B., Christova, P., Shosheva, A., Stura, E., Le Du, M.H., Blouquit, Y., Duchambon, P., Miron, S., and Craescu, C.T. (2006). Crystallization and preliminary X-ray diffraction data of the complex between human centrin 2 and a peptide from the protein XPC. Acta crystallographica *62*, 649-651.

Chen, Z., Indjeian, V.B., McManus, M., Wang, L., and Dynlacht, B.D. (2002). CP110, a cell cycle-dependent CDK substrate, regulates centrosome duplication in human cells. Dev Cell *3*, 339-350.

Chretien, D., Buendia, B., Fuller, S.D., and Karsenti, E. (1997). Reconstruction of the centrosome cycle from cryoelectron micrographs. J Struct Biol *120*, 117-133.

Cowan, C.R., and Hyman, A.A. (2006). Cyclin E-Cdk2 temporally regulates centrosome assembly and establishment of polarity in Caenorhabditis elegans embryos. Nat Cell Biol *8*, 1441-1447.

Dammermann, A., and Merdes, A. (2002). Assembly of centrosomal proteins and microtubule organization depends on PCM-1. J Cell Biol *159*, 255-266.

Dammermann, A., Muller-Reichert, T., Pelletier, L., Habermann, B., Desai, A., and Oegema, K. (2004). Centriole assembly requires both centriolar and pericentriolar material proteins. Developmental cell *7*, 815-829.

Delattre, M., Canard, C., and Gonczy, P. (2006). Sequential protein recruitment in C. elegans centriole formation. Curr Biol *16*, 1844-1849.

Delattre, M., and Gonczy, P. (2004). The arithmetic of centrosome biogenesis. J Cell Sci *117*, 1619-1630.

Delattre, M., Leidel, S., Wani, K., Baumer, K., Bamat, J., Schnabel, H., Feichtinger, R., Schnabel, R., and Gonczy, P. (2004). Centriolar SAS-5 is required for centrosome duplication in C. elegans. Nat Cell Biol *6*, 656-664.

Dictenberg, J.B., Zimmerman, W., Sparks, C.A., Young, A., Vidair, C., Zheng, Y., Carrington, W., Fay, F.S., and Doxsey, S.J. (1998). Pericentrin and gamma-tubulin form a protein complex and are organized into a novel lattice at the centrosome. The Journal of cell biology *141*, 163-174.

Dippell, R.V. (1968). The development of basal bodies in paramecium. Proc Natl Acad Sci U S A *61*, 461-468.

Doxsey, S. (2001). Re-evaluating centrosome function. Nature reviews *2*, 688-698.

Doxsey, S., McCollum, D., and Theurkauf, W. (2005). Centrosomes in cellular regulation. Annual review of cell and developmental biology *21*, 411-434.

Dualan, R., Brody, T., Keeney, S., Nichols, A.F., Admon, A., and Linn, S. (1995). Chromosomal localization and cDNA cloning of the genes (DDB1 and DDB2) for the p127 and p48 subunits of a human damage-specific DNA binding protein. Genomics *29*, 62-69.

Duensing, A., Liu, Y., Perdreau, S.A., Kleylein-Sohn, J., Nigg, E.A., and Duensing, S. (2007a). Centriole overduplication through the concurrent formation of multiple daughter centrioles at single maternal templates. Oncogene *26*, 6280-6288.

Duensing, A., Liu, Y., Perdreau, S.A., Kleylein-Sohn, J., Nigg, E.A., and Duensing, S. (2007b). Centriole overduplication through the concurrent formation of multiple daughter centrioles at single maternal templates. Oncogene.

Duensing, A., Liu, Y., Tseng, M., Malumbres, M., Barbacid, M., and Duensing, S. (2006). Cyclin-dependent kinase 2 is dispensable for normal centrosome duplication but required for oncogene-induced centrosome overduplication. Oncogene *25*, 2943-2949.

Dutcher, S.K. (2003). Long-lost relatives reappear: identification of new members of the tubulin superfamily. Current opinion in microbiology *6*, 634-640.

Dutcher, S.K. (2004). Dissection of Basal Body and Centriole Function in the Unicellular Green Alga Chlamydomonas reinhardtii, In 'Centrosomes in Development and Disease'. E.A.Nigg, editor. Weinheim: Wiley-VCH. pp. 71-92.

Elbashir, S.M., Harborth, J., Lendeckel, W., Yalcin, A., Weber, K., and Tuschl, T. (2001). Duplexes of 21-nucleotide RNAs mediate RNA interference in cultured mammalian cells. Nature *411*, 494-498.

Fode, C., Motro, B., Yousefi, S., Heffernan, M., and Dennis, J.W. (1994). Sak, a murine protein-serine/threonine kinase that is related to the Drosophila polo kinase and involved in cell proliferation. Proc Natl Acad Sci U S A *91*, 6388-6392.

Fry, A.M., Mayor, T., Meraldi, P., Stierhof, Y.D., Tanaka, K., and Nigg, E.A. (1998). C-Nap1, a novel centrosomal coiled-coil protein and candidate substrate of the cell cycle-regulated protein kinase Nek2. The Journal of cell biology *141*, 1563-1574.

Fuchs, S.Y., Spiegelman, V.S., and Kumar, K.G. (2004). The many faces of beta-TrCP E3 ubiquitin ligases: reflections in the magic mirror of cancer. Oncogene *23*, 2028-2036.

Fujiwara, T., Bandi, M., Nitta, M., Ivanova, E.V., Bronson, R.T., and Pellman, D. (2005). Cytokinesis failure generating tetraploids promotes tumorigenesis in p53-null cells. Nature *437*, 1043-1047.

Fukasawa, K., Choi, T., Kuriyama, R., Rulong, S., and Vande Woude, G.F. (1996). Abnormal centrosome amplification in the absence of p53. Science (New York, NY *271*, 1744-1747.

Fuller, S.D., Gowen, B.E., Reinsch, S., Sawyer, A., Buendia, B., Wepf, R., and Karsenti, E. (1995). The core of the mammalian centriole contains gamma-tubulin. Curr Biol *5*, 1384-1393.

Gadde, S., and Heald, R. (2004). Mechanisms and molecules of the mitotic spindle. Curr Biol *14*, R797-805.

Gattiker, A., Gasteiger, E., and Bairoch, A. (2002). ScanProsite: a reference implementation of a PROSITE scanning tool. Applied bioinformatics *1*, 107-108.

Gavet, O., Alvarez, C., Gaspar, P., and Bornens, M. (2003). Centrin4p, a novel mammalian centrin specifically expressed in ciliated cells. Mol Biol Cell *14*, 1818-1834.

Ghadimi, B.M., Sackett, D.L., Difilippantonio, M.J., Schrock, E., Neumann, T., Jauho, A., Auer, G., and Ried, T. (2000). Centrosome amplification and instability occurs exclusively in aneuploid, but not in diploid colorectal cancer cell lines, and correlates with numerical chromosomal aberrations. Genes, chromosomes & cancer *27*, 183-190.

Giet, R., Uzbekov, R., Kireev, I., and Prigent, C. (1999). The Xenopus laevis centrosome aurora/Ipl1-related kinase. Biology of the cell / under the auspices of the European Cell Biology Organization *91*, 461-470.

Glover, D.M., Leibowitz, M.H., McLean, D.A., and Parry, H. (1995). Mutations in aurora prevent centrosome separation leading to the formation of monopolar spindles. Cell *81*, 95-105.

Goepfert, T.M.a.B., W.R. (2004). Centrosome Anomalies in Cancer: From Early Observations to Animal Models. In 'Centrosomes in Development and Disease'. E.A.Nigg, editor. Weinheim: Wiley-VCH.pp. 323-336.

Golsteyn, R.M., Mundt, K.E., Fry, A.M., and Nigg, E.A. (1995). Cell cycle regulation of the activity and subcellular localization of Plk1, a human protein kinase implicated in mitotic spindle function. The Journal of cell biology *129*, 1617-1628.

Gould, R.R., and Borisy, G.G. (1977). The pericentriolar material in Chinese hamster ovary cells nucleates microtubule formation. J Cell Biol *73*, 601-615.

Graser, S., Stierhof, Y.D., Lavoie, S.B., Gassner, O.S., Lamla, S., Le Clech, M., and Nigg, E.A. (2007). Cep164, a novel centriole appendage protein required for primary cilium formation. The Journal of cell biology *179*, 321-330.

Guarguaglini, G., Duncan, P.I., Stierhof, Y.D., Holmstrom, T., Duensing, S., and Nigg, E.A. (2005). The forkhead-associated domain protein Cep170 interacts with

Polo-like kinase 1 and serves as a marker for mature centrioles. Mol Biol Cell *16*, 1095-1107.

Gustafsson, M.G. (2000). Surpassing the lateral resolution limit by a factor of two using structured illumination microscopy. Journal of microscopy *198*, 82-87.

Habedanck, R., Stierhof, Y.D., Wilkinson, C.J., and Nigg, E.A. (2005). The Polo kinase Plk4 functions in centriole duplication. Nat Cell Biol *7*, 1140-1146.

Hagiwara, H., Ohwada, N., and Takata, K. (2004). Cell biology of normal and abnormal ciliogenesis in the ciliated epithelium. International review of cytology *234*, 101-141.

Hannak, E., Kirkham, M., Hyman, A.A., and Oegema, K. (2001). Aurora-A kinase is required for centrosome maturation in Caenorhabditis elegans. The Journal of cell biology *155*, 1109-1116.

Haren, L., Remy, M.H., Bazin, I., Callebaut, I., Wright, M., and Merdes, A. (2006). NEDD1-dependent recruitment of the gamma-tubulin ring complex to the centrosome is necessary for centriole duplication and spindle assembly. The Journal of cell biology *172*, 505-515.

Hart, P.E., Glantz, J.N., Orth, J.D., Poynter, G.M., and Salisbury, J.L. (1999). Testis-specific murine centrin, Cetn1: genomic characterization and evidence for retroposition of a gene encoding a centrosome protein. Genomics *60*, 111-120.

Hell, S.W. (2007). Far-field optical nanoscopy. Science (New York, NY *316*, 1153-1158.

Hildebrandt, F., and Zhou, W. (2007). Nephronophthisis-associated ciliopathies. J Am Soc Nephrol *18*, 1855-1871.

Hinchcliffe, E.H., Li, C., Thompson, E.A., Maller, J.L., and Sluder, G. (1999). Requirement of Cdk2-cyclin E activity for repeated centrosome reproduction in Xenopus egg extracts. Science *283*, 851-854.

Huang, B., Mengersen, A., and Lee, V.D. (1988). Molecular cloning of cDNA for caltractin, a basal body-associated Ca2+-binding protein: homology in its protein sequence with calmodulin and the yeast CDC31 gene product. The Journal of cell biology *107*, 133-140.

Hung, L.Y., Tang, C.J., and Tang, T.K. (2000). Protein 4.1 R-135 interacts with a novel centrosomal protein (CPAP) which is associated with the gamma-tubulin complex. Mol Cell Biol *20*, 7813-7825.

Ishikawa, H., Kubo, A., Tsukita, S., and Tsukita, S. (2005). Odf2-deficient mother centrioles lack distal/subdistal appendages and the ability to generate primary cilia. Nat Cell Biol *7*, 517-524.

Jaspersen, S.L., Giddings, T.H., Jr., and Winey, M. (2002). Mps3p is a novel component of the yeast spindle pole body that interacts with the yeast centrin homologue Cdc31p. The Journal of cell biology *159*, 945-956.

Jones, M.H., and Winey, M. (2006). Centrosome duplication: is asymmetry the clue? Curr Biol *16*, R808-810.

Keller, L.C., Romijn, E.P., Zamora, I., Yates, J.R., 3rd, and Marshall, W.F. (2005). Proteomic analysis of isolated chlamydomonas centrioles reveals orthologs of ciliary-disease genes. Curr Biol *15*, 1090-1098.

Kemp, C.A., Kopish, K.R., Zipperlen, P., Ahringer, J., and O'Connell, K.F. (2004). Centrosome maturation and duplication in C. elegans require the coiled-coil protein SPD-2. Dev Cell *6*, 511-523.

Keryer, G., Witczak, O., Delouvee, A., Kemmner, W.A., Rouillard, D., Tasken, K., and Bornens, M. (2003). Dissociating the centrosomal matrix protein AKAP450 from centrioles impairs centriole duplication and cell cycle progression. Molecular biology of the cell *14*, 2436-2446.

Khodjakov, A., Rieder, C.L., Sluder, G., Cassels, G., Sibon, O., and Wang, C.L. (2002). De novo formation of centrosomes in vertebrate cells arrested during S phase. The Journal of cell biology *158*, 1171-1181.

Kilmartin, J.V. (2003). Sfi1p has conserved centrin-binding sites and an essential function in budding yeast spindle pole body duplication. The Journal of cell biology *162*, 1211-1221.

Kirkham, M., Muller-Reichert, T., Oegema, K., Grill, S., and Hyman, A.A. (2003). SAS-4 is a C. elegans centriolar protein that controls centrosome size. Cell *112*, 575-587.

Klink, V.P., and Wolniak, S.M. (2001). Centrin is necessary for the formation of the motile apparatus in spermatids of Marsilea. Molecular biology of the cell *12*, 761-776.

Ko, M.A., Rosario, C.O., Hudson, J.W., Kulkarni, S., Pollett, A., Dennis, J.W., and Swallow, C.J. (2005). Plk4 haploinsufficiency causes mitotic infidelity and carcinogenesis. Nature genetics *37*, 883-888.

Koblenz, B., Schoppmeier, J., Grunow, A., and Lechtreck, K.F. (2003). Centrin deficiency in Chlamydomonas causes defects in basal body replication, segregation and maturation. J Cell Sci *116*, 2635-2646.

Kochanski, R.S., and Borisy, G.G. (1990). Mode of centriole duplication and distribution. The Journal of cell biology *110*, 1599-1605.

Krishan, A., and Buck, R.C. (1965). Structure of the Mitotic Spindle in L Strain Fibroblasts. J Cell Biol *24*, 433-444.

Kuriyama, R., and Borisy, G.G. (1981). Centriole cycle in Chinese hamster ovary cells as determined by whole-mount electron microscopy. The Journal of cell biology *91*, 814-821.

Kuriyama, R., Dasgupta, S., and Borisy, G.G. (1986). Independence of centriole formation and initiation of DNA synthesis in Chinese hamster ovary cells. Cell motility and the cytoskeleton *6*, 355-362.

La Terra, S., English, C.N., Hergert, P., McEwen, B.F., Sluder, G., and Khodjakov, A. (2005). The de novo centriole assembly pathway in HeLa cells: cell cycle progression and centriole assembly/maturation. J Cell Biol *168*, 713-722.

Lacey, K.R., Jackson, P.K., and Stearns, T. (1999). Cyclin-dependent kinase control of centrosome duplication. Proc Natl Acad Sci U S A *96*, 2817-2822.

Lane, H.A., and Nigg, E.A. (1996). Antibody microinjection reveals an essential role for human polo-like kinase 1 (Plk1) in the functional maturation of mitotic centrosomes. The Journal of cell biology *135*, 1701-1713.

Lange, B.M., and Gull, K. (1996). Structure and function of the centriole in animal cells: progress and questions. Trends Cell Biol *6*, 348-352.

Laoukili, J., Perret, E., Middendorp, S., Houcine, O., Guennou, C., Marano, F., Bornens, M., and Tournier, F. (2000). Differential expression and cellular distribution of centrin isoforms during human ciliated cell differentiation in vitro. J Cell Sci *113 (Pt 8)*, 1355-1364.

Leidel, S., Delattre, M., Cerutti, L., Baumer, K., and Gonczy, P. (2005). SAS-6 defines a protein family required for centrosome duplication in C. elegans and in human cells. Nat Cell Biol *7*, 115-125.

Leidel, S., and Gonczy, P. (2003). SAS-4 is essential for centrosome duplication in C elegans and is recruited to daughter centrioles once per cell cycle. Dev Cell *4*, 431-439.

Leidel, S., and Gonczy, P. (2005). Centrosome duplication and nematodes: recent insights from an old relationship. Developmental cell *9*, 317-325.

Li, S., Sandercock, A.M., Conduit, P., Robinson, C.V., Williams, R.L., and Kilmartin, J.V. (2006). Structural role of Sfi1p-centrin filaments in budding yeast spindle pole body duplication. The Journal of cell biology *173*, 867-877.

Lingle, W.L., Barrett, S.L., Negron, V.C., D'Assoro, A.B., Boeneman, K., Liu, W., Whitehead, C.M., Reynolds, C., and Salisbury, J.L. (2002). Centrosome amplification drives chromosomal instability in breast tumor development. Proceedings of the National Academy of Sciences of the United States of America *99*, 1978-1983.

Lingle, W.L., Lutz, W.H., Ingle, J.N., Maihle, N.J., and Salisbury, J.L. (1998). Centrosome hypertrophy in human breast tumors: implications for genomic stability

and cell polarity. Proceedings of the National Academy of Sciences of the United States of America *95*, 2950-2955.

Lingle, W.L., and Salisbury, J.L. (2001). Methods for the analysis of centrosome reproduction in cancer cells. Methods in cell biology *67*, 325-336.

Luders, J., Patel, U.K., and Stearns, T. (2006). GCP-WD is a gamma-tubulin targeting factor required for centrosomal and chromatin-mediated microtubule nucleation. Nature cell biology *8*, 137-147.

Luders, J., and Stearns, T. (2007). Microtubule-organizing centres: a re-evaluation. Nature reviews *8*, 161-167.

Lupas, A., Van Dyke, M., and Stock, J. (1991). Predicting coiled coils from protein sequences. Science (New York, NY *252*, 1162-1164.

Ma, P., Winderickx, J., Nauwelaers, D., Dumortier, F., De Doncker, A., Thevelein, J.M., and Van Dijck, P. (1999). Deletion of SFI1, a novel suppressor of partial Ras-cAMP pathway deficiency in the yeast Saccharomyces cerevisiae, causes G(2) arrest. Yeast (Chichester, England) *15*, 1097-1109.

Machida, Y.J., and Dutta, A. (2005). Cellular checkpoint mechanisms monitoring proper initiation of DNA replication. The Journal of biological chemistry *280*, 6253-6256.

Marshall, W.F., and Nonaka, S. (2006). Cilia: tuning in to the cell's antenna. Curr Biol *16*, R604-614.

Marshall, W.F., Vucica, Y., and Rosenbaum, J.L. (2001). Kinetics and regulation of de novo centriole assembly. Implications for the mechanism of centriole duplication. Curr Biol *11*, 308-317.

Mathias, N., Johnson, S.L., Winey, M., Adams, A.E., Goetsch, L., Pringle, J.R., Byers, B., and Goebl, M.G. (1996). Cdc53p acts in concert with Cdc4p and Cdc34p to control the G1-to-S-phase transition and identifies a conserved family of proteins. Molecular and cellular biology *16*, 6634-6643.

Matsumoto, Y., Hayashi, K., and Nishida, E. (1999). Cyclin-dependent kinase 2 (Cdk2) is required for centrosome duplication in mammalian cells. Curr Biol *9*, 429-432.

Matsuura, K., Lefebvre, P.A., Kamiya, R., and Hirono, M. (2004). Bld10p, a novel protein essential for basal body assembly in Chlamydomonas: localization to the cartwheel, the first ninefold symmetrical structure appearing during assembly. J Cell Biol *165*, 663-671.

Mayor, T., Stierhof, Y.D., Tanaka, K., Fry, A.M., and Nigg, E.A. (2000). The centrosomal protein C-Nap1 is required for cell cycle-regulated centrosome cohesion. The Journal of cell biology *151*, 837-846.

Meraldi, P., Lukas, J., Fry, A.M., Bartek, J., and Nigg, E.A. (1999). Centrosome duplication in mammalian somatic cells requires E2F and Cdk2-cyclin A. Nat Cell Biol *1*, 88-93.

Meraldi, P., and Nigg, E.A. (2001). Centrosome cohesion is regulated by a balance of kinase and phosphatase activities. Journal of cell science *114*, 3749-3757.

Middendorp, S., Paoletti, A., Schiebel, E., and Bornens, M. (1997). Identification of a new mammalian centrin gene, more closely related to Saccharomyces cerevisiae CDC31 gene. Proc Natl Acad Sci U S A *94*, 9141-9146.

Mizukami, I., and Gall, J. (1966). Centriole replication. II. Sperm formation in the fern, Marsilea, and the cycad, Zamia. J Cell Biol *29*, 97-111.

Murphy, T.D. (2003). Drosophila skpA, a component of SCF ubiquitin ligases, regulates centrosome duplication independently of cyclin E accumulation. Journal of cell science *116*, 2321-2332.

Nachury, M.V., Loktev, A.V., Zhang, Q., Westlake, C.J., Peranen, J., Merdes, A., Slusarski, D.C., Scheller, R.H., Bazan, J.F., Sheffield, V.C.*, et al.* (2007). A core complex of BBS proteins cooperates with the GTPase Rab8 to promote ciliary membrane biogenesis. Cell *129*, 1201-1213.

Nigg, E.A. (2002). Centrosome aberrations: cause or consequence of cancer progression? Nature reviews *2*, 815-825.

Nigg, E.A. (2007). Centrosome duplication: of rules and licenses. Trends Cell Biol *17*, 215-221.

Nishi, R., Okuda, Y., Watanabe, E., Mori, T., Iwai, S., Masutani, C., Sugasawa, K., and Hanaoka, F. (2005). Centrin 2 stimulates nucleotide excision repair by interacting with xeroderma pigmentosum group C protein. Molecular and cellular biology *25*, 5664-5674.

O'Connell, K.F., Caron, C., Kopish, K.R., Hurd, D.D., Kemphues, K.J., Li, Y., and White, J.G. (2001). The C. elegans zyg-1 gene encodes a regulator of centrosome duplication with distinct maternal and paternal roles in the embryo. Cell *105*, 547-558.

O'Connell, K.F., Leys, C.M., and White, J.G. (1998). A genetic screen for temperature-sensitive cell-division mutants of Caenorhabditis elegans. Genetics *149*, 1303-1321.

Ohta, T., Essner, R., Ryu, J.H., Palazzo, R.E., Uetake, Y., and Kuriyama, R. (2002). Characterization of Cep135, a novel coiled-coil centrosomal protein involved in microtubule organization in mammalian cells. J Cell Biol *156*, 87-99.

Oshimori, N., Ohsugi, M., and Yamamoto, T. (2006). The Plk1 target Kizuna stabilizes mitotic centrosomes to ensure spindle bipolarity. Nature cell biology *8*, 1095-1101.

Paintrand, M., Moudjou, M., Delacroix, H., and Bornens, M. (1992). Centrosome organization and centriole architecture: their sensitivity to divalent cations. J Struct Biol *108*, 107-128.

Palazzo, R.E., Vogel, J.M., Schnackenberg, B.J., Hull, D.R., and Wu, X. (2000). Centrosome maturation. Current topics in developmental biology *49*, 449-470.

Paoletti, A., Bordes, N., Haddad, R., Schwartz, C.L., Chang, F., and Bornens, M. (2003). Fission yeast cdc31p is a component of the half-bridge and controls SPB duplication. Mol Biol Cell *14*, 2793-2808.

Paoletti, A., Moudjou, M., Paintrand, M., Salisbury, J.L., and Bornens, M. (1996). Most of centrin in animal cells is not centrosome-associated and centrosomal centrin is confined to the distal lumen of centrioles. J Cell Sci *109 (Pt 13)*, 3089-3102.

Pazour, G.J., and Witman, G.B. (2003). The vertebrate primary cilium is a sensory organelle. Current opinion in cell biology *15*, 105-110.

Peel, N., Stevens, N.R., Basto, R., and Raff, J.W. (2007). Overexpressing Centriole-Replication Proteins In Vivo Induces Centriole Overduplication and De Novo Formation. Curr Biol.

Pelletier, L., O'Toole, E., Schwager, A., Hyman, A.A., and Muller-Reichert, T. (2006). Centriole assembly in Caenorhabditis elegans. Nature *444*, 619-623.

Pelletier, L., Ozlu, N., Hannak, E., Cowan, C., Habermann, B., Ruer, M., Muller-Reichert, T., and Hyman, A.A. (2004). The Caenorhabditis elegans centrosomal protein SPD-2 is required for both pericentriolar material recruitment and centriole duplication. Curr Biol *14*, 863-873.

Pihan, G.A., Purohit, A., Wallace, J., Knecht, H., Woda, B., Quesenberry, P., and Doxsey, S.J. (1998). Centrosome defects and genetic instability in malignant tumors. Cancer research *58*, 3974-3985.

Popescu, A., Miron, S., Blouquit, Y., Duchambon, P., Christova, P., and Craescu, C.T. (2003). Xeroderma pigmentosum group C protein possesses a high affinity binding site to human centrin 2 and calmodulin. The Journal of biological chemistry *278*, 40252-40261.

Raynaud-Messina, B., Mazzolini, L., Moisand, A., Cirinesi, A.M., and Wright, M. (2004). Elongation of centriolar microtubule triplets contributes to the formation of the mitotic spindle in gamma-tubulin-depleted cells. J Cell Sci *117*, 5497-5507.

Rebacz, B., Larsen, T.O., Clausen, M.H., Ronnest, M.H., Loffler, H., Ho, A.D., and Kramer, A. (2007). Identification of griseofulvin as an inhibitor of centrosomal clustering in a phenotype-based screen. Cancer research *67*, 6342-6350.

Rodrigues-Martins, A., Riparbelli, M., Callaini, G., Glover, D.M., and Bettencourt-Dias, M. (2007). Revisiting the Role of the Mother Centriole in Centriole Biogenesis. Science.

Ruiz, F., Beisson, J., Rossier, J., and Dupuis-Williams, P. (1999). Basal body duplication in Paramecium requires gamma-tubulin. Curr Biol *9*, 43-46.

Ruiz, F., Garreau de Loubresse, N., Klotz, C., Beisson, J., and Koll, F. (2005). Centrin deficiency in Paramecium affects the geometry of basal-body duplication. Curr Biol *15*, 2097-2106.

Salisbury, J.L. (2004). Centrosomes: Sfi1p and centrin unravel a structural riddle. Curr Biol *14*, R27-29.

Salisbury, J.L. (2007). A mechanistic view on the evolutionary origin for centrin-based control of centriole duplication. Journal of cellular physiology *213*, 420-428.

Salisbury, J.L., Baron, A., Surek, B., and Melkonian, M. (1984). Striated flagellar roots: isolation and partial characterization of a calcium-modulated contractile organelle. The Journal of cell biology *99*, 962-970.

Salisbury, J.L., Suino, K.M., Busby, R., and Springett, M. (2002). Centrin-2 is required for centriole duplication in mammalian cells. Curr Biol *12*, 1287-1292.

Satir, P., and Christensen, S.T. (2007). Overview of structure and function of mammalian cilia. Annual review of physiology *69*, 377-400.

Sauer, G., Korner, R., Hanisch, A., Ries, A., Nigg, E.A., and Sillje, H.H. (2005). Proteome analysis of the human mitotic spindle. Mol Cell Proteomics *4*, 35-43.

Sawin, K.E., and Mitchison, T.J. (1995). Mutations in the kinesin-like protein Eg5 disrupting localization to the mitotic spindle. Proceedings of the National Academy of Sciences of the United States of America *92*, 4289-4293.

Shinmura, K., Bennett, R.A., Tarapore, P., and Fukasawa, K. (2007). Direct evidence for the role of centrosomally localized p53 in the regulation of centrosome duplication. Oncogene *26*, 2939-2944.

Singla, V., and Reiter, J.F. (2006). The primary cilium as the cell's antenna: signaling at a sensory organelle. Science (New York, NY *313*, 629-633.

Sluder, G. (2004). Centrosome Duplication and its Regulation in the Higher Animal Cell, In 'Centrosomes in Development and Disease'. E.A.Nigg, editor. Weinheim: Wiley-VCH. pp.167-189.

Sorokin, S.P. (1968). Centriole formation and ciliogenesis. Aspen Emphysema Conf *11*, 213-216.

Spang, A., Courtney, I., Fackler, U., Matzner, M., and Schiebel, E. (1993). The calcium-binding protein cell division cycle 31 of Saccharomyces cerevisiae is a component of the half bridge of the spindle pole body. The Journal of cell biology *123*, 405-416.

Spang, A., Courtney, I., Grein, K., Matzner, M., and Schiebel, E. (1995). The Cdc31p-binding protein Kar1p is a component of the half bridge of the yeast spindle pole body. J Cell Biol *128*, 863-877.

Spektor, A., Tsang, W.Y., Khoo, D., and Dynlacht, B.D. (2007). Cep97 and CP110 suppress a cilia assembly program. Cell *130*, 678-690.

Stemm-Wolf, A.J., Morgan, G., Giddings, T.H., Jr., White, E.A., Marchione, R., McDonald, H.B., and Winey, M. (2005). Basal body duplication and maintenance require one member of the Tetrahymena thermophila centrin gene family. Mol Biol Cell *16*, 3606-3619.

Stierhof, Y.D., Humbel, B.M., and Schwarz, H. (1991). Suitability of different silver enhancement methods applied to 1 nm colloidal gold particles: an immunoelectron microscopic study. Journal of electron microscopy technique *17*, 336-343.

Strawn, L.A., and True, H.L. (2006). Deletion of RNQ1 gene reveals novel functional relationship between divergently transcribed Bik1p/CLIP-170 and Sfi1p in spindle pole body separation. Current genetics *50*, 347-366.

Swallow, C.J., Ko, M.A., Siddiqui, N.U., Hudson, J.W., and Dennis, J.W. (2005). Sak/Plk4 and mitotic fidelity. Oncogene *24*, 306-312.

Thein, K.H., Kleylein-Sohn, J., Nigg, E.A., and Gruneberg, U. (2007). Astrin is required for the maintenance of sister chromatid cohesion and centrosome integrity. The Journal of cell biology *178*, 345-354.

Thompson, J.R., Ryan, Z.C., Salisbury, J.L., and Kumar, R. (2006). The structure of the human centrin 2-xeroderma pigmentosum group C protein complex. The Journal of biological chemistry *281*, 18746-18752.

Tsang, W.Y., Spektor, A., Luciano, D.J., Indjeian, V.B., Chen, Z., Salisbury, J.L., Sanchez, I., and Dynlacht, B.D. (2006). CP110 cooperates with two calcium-binding proteins to regulate cytokinesis and genome stability. Mol Biol Cell *17*, 3423-3434.

Tsou, M.F., and Stearns, T. (2006). Mechanism limiting centrosome duplication to once per cell cycle. Nature *442*, 947-951.

Ubersax, J.A., Woodbury, E.L., Quang, P.N., Paraz, M., Blethrow, J.D., Shah, K., Shokat, K.M., and Morgan, D.O. (2003). Targets of the cyclin-dependent kinase Cdk1. Nature *425*, 859-864.

Uetake, Y., Loncarek, J., Nordberg, J.J., English, C.N., La Terra, S., Khodjakov, A., and Sluder, G. (2007). Cell cycle progression and de novo centriole assembly after centrosomal removal in untransformed human cells. J Cell Biol *176*, 173-182.

Uhlmann, F., Wernic, D., Poupart, M.A., Koonin, E.V., and Nasmyth, K. (2000). Cleavage of cohesin by the CD clan protease separin triggers anaphase in yeast. Cell *103*, 375-386.

van Kreeveld Naone, S.a.W., M. (2004). The Budding Yeast Spindle Pole Body: A Centrosome Analog, In 'Centrosomes in Develpoment and Disease'. E.A.Nigg, editor. Weinheim: Wiley-VCH. pp.43-69.

Vidwans, S.J., Wong, M.L., and O'Farrell, P.H. (2003). Anomalous centriole configurations are detected in Drosophila wing disc cells upon Cdk1 inactivation. J Cell Sci *116*, 137-143.

Vorobjev, I.A., and Chentsov Yu, S. (1982). Centrioles in the cell cycle. I. Epithelial cells. J Cell Biol *93*, 938-949.

Winey, M., Goetsch, L., Baum, P., and Byers, B. (1991). MPS1 and MPS2: novel yeast genes defining distinct steps of spindle pole body duplication. The Journal of cell biology *114*, 745-754.

Wojcik, E.J., Glover, D.M., and Hays, T.S. (2000). The SCF ubiquitin ligase protein slimb regulates centrosome duplication in Drosophila. Curr Biol *10*, 1131-1134.

Wolff, A., de Nechaud, B., Chillet, D., Mazarguil, H., Desbruyeres, E., Audebert, S., Edde, B., Gros, F., and Denoulet, P. (1992). Distribution of glutamylated alpha and beta-tubulin in mouse tissues using a specific monoclonal antibody, GT335. European journal of cell biology *59*, 425-432.

Wong, C., and Stearns, T. (2003). Centrosome number is controlled by a centrosome-intrinsic block to reduplication. Nat Cell Biol *5*, 539-544.

Yan, X., Habedanck, R., and Nigg, E.A. (2006). A complex of two centrosomal proteins, CAP350 and FOP, cooperates with EB1 in microtubule anchoring. Mol Biol Cell *17*, 634-644.

Yang, A., Miron, S., Mouawad, L., Duchambon, P., Blouquit, Y., and Craescu, C.T. (2006). Flexibility and plasticity of human centrin 2 binding to the xeroderma pigmentosum group C protein (XPC) from nuclear excision repair. Biochemistry *45*, 3653-3663.

APPENDIX

Parts of this work are published in:

Kleylein-Sohn J., Westendorf J., Le Clech M., Habedanck R., Stierhof Y.-D. and Nigg E.A., Plk4-induced centriole biogenesis in human cells. Dev. Cell, 2007 Aug;13(2):190-202

CURRICULUM VITAE

Julia Kleylein-Sohn
Date of birth: 20th March 1978
Place of birth: Munich
Nationality: German

April 2004 – Present
PhD Student at the Max-Planck Institute for Biochemistry, Martinsried, Germany
Department of Cell Biology,
Prof. E.A. Nigg

October 1997 – February 2004
Diploma (M.S.) Biology,
Ludwigs-Maximilians-University, Munich, Germany

1988 – 1997
High School Diploma,
Wilhelm-Hausenstein Gymnasium, Munich, Germany

PUBLICATIONS:

Kleylein-Sohn, J., Stierhof, Y-D., Westendorf, J., Le Clech, M. , Habedanck, R. and Nigg, E. A., Plk4-induced centriole biogenesis in human cells; 2007, Dev Cell.

Thein, K. H., Kleylein-Sohn, J., Barr, F. A., Nigg, E. A. and Gruneberg, U., Astrin is required for the maintenance of sister chromatid cohesion and centrosome integrity, 2007, J Cell Biol.

Dünsing, A., Ying, L., Perdreau, S. A., Kleylein-Sohn, J., Nigg, E. A. and Dünsing, S., Centriole overduplication through the concurrent formation of multiple daughter centrioles at single maternal templates, 2007, Oncogene.

Rehberg, M., Kleylein-Sohn, J., Faix, J., Ho, T. H., Schulz, I., Graf, R., Dictyostelium LIS1 is a centrosomal protein required for microtubule/cell cortex interactions, nucleus/centrosome linkage and actin dynamics, 2005, Mol Biol Cell.

Gordon Research Conference 'Cell Growth and Proliferation', June 2007, Boston (USA, MN)
Kleylein-Sohn, J., Stierhof, Y-D., Westendorf, J., LeClech, M., Habedanck, R. and Nigg, E. A. Posterpresentation: Plk4-induced centriole biogenesis in human cells.